

# **Complex systems models of financial and systemic risk**

*Christopher Michael Wray*

A dissertation submitted in partial fulfilment  
of the requirements for the degree of

**Doctor of Philosophy**

of

**University College London.**

Department of Mathematics

University College London

22 November, 2015

I, Christopher Michael Wray, confirm that the work presented in this thesis is my own. Where information has been derived from other sources, I confirm that this has been indicated in the thesis.

# Abstract

The primary purpose of this thesis is to develop mathematical models and tools that aid the understanding of financial systemic risk, by analysing and applying techniques from complexity science. Large systemic risks that arise in financial asset markets have proved that they can emerge virtually without warning, and create large financial and social costs. I argue that herd behaviour in asset markets is a source of such systemic risk.

In this thesis, I present a new mathematical model of cascades on a stochastic pulse-coupled network, in the presence of binary opposing influences, and analyse it as both a mean field dynamical system, and probabilistically. I demonstrate that a critical coupling parameter exists separating a quiescent regime, from a volatile synchronous regime consisting of large cascades. Second, as an application to systemic risk, I develop a new model of a stylised financial market, using only minimal assumptions, and demonstrate how this replicates important empirical features of financial asset returns, such as long-memory volatility patterns, without recourse to strategy switching or stochastic volatility. Numerical evidence is presented that suggests this minimal market model self-organises to a critical regime, assuming only mild plausible optimising behaviour on the part of the agent. Lastly, I consider some implications for policy scenarios in light of my findings.

# Acknowledgements

I wish to thank a number of people whose time, support and guidance have made undertaking and completion of this thesis possible, in various ways.

First, I wish to thank my supervisor, Prof. Steve Bishop, for his infinite patience, sound advice and the time he has generously taken to guide and encourage my research. Financial mathematics is truly an interdisciplinary field of research, that intersects and borrows from a range of fields. And while it is fascinating to work at the intersection between disciplines, constructing a focussed thesis can be daunting. It is testament to Steve's stoic resolve and broad mathematical interests that not only have I seemingly managed to avoid the "intellectual homelessness" that can beset early-career interdisciplinary researchers but he has helped to extend my mathematical thinking to new areas. For this I am most grateful.

The seed that grew into this thesis was planted while working, on secondment, in New York during Summer 2007, which coincided with the onset of the global financial crisis. For making this "financial crash front row seat" possible, I have Pierre Sarrau, Ed Fishwick and Ben Golub to thank. Special thanks go to Louise "Vord at the Board" Murray and Nigel Foster for stimulating discussions about markets and derivatives, and for correcting my equations. This list would not be complete without acknowledging, in addition to those named above, (in alphabetical order): Nosrut & Shyda Asghar, Rachel Basarab-Horwath, Olga Beschastnykh, Belinda Boa, Simon Brace-Stacey, Richard Bravery, Vivek Gupta, Mark Higgins, Guibin Li, Paul Reid, Paul Scorer, and the wider RQA, FMG, PMG, PAG teams. It was via an amalgam of thought provoking discussion and insightful analysis, with those named above, that my interest in mathe-

mathematical finance was formed. They also helped to make going to work fun.

I would like to take this opportunity to thank Piotr Karasinski, of the European Bank of Reconstruction and Development, and Doyne Farmer, of Oxford University and the Santa Fe Institute, for taking the time to introduce me to the physics of financial markets and agent-based models. Similarly, without support from the UCL DTC in Financial Computing, and in particular Philip Treleaven, Yonita Carter and Damon Wischik, this thesis would not have left the ground. Special thanks are extended to Irena Borzym, whose infectious enthusiasm for mathematics has stayed with me longer than I ever imagined it would.

The science of non-linear systems shows us that to reach certain destinations, one must begin from an appropriate origin. And much of what I have accomplished would not have been possible without Ed and Bernice Patient helping me to find that origin. “Progress is possible”...but it helps if you start at the right place. On a similar note, I am indebted to Peter Stannard, whose steadfast belief in me, and wise advice, have been a great source of encouragement.

To my close friends and family: Miriam, Net, Jo, Paul, Tanya and John Arvanitopoulos, thanks for the intelligent non-mathematical discussion, the relaxing breaks away from work, and for never complaining about the numerous social events I cancelled. Without the unwavering support of Edward Gunn and Paul Stock this thesis would never have been started, nor completed - heartfelt thanks. Finally, to my mother Khoriah and father Michael, brother Dan and sister Nardya, Sarah, Sadie and Roberto - thanks for always being there, to push me on.

# Contents

<b>1</b>	<b>Introduction</b>	<b>13</b>
1.1	Motivation and background . . . . .	16
1.1.1	Financial markets as a complex system . . . . .	17
1.2	Thesis outline . . . . .	22
<b>2</b>	<b>Mathematical Background</b>	<b>24</b>
2.1	Network models . . . . .	24
2.2	Tools for analysing complex systems . . . . .	31
2.2.1	Topological structure . . . . .	31
2.2.2	Analysing dynamics . . . . .	31
2.3	Agent based models in finance . . . . .	34
2.4	Integrate-and-fire and pulse coupled oscillators . . . . .	36
2.5	Empirical facts of financial asset prices . . . . .	41
2.5.1	Notation . . . . .	41
2.5.2	A brief historical perspective of stylised facts . . . . .	45
<b>3</b>	<b>Standard economic theory and a socio-economic perspective</b>	<b>51</b>
3.1	Classical economic modelling: Dynamic stochastic general equilibrium models . . . . .	51
3.2	What are Dynamic Stochastic General Equilibrium models? . . . . .	52
3.2.1	A basic New-Keynesian DSGE model . . . . .	53
3.2.2	Criticism of DSGE models and methodology . . . . .	54
3.3	A socio-economic perspective . . . . .	55

3.3.1	Herding as a contributor to systemic risk . . . . .	56
3.3.2	Classes of agent-based models of herding . . . . .	57
3.3.3	Lux's categorisation of behavioural agent-based models . . . . .	57
<b>4</b>	<b>Stochastic pulse-coupled network: A threshold model of emergent behaviour</b>	<b>60</b>
4.1	Model motivation: Cascade phenomenon in the presence of opposing influences . . . . .	62
4.2	Model description . . . . .	63
4.3	Numerical Analysis of the stochastic system . . . . .	65
4.4	Solution of the model in mean field approximation . . . . .	68
4.5	Path to synchronicity . . . . .	74
4.6	Analysis of the stochastic system: finite state-space . . . . .	75
4.6.1	Cascade distribution of the $K = 1$ system . . . . .	76
4.6.2	Analysis and approximation of systems with $K \geq 1$ . . . . .	81
4.6.3	Fitting a negative binomial distribution. . . . .	81
<b>5</b>	<b>Complexity model of herding in financial markets</b>	<b>84</b>
5.1	Financial market model . . . . .	90
5.2	Comparison to market data . . . . .	93
5.2.1	Volatility clustering and long-memory . . . . .	99
5.2.2	Volatility clustering in the finite state space case . . . . .	102
5.3	Analysis of the stochastic system: semi-infinite state-space . . . . .	108
5.3.1	Volatility clustering in the semi-infinite state-space case . . . . .	111
<b>6</b>	<b>Financial complexity and its use in policy scenarios</b>	<b>119</b>
6.1	A brief outline of broad UK economic policy before and after the financial crisis . . . . .	120
6.2	Bank capital adequacy and delayed transitions . . . . .	121
6.3	Asset bubbles and herding as a precursor to systemic risk . . . . .	126

6.4	General comments on the use of complexity models by policymakers . . .	129
<b>7</b>	<b>Conclusions</b>	<b>132</b>
7.1	Summary of results . . . . .	132
7.2	Extensions and future research and limitations . . . . .	135
	<b>Appendices</b>	<b>137</b>
<b>A</b>	<b>A New Keynesian DSGE model - for chapter 3</b>	<b>137</b>
A.0.1	Exogenous variables . . . . .	138
A.0.2	Households . . . . .	139
A.0.3	Firms . . . . .	140
A.0.4	Monetary policy . . . . .	141
A.1	Estimating the model and fitting data . . . . .	141
<b>B</b>	<b>Pulse-coupled model details and proofs - for chapter 4</b>	<b>145</b>
B.1	Construction of the map $G_0$ . . . . .	149
B.2	Combinatorial methods for cascade probability . . . . .	151
B.3	Mixture distribution moments and negative binomial density . . . . .	153
B.4	Power law distribution and Kolmogorov-Smirnov test . . . . .	154
<b>C</b>	<b>Complexity model of herding in financial markets details - for chapter 5</b>	<b>155</b>
C.1	Model description . . . . .	155
C.2	Recovery of the implied volatility smile . . . . .	156
C.3	Market data: implied volatility of 1-month expiry European call option on S&P 500 afternoon settled index . . . . .	156
<b>D</b>	<b>A result on the first passage time of <math>N</math> Brownian motions - a result used in numerical programming</b>	<b>158</b>
	<b>References</b>	<b>163</b>

# List of Figures

1.1	S& P500 Index value with European Central Bank deposits . . . . .	20
2.1	Examples of basic networks . . . . .	27
2.2	Small-world mean path and clustering . . . . .	29
2.3	Evolution of an integrate-and-fire oscillator . . . . .	37
2.4	Phase response of an oscillator after pulse coupling . . . . .	39
2.5	Evolution of order parameter $S$ of a pulse-coupled system . . . . .	40
2.6	Probability densities for Power laws versus Gaussian . . . . .	46
2.7	Volatility clustering of the S & P 500 Index 2006-2014 . . . . .	48
2.8	Implied volatility smile of S & P Index options as of 26 November 2014	49
3.1	Schematic of a simple DSGE model . . . . .	53
4.1	Cascade size progression of the stochastic pulse-coupled model (finite state-space) . . . . .	66
4.2	Cumulative absolute cascade size of the stochastic pulse-coupled model	67
4.3	Bifurcation diagram of stochastic and mean field system. . . . .	68
4.4	Cascade size progression for a normalised mean field system . . . . .	69
4.5	Phase transition in mean field systems: transition from asynchronous to synchronous . . . . .	70
4.6	Cascade size analytic versus numerical for $K = 1$ system . . . . .	73
4.7	Tree representations of a single arbitrary cascade incorporating depen- dency between levels. . . . .	79
4.8	Log-log probability plots of cascade distributions. . . . .	80

4.9	Extracting negative binomial parameters. . . . .	82
4.10	Kolmogorov-Smirnov statistic values obtained by fitting a power law and negative binomial model to absolute cascade size data. . . . .	83
5.1	Comparison of simulated standard deviation and closed form approxi- mation. . . . .	92
5.2	Log-log probability plots of $(K, q)$ model output compared with mid price market data. . . . .	94
5.3	Fitting the implied volatility smile for index options. . . . .	95
5.4	Log-linear plot of maximal cascade size for various $K$ . . . . .	98
5.5	Simulation of the financial market model with finite state-space, homo- geneous firing thresholds. . . . .	103
5.6	Simulation of the financial market model with finite state-space, inho- mogeneous firing thresholds. . . . .	105
5.7	Simulation of the financial market model with finite state-space, homo- geneous firing thresholds and time-varying coupling. . . . .	107
5.8	Implied bias probability when the threshold distribution is of power law type with exponent 2. . . . .	109
5.9	Simulation of the financial market model with semi-infinite state-space and homogeneous firing thresholds (1). . . . .	114
5.10	Simulation of the financial market model with semi-infinite state-space and homogeneous firing thresholds (2). . . . .	115
5.11	Simulation of the financial market model with semi-infinite state-space and inhomogeneous firing thresholds. . . . .	116
5.12	Mean hitting times for a battery of distributions for the firing threshold .	117
5.13	Mean hit time for the semi-infinite system with left-skew threshold dis- tribution. . . . .	118

5.14	Log-log plot showing slow convergence to a Gaussian. Kolmogorov-Smirnov two sample test statistic and excess kurtosis of the financial market model plotted against increasing price return interval. . . . .	118
6.1	Transition from small cascade regime to large cascade size regime shown against $q$ for $K=1, 2, 3, 5, 8, 10$ - finite state-space . . . . .	124
6.2	The rate of change in the size of the maximal cascade as coupling probability is perturbed . . . . .	125
6.3	Monthly index values of the Case-Shiller United States National House Price Index. . . . .	127
6.4	Smoothing an abrupt tipping point in a 100 node network of average degree 10, undergoing systematic node failure . . . . .	130
A.1	Input-response function diagram: relations to policy shock . . . . .	143
A.2	Input-response function diagram: relations to technology shock . . . . .	144
D.1	Appendix: First-passage times of multiple Brownian motions. For numerical analysis . . . . .	162

# List of Tables

2.1	Average shortest path lengths and average clustering for ring lattice and random network . . . . .	29
2.2	Modelling different interaction structures in complex systems. . . . .	32
2.3	Suitable analysis tools based upon properties of a complex system. . . . .	32
5.1	Parameter values of simulation corresponding to Figs. 5.5-5.11 . . . . .	101
C.1	Implied volatility of SPXpm European call options of 1-month expiry as of November 25 2014 . . . . .	157

# Chapter 1

## Introduction

The primary purpose of this thesis is to develop mathematical models and tools that aid the understanding of financial systemic risk, by analysing and applying techniques from complexity science. The study of systemic risk is intimately connected to the notion of a system which, throughout this thesis, is taken to refer to a collection of interacting components that contribute to the function, or objective, of the system. There is currently no agreed definition of systemic risk, financial or otherwise, although Haldane and May [2011] consider risk and instability to the whole financial system as important components of financial systemic risk. Another view of systemic risk is offered by D. Helbing, who suggests such risks

‘can trigger unexpected large-scale changes of a system or imply uncontrollable large-scale threats to it’ [Helbing, 2012]

For this thesis, systemic risk is taken as referring to large-scale, macroscopic, change among system components that either adversely impacts the functioning of the system under consideration, or places the system in to an undesirable state. Systemic risk events that arise within a system may do so endogenously, or be triggered by an exogenous event.

The costs associated with a systemic risk event occurring within a particularly critical, or interdependent system, can be immense. Even if the numéraire of cost is simply the time required to return the system to its original state, it would be reasonable to surmise

that opportunity costs had been incurred. For example, case studies of severe disruption in electricity supply (blackouts) reveal economic costs to be in excess of four billion U.S. dollars for a 2003 blackout in Canada, lasting a few days [Walker et al., 2014]. In relation to financial systems, systemic risk events can be extraordinarily costly in both the social dimension, through unemployment and poor public health [Stuckler et al., 2009], and the monetary dimension, with estimates of the financial losses incurred as a result of the financial crisis are of the order of trillions of U.S. dollars [The Financial Crisis Inquiry Commission, 2011].

Given the potential for large social and economic costs, researchers and policy makers are particularly interested in understanding systems that possess the ability to generate endogenous systemic risk events [Helbing et al., 2011]. Gaining an understanding of such systems may lead to better contingency plans, mitigation strategies and techniques for predicting the onset of large scale system failure, or a shift to an undesirable state.

Systemic risk events in financial systems manifest in a number of ways, the classical example being a bank run [Allen and Gale, 1998], during which many depositors withdraw their funds from a bank near simultaneously, and attract others to do the same, severely impairing the functioning of the bank as a result. Other examples include a cascade of insolvencies occurring among financially important institutions - whose impairment places the stability of the financial system at risk - as what occurred in 2007 and 2008 during the global financial crisis [Haldane, 2009].

This thesis is concerned with systemic risk arising in financial asset markets, as a result of herd behaviour [Bikhchandani and Sharma, 2000]; how it may be quantified and identified, and the consequence for asset price dynamics. This is achieved by placing the simple theory of information cascades [Bikhchandani et al., 1992; Banerjee, 1992; Shiller, 2015] into a mathematical context, and utilising techniques from complex systems in the subsequent analysis. By framing this problem in complex systems science, it is argued that such systemic risk endogenously occurs as emergent behaviour, in accordance with typical features of a complex system. In addition, some pertinent policy

implications are considered in light of this.

The contributions to knowledge that this thesis has made, can be separated in to three areas. First, a new mathematical model [Wray and Bishop, 2014] of cascades occurring on a stochastic network in the presence of binary opposing influence, is presented and analysed both as a mean field dynamical system and probabilistically. The model is demonstrated to possess a critical transition separating a quiescent regime, in which cascade sizes are small relative to the system size, and a regime in which cascade sizes are macroscopic in size. This contributes to the literature on phase transitions occurring in processes that take place on a network.

Second, as an application to financial systemic risk in asset markets, a new minimalistic model describing herd behaviour in a stylised financial market is developed [Wray and Bishop, 2015]. The novel feature of this model is its ability to replicate important features of asset returns time series, without explicit recourse to two of the commonly assumed behavioural mechanisms presented in the literature to-date (namely strategy switching amongst economic agents, and agents operating over fixed but heterogeneous time scales). Although the model described here requires economic agents to operate over a specific parameter range in order for the stylised facts to emerge, I reason, supported by numerical findings, that an economically plausible and simple optimising mechanism (minimisation of the time duration between trades) drives agents to this critical parameter range.

Third, this thesis as a whole contributes to a more constructive framing of certain financial market risks related to herd behaviour, than has previously been the case. The relationship between individuals and financial systems evolve through time, not only in terms of participation, but also in how individuals (policy makers, researchers, citizens) perceive and interpret events that may occur. To be specific, I am arguing that the historic framing of possible systemic risk events as ‘anomalous’, suggesting such events should conform to an already existing body of knowledge, or do not warrant explanation, is non-constructive in the sense of deterring potential scholarly attention [see

Frankfurter and McGoun, 2001, for a fuller account of this line of reasoning]. This, I argue, is in contrast to the less emotive and more constructive framing of systemic risk, that actively seeks interdisciplinary understanding in the pursuit of solutions to difficult problems.

## **1.1 Motivation and background**

In his, by now well known, opening speech of the 2010 European Central Bank (ECB) annual conference Jean-Claude Trichet, then President of the ECB, made the following profound remarks in relation to the Eurozone Sovereign debt crisis, that started in 2009, and the shortcomings of available policy tools:

‘When the crisis came, the serious limitations of existing economic and financial models immediately became apparent. Macro[economic] models failed to predict the crisis and seemed incapable of explaining what was happening to the economy in a convincing manner. As a policy-maker during the crisis, I found the available models of limited help. In fact, I would go further: in the face of the crisis, we felt abandoned by conventional tools.’ [Trichet, 2010].

Trichet continues, with an appeal for economists to work in conjunction with scientists and experts of complex dynamic systems:

‘... we need to develop complementary tools to improve the robustness of our overall framework. In this context, I would very much welcome inspiration from other disciplines: physics, engineering, psychology, biology. Bringing experts from these fields together with economists and central bankers is potentially very creative and valuable. Scientists have developed sophisticated tools for analysing complex dynamic systems in a rigorous way. These models have proved helpful in understanding many important but complex phenomena: epidemics, weather patterns, crowd psychology, magnetic fields.’ [Trichet, 2010].

It is clear that Trichet does not say economics needs to be replaced, nor from his comments can one infer he believes economic models possess no value. Although, for a highly regarded administrator to publicly question the efficacy of policy tools based upon classical economic models, at a time when they are most needed, is excellent motivation to develop financial-economic models using techniques from the science of complex systems.

### **1.1.1 Financial markets as a complex system**

The beginnings of complexity science, (as it most closely resembles the endeavour today) can be traced back to two seminal contributions. Anderson [1972], who questioned the reductionist point of view which postulates fundamental laws of physics are only those that apply to elementary particles - arguing instead that such laws depend on a hierarchy of scales. This argument led to the concept of emergence, a central concept in complexity science. May [1972], demonstrated that a large (highly connected) complex system need not be considered stable (contrary to the prevailing wisdom at the time), and provided criteria for when stability exists - a concept which continues to be central to the study of complex systems, and of clear relevance to the highly interconnected financial systems that exist today.

It remains an unresolved question as to whether complexity is a universal phenomenon, or if different disciplines exhibit domain-specific complexity. As a result, there is a lack of consensus as to what exactly constitutes complexity, and therefore no agreed definition exists. Researchers have therefore focused on describing core qualitative features that are considered to be common to many complex systems. Three features that appear to be present in most descriptions of complex systems are [Boccaro, 2010]

1. Consisting of many interacting components.
2. Present emergent macroscopic phenomena not present at the microscopic level.
3. Emergent behaviour does not result from the existence of a central controller.

Depending upon the particular system under study, the components of a complex system may themselves have diverse properties. In the case of financial markets, and of direct relevance to this thesis, these features are often taken to be agent (component) heterogeneity [Page, 2010] and adaptive behaviour [Johnson et al., 2003]. It is noted, that component heterogeneity is not a prerequisite to producing interesting complex phenomena: paradigmatic models consisting of homogeneous components include the cellular automata studied by Wolfram [1983], and the Ising [1925] lattice interaction model. Both models continue to influence current research across a diverse range of disciplines.

The classic examples of complex systems, together with corresponding emergent phenomena include [Newman, 2011]

1. Condensed matter physics and spontaneous symmetry.
2. The brain and cognitive ability.
3. Ecosystems and extinction (and life) events.
4. Transport networks and congestion.
5. Financial markets and financial crashes/asset bubbles.

Aside from the classic examples listed above, other significant applications of ideas arising from complexity science have occurred in urban planning and the theory of cities [Batty, 2007], epidemic spreading [Pastor-Satorras and Vespignani, 2001; Newman, 2002] and more recently network collapse [Majdandzic et al., 2013]. Tools used to study complex systems, such as networks, are described in chapter 2.

The view of financial markets (and the economy, more broadly) as a complex system has long been established by certain economists [Arthur, 1995; Anderson et al., 1988; Arthur et al., 1997] (see Hommes [2013], and references therein for a recent review), although neither this view, nor its implications, are shared universally amongst all economists or policy makers. Notwithstanding this, it has been suggested that financial systems represent one of the best examples of a complex adaptive system [Havlin

et al., 2012], since financial markets consist of many interacting heterogeneous agents, acting with no central coordination and capable of producing seemingly macroscopic emergent phenomena, such as crashes and asset bubbles [Sornette, 2003]. Moreover, financial systems feature multiple hierarchies of feedback, ranging from performance tracking of investment fund managers and the subsequent scrutiny of their portfolio holdings, companies that sell stock and subsequent buy it back if it falls too low, and feedback between a financial index and its constituent stocks [Kenett et al., 2013].

With the onset of the financial crisis that began in 2007, researchers have had another piece of evidence that supports the view that financial markets generate endogenous systemic risk events, and this has been followed by a range of studies examining the conditions under which such events may arise and propagate in the interbank network [Haldane and May, 2011; May et al., 2008; Gai and Kapadia, 2010; Tedeschi et al., 2012b]. Although this is exceptionally important and necessary work, an influential report [The Financial Crisis Inquiry Commission, 2011] states the most recent financial crisis first transpired in the asset market for financial securities derived from home loans, whose collapse was preceded by the collapse of the U.S. housing bubble in existence at the time.

‘While the vulnerabilities that created the potential for crisis were years in the making, it was the collapse of the housing bubble fueled by low interest rates, easy and available credit, scant regulation, and toxic mortgages that was the spark that ignited a string of events, which led to a full-blown crisis in the fall of 2008.’ [The Financial Crisis Inquiry Commission, 2011, page. 16].

This raises the question of why so many independent professional investors arrived at the same false conclusion (that the assets in question were correctly priced), when in fact they were extremely mis-priced. One explanation is that such investors have identical (or near identical) thought processes and information sets - although, this raises many difficulties in relation to prior and subsequent decisions. Another reason can be

found in the context of herd behaviour and information cascades, first introduced by Bikhchandani et al. [1992] and Banerjee [1992], which theorises how individuals may eventually ignore their own private information, or preferences, as a result of taking into account the judgements, or actions, of others [see Shiller, 2015, for an account].

Herd behaviour has been suspected, or known to be, the catalyst of many financial crises and numerous asset bubbles (for example, Black Monday in 1987 and the Dot Com crash in 2000. For a review of these events see Sornette [2003]). It follows that herd behaviour can be considered a significant (but not exclusive) component of systemic risk events.

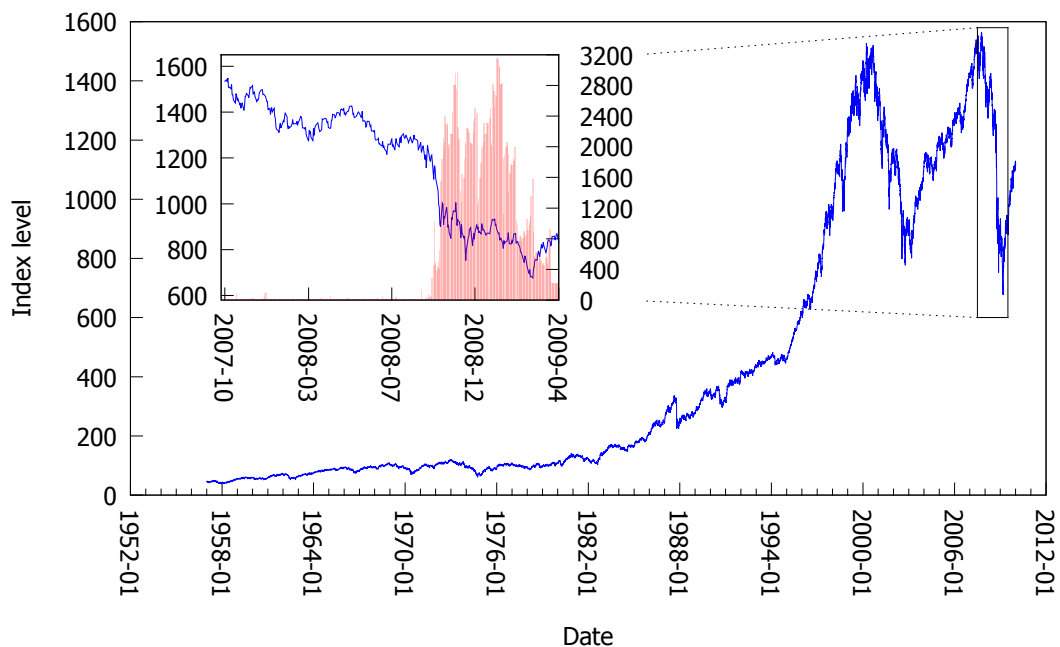


**Figure 1.1.** Value of the S&P 500 index, with inset additionally detailing bank deposits (right hand scale EUR billions) placed with the European Central Bank, indicating the extent of liquidity hoarding by European banks during the financial crisis.

### **Contextual economic background and summary of official U.S. government report**

It is important to understand the context in which Trichet's remarks [Trichet, 2010] were made (during the global financial crisis that began in the U.S), if only to eradicate any notion of exaggeration or hyperbole on his part. In a bid to increase home ownership, the U.S. department for Housing and Urban Development (HUD) relaxed the

restrictions on Freddie Mac and Fannie Mae (government-sponsored enterprises whom were overseen by the HUD) in securitizing sub-prime mortgages. During this time, investment banks, and private non-government enterprises, increased their securitization of these riskier loans. While Government enterprises guaranteed the performance of their securities, private and investment bank securitizations provided no such guarantees, and mitigated their risk, by buying insurance, in the form of a credit default swap (CDS), thus transferring the credit risk to a third party. As the government enterprises, Fannie Mae and Freddie Mac, lost market share they too loosened their guarantee business and underwriting standards, in a race to the bottom to attract a larger share of the sub prime market. By mid 2004, sub-prime mortgages made up around 13% of total mortgages, jumping from around 3% in 2003. By 2006, default rates of sub-prime mortgages stood at 12.2%. The United States entered a national recession towards the end of 2007, that caused real-estate prices to collapse from all-time historical highs, driving up homeowner loan defaults (see Fig. 1.1). This in turn caused the value of securities linked to real-estate loans (so-called asset backed securities) to plummet, which incurred unexpected losses for institutions holding such securities. These events marked the beginning of what has become known as the global financial crisis of 2007-2008. The two years that followed revealed how the complex interplay between US administration policy, rating agencies, regulators, banking practices and solvency provisions can lead to a build up of systemic risk, having the potential to severely impact the global economy. During 2008 and 2009 a large number (39 in 2008, and 10 in 2009, in addition to the 140 smaller U.S. commercial banks and savings associations) of systemically important financial institutions experienced exceptionally negative liquidity problems and capital shortfalls as a result of sub-prime contagion, and either failed and filed for bankruptcy (Lehman Brothers), or were acquired by competitors with government assistance (Merril Lynch by Bank of America), or given restrictive bailout loans by central authorities (American Insurance Group). Lending between banks on the interbank market froze as they began liquidity hoarding: depositing their available cash with central banks (deemed as safe), rather than make short term loans to another bank

(seen as risky). The inset bar chart in figure 1.1 shows the marked increase in deposits taken by the European Central Bank. In the short term, liquidity hoarding could be seen as bolstering healthy banks, but eventually reduces the resilience of all banks due to negative system-wide feedback effects. For a fuller account of the background, see the comprehensive financial crisis inquiry report, compiled by the U.S. government [The Financial Crisis Inquiry Commission, 2011].

## **1.2 Thesis outline**

In chapter 2, mathematical and financial background material to this thesis is presented.

In chapter 3, a modern economic dynamic stochastic general equilibrium model is constructed and evaluated which is used to frame the remaining work and discussion, and highlight the significant conceptual differences between classical economic modelling, and the methods and models suggested in the rest of the thesis.

In chapter 4, a new model of cascades on a stochastic pulse-coupled network is developed, and analysed as a mean field dynamical system. The existence of a critical network coupling is demonstrated both analytically and numerically, and a correspondence with standard bond percolation. The model is demonstrated to possess a critical transition separating a quiescent regime, in which cascade sizes are small relative to the system size, and a regime in which cascade sizes are macroscopic in size. The transition of the system between regimes can be thought of as analogous to bond percolation Grimmett [1999], which is recovered as a special case of the model. In general, the model displays transitions that occur at a sharper rate than in the case for standard bond percolation - a point which is discussed in relation to bank capital adequacy buffers in chapter 6.

In chapter 5, two variants of a new financial market model are derived from the model presented in chapter 4. It is demonstrated how the new model can be applied in the context of herding in financial asset markets, and substantial numerical analysis is presented, showing the ability of the model to reproduce a number of observed empirical facts concerning financial time series, in a robust and parsimonious manner. By

reference to economic literature, a detailed economic justification is provided for the modelling choices, showing that such choices are not at odds with certain economic evidence. Second, as an application to financial systemic risk in asset markets, a new minimalistic model describing herd behaviour in a stylised financial market is developed [Wray and Bishop, 2015]. Substantial numerical results are presented as evidence of the models ability to generically replicate some of the important features empirically observed in the time series of returns of financial assets (known as the stylised facts of financial markets, in the lexicon of financial markets), and an economic rationale for specific modelling choices is stated. The novel feature of this model is its ability to generate these stylised facts without explicit recourse to two of the commonly assumed behavioural mechanisms presented in the literature to-date (namely strategy switching amongst economic agents, and agents operating over fixed but heterogeneous time scales). and an economic rationale for specific modelling choices is stated.

In chapter 6, policy scenarios are discussed in light of the findings of this thesis. In particular, the policy implications of considering asset bubbles as a precursor to systemic risk are discussed, and bank capital adequacy buffers - one result from the policy response to the most recent financial crisis - are discussed in the presence of sharp transitions.

Chapter 7 concludes with a summary of findings, and implications to the economic literature. In particular, the classical economic belief that the absence of external news implies the absence of trading (and consequently the absence of fundamental price changes) is reconciled with the threshold model developed in this thesis. Finally, some ideas for further research are presented.

# Chapter 2

## Mathematical Background

This chapter collects much of the background mathematical terms, tools, concepts and notation that will be used in this thesis. Networks, or graphs as they are known in the mathematical literature, have become valuable tools for modelling complex systems, and this chapter starts by describing the basic network models, and a selection of their properties. This is followed by a brief description of a selection of methods and tools commonly used to analyse complex systems and employed in this thesis (namely dynamical systems and probabilistic methods). A description of agent-based models follows, with an emphasis on finance and economics, as such models are frequently employed to study complex systems, and because the financial market model in chapter 5, can be viewed as an agent-based model. This is followed by background material on deterministic pulse-coupled oscillators and the integrate-and-fire methodology that is used in chapters 4 and 5, to model the communication structure between components of the system considered therein. The latter part of this chapter collates notation and fundamental concepts associated with the so-called stylised facts of financial asset prices, that are referenced in chapter 5.

### 2.1 Network models

The vast literature on network theory has evolved from its roots in pure mathematics [Erdős and Rényi, 1959] along a diverse interdisciplinary path finding application in a wide range of research areas. Notable applications of network theory are: epidemiol-

ogy and the spreading of disease on networks [Pastor-Satorras and Vespignani, 2001; Castellano and Pastor-Satorras, 2010]; neuroscience and the modelling of neuronal networks [Brunel, 2000], and the study of man-made technological and transportation structures [Colizza et al., 2006; Kaluza et al., 2010]. In economics and finance, a significant amount of research utilising networks has been catalysed by the global financial crisis, in particular to model financial contagion [Gai et al., 2011]. Boccaletti et al. [2006] presents a comprehensive account of other areas where networks have been applied.

Recent research concerning networks explores multiplex networks [Nicosia et al., 2013], explosive percolation on networks [Achlioptas and Spencer, 2009], dynamic failure and recovery of networks [Majdandzic et al., 2013] and cascades both on, and within, networks [Buldyrev et al., 2010; Crucitti et al., 2004], and opinion dynamics and general spreading phenomena [Watts, 2002; Singh et al., 2013; Hackett and Gleeson, 2013].

For complex systems that do not require an idiosyncratic or specialised model to describe their interaction structures, network theory has, for some time now, come to be the methodology of choice when modelling component interaction [Strogatz, 2001]. In this section I provide an overview of basic networks.

### **Basic network models**

A network is a collection of abstract objects, some of which may be pairwise connected via links (interchangeably known as edges). The objects which comprise a network are called vertices (interchangeably known as nodes), and may be labelled using enumeration, so that reference can be made to node 1 or, in general, node  $i$  or simply  $n_i$ , depending upon the context.

A simple network is one where nodes are distinct; two nodes may have at most one edge between them (no multi-edges), and nodes cannot have an edge with themselves (no self-loops). In the case of simple networks, the collection of nodes and edges can be conveniently represented by the so-called adjacency matrix,  $A$ , with entries  $A_{ij}$

satisfying

$$A_{ij} = \begin{cases} 1, & n_i \text{ connects to } n_j. \\ 0, & \text{otherwise.} \end{cases} \quad (2.1)$$

Edges may be either undirected, implying the adjacency matrix is symmetric, or directed with the corresponding adjacency matrix, in general, non-symmetric. The degree of a node within an undirected network is taken as the number of edges incident to the node. In the case of a network with directed edges, it is possible to make a distinction between incoming incident edges to a node (in-degree) and outgoing incident edges to a node (out-degree). A central idea in network theory is that of the degree distribution, which is the probability distribution of node degree, taken over the entire network. Since the degree distribution is a fundamental global network property, it is often used for preliminary classification, or analysis, of networks. Another important network measure is the clustering coefficient, introduced in a local-network form by Watts and Strogatz [1998]. Before defining the clustering coefficient for a node in an undirected network, we first define the neighbourhood,  $N(i)$ , of node  $n_i$  to be the set of nodes that directly connect to  $n_i$ . Let  $E$  denote the set of all edges of the network; the number of nodes in the neighbourhood of node  $i$  by  $|N(i)|$ , and an edge between two nodes ( $n_i$  and  $n_j$ ) by  $(i, j)$ , then the local clustering coefficient [Watts and Strogatz, 1998],  $C_i$ , for an arbitrary node  $n_i$  is

$$C_i = \frac{2|\{(j, k) : n_j, n_k \in N(i), (j, k) \in E\}|}{|N(i)|(|N(i)| - 1)}. \quad (2.2)$$

Intuitively,  $C_i$  measures the density of connections between the nodes in the neighbourhood of a given node. A global measure of clustering,  $C(N)$ , can be obtained by taking the average local clustering coefficient, Eqn. (2.2), over all  $N$  nodes in the network. Another widely used measure of network topology is the average path length,  $L(N)$ , and is simply the average number of edges along the shortest paths between all possible pairs of nodes.

Models for generating networks are invaluable for understanding and classifying real-world networks. Not only can it be resource intensive, time consuming or impractical to gather enough data to reconstruct a specific network. In some cases, such as financial or trade related networks, there may be regulatory barriers or competitive restrictions in obtaining relevant network data. The main types of network models, and how they are constructed, are presented below.

### **Erdős-Rényi networks.**

The paradigmatic random graph model (or random network), introduced by Erdős and Rényi [1959] is a simple probabilistic graph construction model lacking any informed edge creation mechanism. Instead, undirected edges between nodes exists randomly, and independently from other edges and the size of the network.

Equivalent to the Erdős-Rényi network, is the binomial network, that consists of  $N$  nodes, with each of the  $N(N - 1)/2$  possible edges having an independent probability  $p$  of being present and probability  $1 - p$  of being absent, from the network. For a given  $N, p$  we can compute the degree distribution explicitly. Let  $P(z)$  be the probability that a node of degree  $z$  is present in the network. In a network of  $N$  nodes, consider a node of some degree  $0 < z < N$  that necessarily connects to  $z$  other nodes, and does not connect to the other  $N - z - 1$  nodes. Since each connection exists independently with probability  $p$ , we can use the binomial distribution to show that

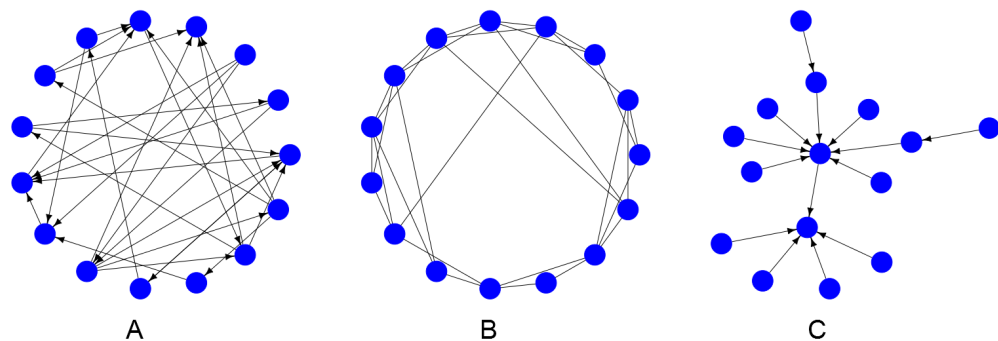


**Figure 2.1.** A) directed Erdős-Rényi, B) undirected Watts-Strogatz ‘small-world’ showing ring-lattice with some rewired edges, C) scale-free network produced via the Barabási-Albert preferential attachment mechanism

$$P(z) = \binom{N-1}{z} p^z (1-p)^{N-z-1} \quad (2.3)$$

$$\approx e^{-\langle z \rangle} \frac{\langle z \rangle^z}{z!}, \quad (2.4)$$

where  $\langle z \rangle$  represents the average (mean) node degree, and the approximation in equation (2.4) follows from the Poisson approximation for large  $N$  and bounded  $\langle z \rangle = (N-1)p$ .

### **Watts-Strogatz network.**

Watts and Strogatz [1998] introduced a single parameter ( $\beta \in [0, 1]$ ) family of networks, known as small-world networks, to analyse the small-world character of real-world networks that simultaneously have a high clustering coefficient and low average path length. The method of constructing a small-world network (in one dimension) utilises two features: the high clustering value of ring-lattices ( $\beta = 0$ ), and secondly, the low average path length of random networks ( $\beta = 1$ ). The small-world network construction method produces a small-world network as the result of an interpolation between these two network types. A small-world network with  $N$  nodes and average (even) degree  $Z$ , with  $N \gg Z \gg \log N \gg 1$ , can be constructed in two stages. First, a regular ring lattice of  $N$  nodes, with each node connected to its  $Z/2$  nearest neighbours on either side of the node, is produced. Each edge can be represented by the nodes it connects, so that  $(i, j)$  represents the edge connecting nodes labelled  $i$  and  $j$ . We say an edge is rewired when the edge  $(i, j)$  is replaced by  $(i, r)$  where  $r \neq i$  is selected to avoid self-loops and edge duplication, but randomly selected otherwise. The second stage of the construction consists of rewiring each edge  $(i, j)$ , for  $i < j$ , with probability  $\beta$  or leaving it unchanged with probability  $1 - \beta$ . This mechanism produces an undirected small-world network, parametrised by  $\beta$ .

The key mechanism for producing small-world graphs with high clustering values is how quickly the average path length drops as the edge-rewiring probability increases from zero, and importantly how it does so more quickly compared to the normalised mean clustering. By considering average network clustering and shortest path length

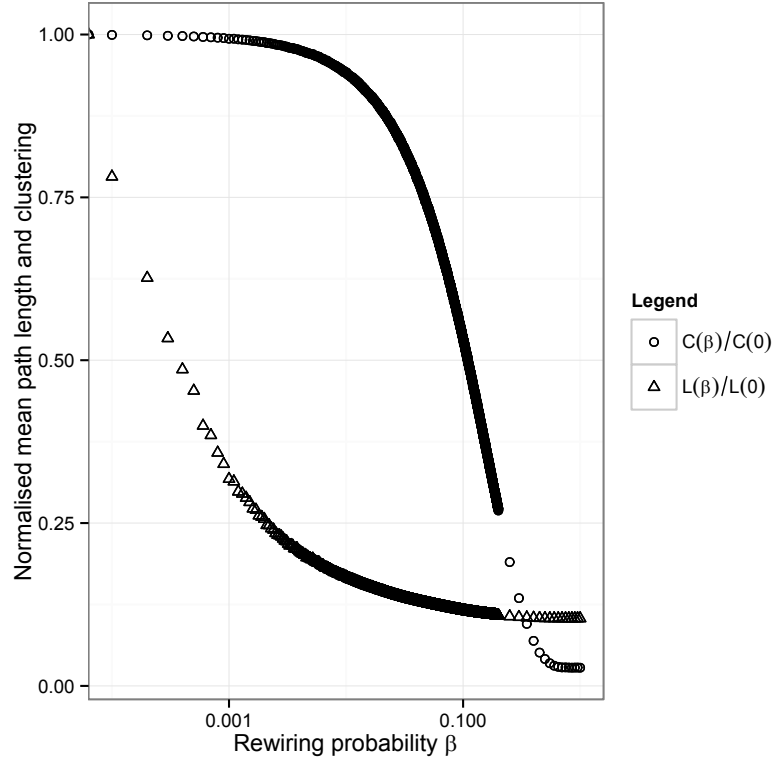


**Figure 2.2.** The normalised mean clustering coefficient ( $\circ$ ) and mean path length ( $\triangle$ ), plotted against the Watts-Strogatz  $\beta$  parameter using log scale. The x-axis is shown in log scale. The networks have 1000 nodes and average degree of 20. Each point is the average of 1000 realisations.

Network type	Average clustering	Average path length
Ring-lattice ( $\beta = 0$ )	$\frac{N}{2Z}$	$\frac{3(Z-2)}{4(Z-1)}$
Random network ( $\beta = 1$ )	$\frac{\log N}{\log Z}$	$\frac{Z}{N}$

**Table 2.1.** Average shortest path lengths and average clustering for ring lattice and random network

parameterised by  $\beta$ , Fig. 2.2 shows that as  $\beta$  increases from 0 to approximately 0.001, the normalised path length drops from one to,  $\frac{L(\beta)}{L(0)} \approx 0.3$ , while the normalised average clustering coefficient changes from one to  $\frac{C(\beta)}{C(0)} \approx 0.99$ . Showing that even a small perturbation of  $\beta$  can have a drastic impact upon the topological connectivity of the network. Table. 2.1 compares the average clustering and shortest path length for ring-lattices and random networks, expressed in terms of total number of nodes ( $N$ ), and average degree ( $Z$ ).

### Scale-free networks: Barabási-Albert.

In a seminal article, Barabási and Albert [1999] introduce a preferential attachment mechanism for constructing networks that possess a scale-free degree distribution. Although the small-world network [Watts and Strogatz, 1998] reproduces some features possessed by many empirical networks, there are other attributes it does not reproduce or explain. One such phenomena is that of a scale-free degree distribution. A Barabási-Albert network is constructed via a growth and preferential attachment mechanism, which means that new nodes joining a network are more likely to connect to nodes that are already well connected, and results in a power-law degree distribution,  $P(z) \sim z^{-3}$ . The algorithm used to create a Barabási-Albert network is simple: start with a connected network of  $N_0$  nodes, and then at each time-step add a new node with  $m < N_0$  edges. Each edge connects to one of the existing nodes with a probability proportional to the node degree. Once all the new edges have been attached to nodes in the system, the process is repeated with updated probabilities until a network with the desired number of nodes, ( $N$ ), is reached. The average clustering coefficient, for a Barabási-Albert network is [Klemm and Eguíluz, 2002]

$$C(N) = \frac{m}{8N}(\log N)^2, \quad (2.5)$$

while Bollobás and Riordan [2003] show that average path length scales like

$$L(N) \approx \frac{\log N}{\log \log N}. \quad (2.6)$$

Scale-free networks (obtained via a method such as growth plus preferential attachment) explain the formation of hubs, or highly connected nodes, within networks. Such nodes are considered important, due to their high topological relevance within a network [see Albert et al., 2000; Doyle et al., 2005, for a description of so-called robust-yet-fragile systems]. It is reported that many important networks, such as the World Wide Web and metabolic networks, appear to possess power-law degree distributions [see Albert and Barabási, 2002].

## **2.2 Tools for analysing complex systems**

### **2.2.1 Topological structure**

One of the earliest tools to study complexity was popularised by Stephen Wolfram, who carried out pioneering research on complexity in one-dimensional cellular automata [Wolfram, 1983]. An elementary cellular automata can be thought of as an array of discrete cells each consisting of a state variable whose value depends upon the states of cells in the immediate neighbourhood, at the previous time step. Updates to cell states typically occur in parallel, although other schemes are possible. Cellular automata are particularly suited for describing local interactions, between homogeneous units when the cell update rule is both spatially and temporally homogeneous. There are numerous extensions and generalisations of cellular automata, including stochastic cellular automata, asynchronous updating cellular automata and cellular automata in higher dimensions [a comprehensive survey can be found in Kari, 2005]. An important property of cellular automata is the ability to realise coherent global patterns from strictly local rules. Furthermore, because such systems lack central control, cellular automata represent a useful tool to model self-organisation, as well as emergent behaviour. It is noted that an agent based model may be depicted as a cellular automata, that is no longer required to be homogeneous, or act in accordance with the same (local) rule-set.

When modelling a complex system, there is a certain freedom in choosing the representation of interactions. For spatially constrained systems consisting of homogeneous components, cellular automata represent a natural modelling choice. Similarly, lattices may be employed to represent a constrained interaction neighbourhood of each component (each component in a  $d$ -dimensional regular cubic lattice has  $2d$  nearest neighbours). Table. 2.2 lists some common topological structures, and tools used to model interactions.

### **2.2.2 Analysing dynamics**

Aside from the significant amount of research in complex networks, few tools exist that have been specifically designed to analyse complex systems. As a result, a range

<b>Topological structure</b>	<b>Tool</b>
Homogeneous and local interaction	Cellular automata / lattice
Spatially distributed	Cellular automata / lattice
High dimensional / random interaction	Random network
High dimensional / structured interaction	Small-world / Scale-free network
High dimensional / ensemble of networks	Multiplex network

**Table 2.2.** Modelling different interaction structures in complex systems.

of domain specific tools are often employed. Although certain tools are better suited to certain circumstances, as summarised in Table. 2.3.

<b>Analysis type</b>	<b>Topological structure</b>
Deterministic non-linear dynamical systems	Small to medium number of components
	Small number of homogeneous component groups
	Weak stochasticity
	Bifurcation and abrupt qualitative transitions
Probabilistic	Large number of components
	Many inhomogeneous component groups
	Weak interactions
	Smooth divergence

**Table 2.3.** Suitable analysis tools based upon properties of a complex system.

Due to the multiplicity of choice that can arise in a complex system, coupled with sensitive path dependence of system trajectories, the variability of outcomes can be viewed probabilistically [Nicolis and Nicolis, 2009]. This stochasticity is innate to the system, rather than imposed exogenously, making a probabilistic description of a complex system useful in extracting information concerning aggregate system behaviour. An alternative approach consists of using (non-linear) dynamical systems to model the behaviour of systems, a benefit of which is the substantial body of mathematical knowledge that exists to describe such models. Aggregate qualitative phenomena, such as phase transitions, are naturally described by the bifurcation theory of dynamical systems. Although, both of the aforementioned approaches have their drawbacks. Probabilistic methods require careful construction to avoid excessive simplification via assuming the independence of events. Analogously, the theory of non-smooth dynamical systems is much less developed than the standard smooth theory. Significant stochastic-

ity may also present problems when utilising the standard theory of dynamical systems, which can often be simplified by resorting to the mean field approximation [Stanley, 1988], or other more recent moment closure methods.

A parsimonious way to capture such dominating features of a complex system is to study the phase transitions, if present. This is analogous to the insights provided by bifurcation analysis of dynamical systems. A phase is interpreted as a region of parameter space in which the macroscopic behaviour of a system is qualitatively similar, and macroscopic variables change smoothly. In contrast, at a phase transition a small variation in control parameters induce qualitative changes in macroscopic system behaviour and macroscopic variables change abruptly, either discontinuously or continuously. In summary, phase transitions can be regarded as demarcating regions of parameter space, known as states, where the system macroscopic behaviour is equivalent.

Many physical systems can be analysed in this way. Water, considered as a thermodynamic system, undergoes phase transitions between solid, liquid, gas and plasma phases, that occur at various temperatures and pressures. So useful is this method of analysing complicated (or complex) systems, that these ideas have been applied in a wide variety of contexts, including population dynamics and ecology, financial markets and climate science [see Scheffer et al., 2009, and references therein].

To ease the burden of attempting to determine the macroscopic phases and associated phase transitions of many-particle systems, a mean field approximation, is often made about the microscopic interaction effects between components. Rather than attempt to capture each and every interaction between components and the effect on the macroscopic system variables, one can allow each component (or groups of components) to experience a mean, or statistically average, effect. The benefit of this transformation is to replace a large number of stochastic interactions, with a smaller number of deterministic ones, making aggregation and the determination of macroscopic variables tractable.

## 2.3 Agent based models in finance

For the basic modelling unit of the economic agent, its behaviour may not be easily and directly described, in a given context. On the contrary, the rules that govern behaviour may be known with much greater certainty or depend upon physical, commercial or monetary constraints that are easily computerised. Moreover, in most situations, economic agents can be assumed to possess a memory of events which may influence their future decisions. Capturing such path-dependency using traditional, or equation-based, techniques is extremely challenging.

For the reasons cited above, there is a persistent interest in agent based models, and especially so in the domain of financial and economic modelling. The analytically tractable, but often highly simplified, traditional economic models rely upon assumptions that render them inappropriate for a range of important situations. For instance, the recent global economic crisis brought to wide attention the dearth of tools available to economists wishing to study economic and financial crises [Trichet, 2010]. Although this point has been made both before [Bouchaud, 2008; Farmer and Foley, 2009] and since [Kirman, 2010a; Gallegati and Kirman, 2012], it remains true that agent based models are an important modelling tool, applicable to situations in which traditional economic and financial models either do not apply, or become impractical to apply. A brief chronology of important financial agent based models is presented below.

- **Kim and Markowitz 1989.** An early agent based model [Kim and Markowitz, 1989], developed with the aim of understanding the Black Monday crash in 1987 during which the largest one-day percentage decline in the Dow Jones index occurred. The agent based model is designed to investigate whether hedging and Constant Proportion Portfolio Insurance (CPPI) strategies could be the cause of the crash via endogenous instability and explosive market volatility. Using a series of simulations in which each agent is one of two possible types: a ‘rebalancer’ or portfolio insurer, it was demonstrated that as the proportion of agents following CPPI strategies increases, asset volatility, and transaction volume, in-

crease.

- **The Santa Fe Artificial Stock Market.** A pioneering agent based model [Arthur et al., 1996] investigating the efficient market hypothesis and agent rationality. The model sets out to test the possibility of allowing heterogeneity in agents' price expectations, whilst remaining economically valid otherwise, and the consequences for market dynamics.
- **Minority Game.** A much-studied game-theoretic agent based model, first posed by Arthur [1994] as the so-called El-Farol Bar Problem and later studied and extended by Challet et al. [2001b]. The model investigates agent choice in the presence of a reward structure - with agents rewarded for selecting the minority decision. Later versions of the model incorporate agent memory, adaptability and strategy-switching.
- **Behavioural heterogeneous agent models.** Brock and Hommes [Brock and Hommes, 1998; Brock et al., 2005] take a behavioural finance approach to agent-based models, and relax a number of traditional economic assumptions, namely that of the representative agent (replaced by agents with heterogeneous beliefs) and rationality (replaced by bounded rationality). Chaotic market dynamics are produced by the models.

A review is carried out by Iori and Porter [2012]. More recently, agent based models have been applied to problems and scenarios relevant to central banks and policy makers, that have historically been analysed using traditional economic modelling tools. These include, the Bank of England agent based model modelling of payment systems [Galbiati and Soramäki, 2008], and the European Commission-backed CRISIS project [Hommes and Iori, 2015], that aims to build a fully functioning agent based economy, are prominent examples.

## 2.4 Integrate-and-fire and pulse coupled oscillators

Pulse coupled oscillators are simple dynamical units that occupy a prominent role in the study of synchronisation. A seminal contribution to this area was made by Mirollo and Strogatz [1990], who proved and generalised a previous conjecture of Peskin [1975] concerning the synchronisation of a general number of deterministic oscillators. Since then, synchronisation on more general topologies have been studied (on complex networks [Timme et al., 2002], and small-world networks [Rothkegel and Lehnertz, 2009]). Arenas et al. [2008] provides a comprehensive overview of this area.

Pulse-coupled integrate-and-fire (IF), oscillators have been used to model various biological processes for some time. Here, the essential characteristics of pulse-coupled IF oscillators are initially presented using a simple model, followed by statements of the original Peskin [1975] model of a cardiac pacemaker, and the associated conjectures concerning the synchronised firing of an ensemble of pulse-coupled IF oscillators. Finally, a sketch of the generalised IF framework used by Mirollo and Strogatz [1990] to prove one of the conjectures of Peskin is given.

The inclusion of this material serves two purposes. First, as an aid to understanding subsequent models of this thesis (chapter 4 and chapter 5) that incorporate a network of (stochastic) pulse-coupled IF oscillators to represent the implicit, and minimalistic, interaction between components of a system. Second, an understanding of the method of proof used by Mirollo and Strogatz [1990] to prove Peskin's conjecture illuminates why their result does not carry over in the case of stochastic pulse-coupled oscillators.

A population of coupled integrate-and-fire oscillators, with state  $x_i$  is characterised by the pulsat coupling, initiated upon an oscillator's phase (also known as potential) reaching a certain threshold, and then resetting back to some rest level. For  $i \neq j \in \{1, 2, \dots, N\}$ , let  $N(i)$  represent the neighbourhood of oscillator  $i$  - that is the

set of all those oscillators directly pulse-coupled to oscillator  $i$

$$\dot{x}_i = \frac{1}{\tau}, \quad x_i(t) \in [0, 1], \quad (2.7)$$

$$\text{if } x_i(t) = 1 \text{ with } j \in N(i) \implies x_j(t^+) = \min(1, x_j(t) + C), \quad x_i(t^+) = 0$$

where  $C$  is the coupling strength (pulse), and when a pulse is sent at some time  $t = t_i$ , the time immediately after a firing of the pulse is  $t = t_i^+$  (see Fig. 2.3).

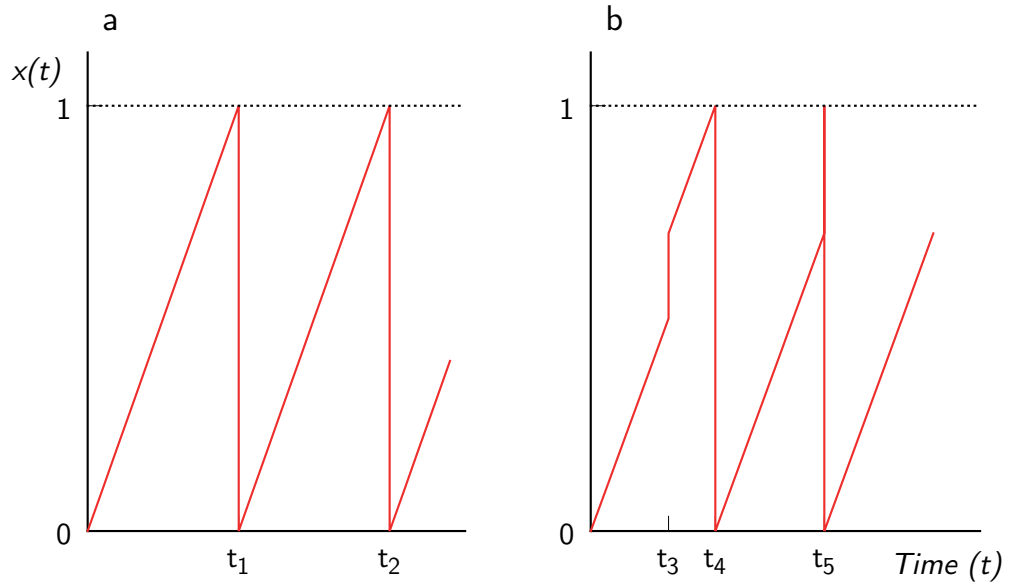


**Figure 2.3.** a) The unperturbed oscillator, given by Eqn. (2.7), reaches threshold  $x(t) = 1$  at times  $t = t_1$  and  $t = t_2$ . b) At  $t = t_3$  the oscillator described by  $x(t)$  experiences a pulse, which brings it closer to threshold, reached at  $t = t_4$ . At  $t = t_5$  the oscillator experiences a pulse which brings it to threshold.

The Peskin [1975] model consists of a globally coupled network of  $N$  identical integrate-and-fire oscillators  $x_i$  (indexed by  $i \in \{1, 2, \dots, N\}$ ), characterised by

$$\dot{x}_i = -\gamma x_i + S_0, \quad x_i(t) \in [0, 1], \quad (2.8)$$

where  $S_0$  and  $\gamma$  are constants. When an oscillator reaches the threshold  $x_i(t) = 1$  it fires and compels all other oscillators to move closer to the threshold, by an amount  $\varepsilon/N > 0$ , which may result in further oscillator firings. Once an oscillator has fired, its state is reset to zero,  $x_i(t^+) = 0$ , where  $t^+$  is the time immediately after firing. Peskin stated the following conjectures:

1. For arbitrary initial conditions, the system approaches a state in which all the oscillators fire in synchrony.
2. Synchronous firing of oscillators is reached even when oscillators are not identical.

In Peskin [1975], the case  $N = 2$  with the product  $\varepsilon\gamma > 0$  small, was proved to result in synchronous firing of oscillators.

In the seminal text, Mirollo and Strogatz [1990] generalised Peskin's ideas, to the case of  $N$  arbitrary oscillators, making use of a phase resetting function,  $f$ , satisfying concavity constraints

$$x_i = f(\phi_i), \quad (2.9)$$

where  $x_i$  is called the *state* of the oscillator;  $f' > 0$  (increasing);  $f'' < 0$  (concave);  $f(0) = 0, f(1) = 1$  and  $\phi_i \in [0, 1]$  is the phase variable with  $\dot{\phi}_i = \frac{1}{T}$ . The conditions on  $f$  guarantee the existence of  $f^{-1}$ . Under this generalised IF model, with pairwise interactions between oscillator- $i$  and oscillator- $j$  given by  $C_{ij}$ , the phase update equations can be written

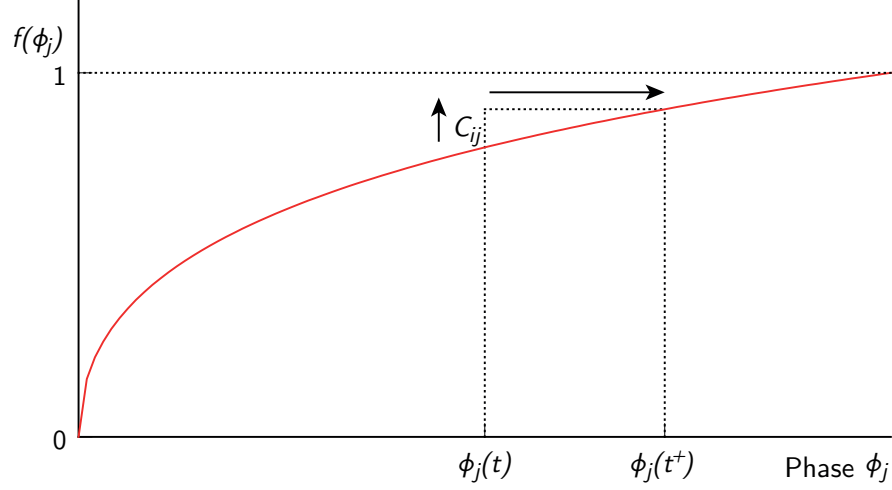
$$\phi_i(t) = 1 \Rightarrow \begin{cases} \phi_i(t^+) = 0 \\ \phi_j(t^+) = \min(1, f^{-1}(f(\phi_j(t)) + C_{ij})). \end{cases} \quad (2.10)$$

Figure. 2.4 shows a diagram of the phase advance of oscillator  $j$  due to pulse-coupling from oscillator  $i$ .

Mirollo and Strogatz [1990] show that the phase resetting function  $f$ , as in Eqn. (2.9), for Peskin's model (Eqn. (2.8)) is given by

$$f(\phi_i) = \frac{1 - e^{-\gamma\phi_i}}{1 - e^{-\gamma}}. \quad (2.11)$$

Using the generalised IF model, Mirollo and Strogatz [1990] show that Peskin's conjecture holds for all  $N$  and all  $\varepsilon, \gamma > 0$ . An outline of the proof in the  $N = 2$  oscillators



**Figure 2.4.** Phase response of an oscillator  $j$  after a pulse from oscillator  $i$ , according to Eqn. (2.10)

case is presented below.

### Synchronisation of IF models.

For the case of two oscillators, assume oscillator  $A$  has reached threshold and fired and has thus reset to zero. Let  $\phi$  be the phase of oscillator  $B$  at this point. Define the *return map*,  $R(\phi)$  as the phase of  $B$  immediately after the next firing of  $A$ , and the *firing map*,  $h(\phi) = f^{-1}(C + f(1 - \phi))$ . Initially the system has a macro state of  $(\phi_A, \phi_B) = (0, \phi)$ . After a time equal to  $1 - \phi$ , oscillator  $B$  will be at threshold, and so will fire and reset to zero. And  $A$  will have a phase of  $h(\phi)$  (see Eqn. (2.10)). The macro state at this point is  $(h(\phi), 0)$ . Clearly after the next firing of  $A$ , which occurs after a time of  $1 - h(\phi)$ , we can deduce that  $B$  phase will be  $h(h(\phi))$ , and the system will have a macro state of  $(0, h(h(\phi)))$ , and so on. From the definition of  $R(\phi)$  (the phase of  $B$  after the next firing of  $A$ ), we see that  $R(\phi) = h(h(\phi))$ . Mirollo and Strogatz [1990] showed that the return map,  $R(\phi)$  has a unique repelling fixed point, by showing that  $h$  has such a fixed point. This means that starting from any arbitrary phase, except the single unique fixed-point of  $R$ , will evolve the system to  $\phi = 0$ , or  $\phi = 1$  implying the system *always* settles to a synchronous regime. Generalising this to the  $N$  oscillator case is based upon similar ideas, and full details can be found in Mirollo and Strogatz [1990].

It is reasonable to consider the values of various quantities, such as time to synchro-

nisation and degree of synchronisation. With this in mind, for a reference oscillator  $j$ , define

$$S = \frac{1}{N} \sum_{i=1}^N \left( 1 - \phi_i(t_j^+) \right), \quad (2.12)$$

which is estimated per cycle of the reference oscillator, that is, each time it resets to  $\phi_j = 0$ . As the system tends towards full synchronisation, all the oscillators ( $i$ ), begin to reset simultaneously, and therefore  $S \rightarrow 1$ . Figure. 2.5 shows a plot of  $S$  against cycle number for a system with  $N = 100$  oscillators, for two different pulse-coupling strengths  $C_1 > C_2$ . Motter et al. [2005] presents further analysis of the time to synchronisation.

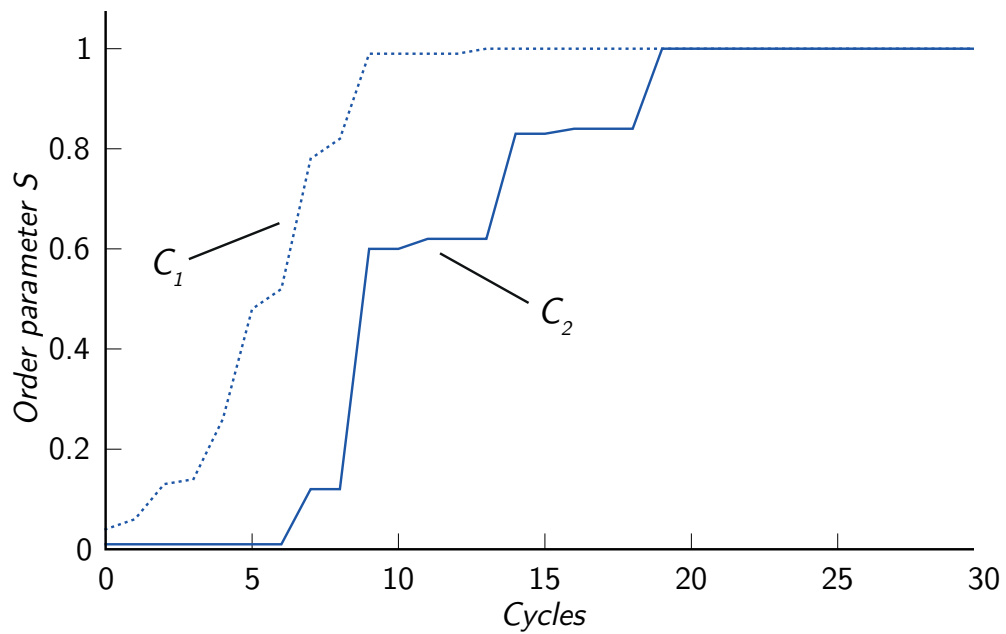


**Figure 2.5.** The quantity  $S$  defined by Equation (2.12) for the cycles of an arbitrary oscillator of a system of  $N = 100$  integrate and fire oscillators plotted for two different pulse strengths,  $C_1 > C_2$ . Coupling is all-to-all and the onset of complete synchronisation is shown to be sooner for the larger pulse magnitude, as expected. The phase-to-state function used is  $x = f(\phi) = \log(1 + (e - 1)\sqrt{\phi})$ , with inverse  $f^{-1}(x) = \left(\frac{e^x - 1}{e - 1}\right)^2$ .

As mentioned above, in chapters 4 and 5, the pulse-coupled oscillators are stochastic, meaning they do not proceed smoothly through the integrate phase (Eqn. 2.7). The synchronisation result of Mirollo and Strogatz [1990], in particular, does not carry over in this case.

## 2.5 Empirical facts of financial asset prices

Certain empirical facts concerning financial asset prices are widely referred to [Chakraborti et al., 2011b] using the phrase *financial stylised facts*, in the same sense as originally expressed in Kaldor [1961]. This phrase is used to describe the collection of simplified, but otherwise non-trivial, observations and generalisations about aspects of the financial market, and in particular the nature of asset prices. Typically, such facts are empirical in nature, and are unaccounted for by standard economic theory. Here, we collect the facts and observations most relevant to this thesis, for future reference. Much of this discussion will be brief, as excellent references exist [Chakraborti et al., 2011b; Cont, 2007]

### 2.5.1 Notation

Throughout this thesis the use of log refers to the natural logarithm, of base  $e$ . When a logarithm to any other base is required, it will be explicitly stated. Standard probability and statistical notation is used throughout, such as that used by Feller [1968]. Let  $P_t$  be the price of a traded asset - such as a stock, bond or commodity and let the (logarithmic) price return,  $r_{t,\Delta t}$  over some interval  $\Delta t$  starting at time  $t$  is given by

$$r_{t,\Delta t} = \log P_{t+\Delta t} - \log P_t = \log \left( \frac{P_{t+\Delta t}}{P_t} \right). \quad (2.13)$$

The volatility of the returns,  $\sigma$  when returns are considered to be a random variable is

$$\sigma(\Delta t) = \sqrt{\text{Var}(r_{t,\Delta t})}, \quad (2.14)$$

and the estimate, or measurement, from a sample is

$$\sigma(\Delta t) = \text{St.dev} \left\{ \frac{P_{t_1+\Delta t}}{P_{t_1}}, \frac{P_{t_2+\Delta t}}{P_{t_2}}, \dots, \frac{P_{t_n+\Delta t}}{P_{t_n}} \right\}, \quad (2.15)$$

When  $R$  is a random variable representing the returns of some asset, the tails of the probability distributions are the regions defined by (typically large  $x > 0$  and large

$y < 0$ ),

$$\mathbb{P}(R > x) \text{ and } \mathbb{P}(R < y). \quad (2.16)$$

The tail probability decay can be captured using generic functional forms,  $\mathbb{P}(R > x) \sim F(x)$ , and categorised into three classes

$$F(x) = e^{-g(x)} \quad \text{exponential decay} \quad (2.17)$$

$$F(x) = x^{-\alpha+1} \quad \text{power law decay} \quad (2.18)$$

$$F(x) = x^{-\alpha} e^{-h(x)} \quad \text{exponentially truncated power law decay,} \quad (2.19)$$

where  $\alpha > -1$  is the power law exponent, and  $g(x) > 0, h(x) > 0$  are regular functions. Capturing accurate behaviour of extreme (either positive or negative) asset returns is of central importance to financial risk managers, investors and other financial market participants, and as a result the specification, and identification, of tail probabilities for asset return distributions has received much attention (see Chakraborti et al. [2011b] for a review). This topic will be revisited in the section 2.5.2.

Differentiating Eqn. (2.18) gives the generic probability density for a (continuous) power law distribution (up to scale) as  $f(x) = x^{-\alpha}$ . Furthermore, power laws admit scale-invariance, so that for  $\lambda > 0$

$$f(x) = x^{-\alpha} \implies f(\lambda x) = \lambda^{-\alpha} f(x). \quad (2.20)$$

### **Black-Scholes-Merton model**

In chapter 5, consideration is given to the pricing of a financial asset. In order to provide some contextual background and motivation to the methodology employed in later chapters, the Black-Scholes-Merton (BSM) model for option pricing, presented in Black and Scholes [1973]; Merton [1973] is stated here for reference.

We start by modelling the price at time  $t$  of a financial asset (hereafter and without loss of generality an equity stock),  $P_t$  as a geometric Brownian motion. That is,  $P_t$  solves

the stochastic differential equation

$$dP_t = \mu P_t dt + \sigma P_t dW_t, \quad \mu, \sigma \in \mathbb{R}, \sigma > 0, \quad (2.21)$$

where  $W_t$  is a standard Brownian motion with  $W_0 = 0$ ,  $\mu$  is known as the drift, and  $\sigma$  the volatility. Solving this equation reveals,

$$P_t = P_0 \exp \left( \left( \mu - \frac{\sigma^2}{2} \right) t + \sigma W_t \right), \quad (2.22)$$

for some initial price  $P_0$ . An important consequence under this framework, is that log-returns,  $\log(P_t/P_0)$ , are normally distributed since  $W_t \sim N(0, t)$ , which does not accommodate so-called fat-tails (or excess kurtosis). Indeed, the tail probability decay is exponential, as characterised by Eqn. (2.17). As will be discussed in the following section, such tail behaviour is at odds with what is observed in real financial markets (where return distributions do generally exhibit excess kurtosis over a range of time horizons). The inability of geometric Brownian motion to capture realistic return distributions is one motivating factor for the financial market model presented in chapter 5 which generates power-law tail probability behaviour, characterised by Eqn. (2.18).

A European option is a financial asset that endows the buyer of the option the right (but not the obligation) to purchase (known as a call option) or sell (known as a put option) the underlying stock at a fixed future date (the expiry) in  $T$  years, at some predetermined price known as the strike price,  $K$ . Let  $C = C(P, t)$  denote the time  $t$  price of a European call option with expiry  $T$  and strike price  $K$ . The stock price,  $P$ , is written without explicit time dependence, for notational ease. By employing the technical probabilistic tools of Itô's lemma and the Girsanov change of measure theorem, it is possible to derive the Black-Scholes-Merton (BSM) equation (Eqn. (2.23)) by forming a so-called risk-free portfolio (attracting the risk-free interest rate  $r$ ) that replicates the

value of a call option,  $C$ , from dynamic holdings in cash and the underlying stock.

$$\text{BSM equation:} \quad \frac{\partial C}{\partial t} + \frac{1}{2}\sigma^2 P^2 \frac{\partial^2 C}{\partial P^2} + rP \frac{\partial C}{\partial P} - rC = 0. \quad (2.23)$$

$$\text{Call option boundary conditions:} \quad C(P, T) = \max(P_T - K, 0), \quad (2.24)$$

$$\lim_{P \rightarrow 0} C(P, t) = 0, \quad \lim_{P \rightarrow \infty} C(P, t)/P = 1.$$

$$\text{BSM formula:} \quad C(P, t) = \Phi(d_1)P - \Phi(d_2)Ke^{-r(T-t)}, \quad (2.25)$$

See Karatzas and Shreve [1991] for probabilistic details and a thorough derivation of Eqn. (2.23). The celebrated Black-Scholes-Merton formula for finding the time  $t$  price of a European call option (Eqn. (2.25)), is obtained by solving Eqn. (2.23) for the particular ‘payoff’ and boundary values in Eqn. (2.24). It is of particular note that the BSM formula in Eqn. (2.25) contains a constant volatility parameter  $\sigma$ . As will be discussed in the following section, option prices observed in markets imply that the BSM volatility parameter (when option prices are used to infer the volatility parameter  $\sigma$ , the result is known as implied volatility) varies non-linearly with strike price for a given expiry. In particular, the implied volatility is generally higher at very low and very high strike prices, compared to when the strike price is very close to the current stock price; a phenomenon known as the volatility smile. The financial market model presented in chapter 5 is demonstrated to produce ‘fat-tailed’ return distributions for a range of parameters, and recovers plausible market option prices (tested on 1-month expiry European call options), from the (simulated) return distribution of the underlying asset.

The variables and parameters relevant to Eqns. (2.23)-(2.25) are collected here for ease

of reference

$C(P, t)$  is the value of a European call option.

$P$  is the price of the underlying stock.

$\Phi$  the cumulative standard normal distribution function.

$\sigma$  is the volatility parameter of the Brownian motion describing the price process.

$T$  is the expiry of the option.

$r$  is the short-term interest rate.

$K$  is the strike price of the option.

$$d_1 = \frac{1}{\sigma\sqrt{T-t}} \left( \log \frac{P}{K} + (T-t) \left( r + \frac{\sigma^2}{2} \right) \right)$$

$$d_2 = d_1 - \sigma\sqrt{T-t}$$

$t$  time.

For a review and derivation of the BSM formula and equation, see Hull [2011].

## 2.5.2 A brief historical perspective of stylised facts

Standard deviation, the second central moment and volatility are different names for the same statistical property: the dispersion of observations around the average observation. Within finance, volatility is one of the most important metrics used to characterise the distribution of price returns. The standard financial model, different aspects of which originate from the amalgam of work by Friedman, Samuelson and Fama [Friedman, 1953; Samuelson, 1965; Fama, 1970], considers asset price returns to be Gaussian (normally distributed), with zero-mean and constant volatility.

- Observation 1: *The level of volatility of financial returns is unexplained by other fundamental macroeconomic factors.*

The magnitude of volatility was first seriously investigated by Shiller [1981], who demonstrated that the volatility of financial stock returns is not explained by changes in the rationally expected dividend stream of a stock. Whereas the standard financial

model asserts that returns of assets reflect the arrival of new information and incorporated into forecasts of future dividends.

- Observation 2: *The distribution of price returns is non-Gaussian, and in particular exhibits positive excess kurtosis.*

The distribution of price returns for virtually all financial securities (stocks, bonds, exchange rates) have been documented as displaying positive excess kurtosis [Chakraborti et al., 2011a]. This implies that observations in the tails of the distribution (either very negative returns or very positive returns) are more likely to occur than when modelled using a Gaussian random variable (which has zero excess kurtosis). The seminal contribution to the non-Gaussian nature of financial returns was made by Mandelbrot [1963], and further refined by Gopikrishnan et al. [1999]; Gabaix et al. [2003] who present evidence suggesting such returns are better described by power law distributions.

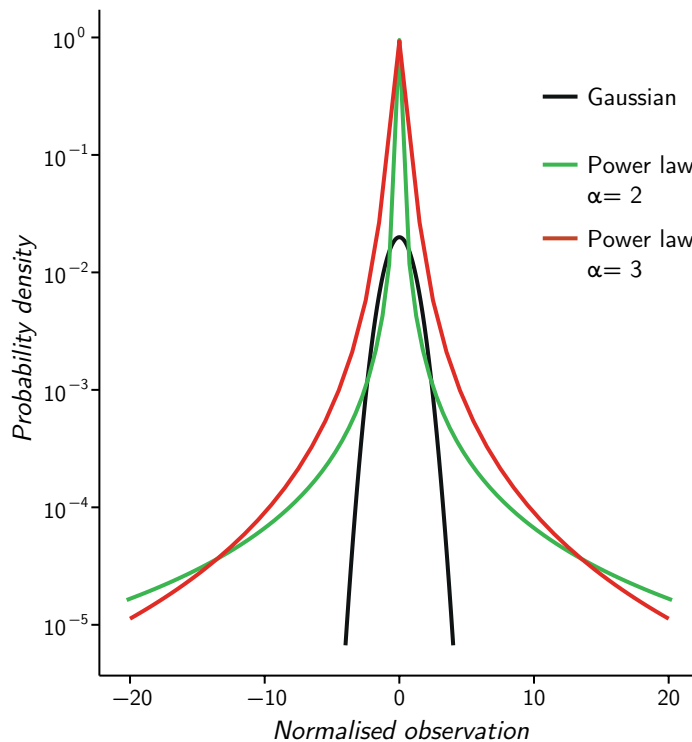


**Figure 2.6.** Linear-log plot showing the comparison of power law densities, with exponent  $\alpha$ , compared to standard Gaussian.

- Observation 3: *The time-series of financial return exhibit intermittent behaviour, and auto-correlated volatility.*

Volatility clustering, can be summarised with the maxim: large increments in price tend to follow similarly large increments, while small increments in price tend to follow similarly small price increments. This implies that while (raw) returns may be serially uncorrelated, they are not statistically independent as periods of large returns (positive or negative) tend to cluster together, as reported in Fig. 2.7. This statement can be formalised mathematically by examining the time series of the magnitude, or absolute value, of price returns for positive serial correlation [Ding et al., 1993]. As a function of the time-lag  $L$  and price return over the interval  $d$ , the autocorrelated volatility  $C(L, d)$  may be written in terms of the returns time series  $r$  as defined by Eqn. (2.13)

$$C(L, d) = \text{Corr}(|r_{t+L,d}|, |r_{t,d}|). \quad (2.26)$$

Volatility is said to possess long memory [Baillie, 1996; Zumbach, 2004] when autocorrelation remains positive and, in particular, decays hyperbolically over large time-lags. Formally,

$$C(L, d) \sim AL^\gamma \text{ as } L \rightarrow \infty, \quad A > 0, \gamma < 0. \quad (2.27)$$

Research into the causes of volatility clustering remains active [Thurner et al., 2012], particularly so in the search for behavioural explanations [Feng et al., 2012].

The identification of volatility persistence in financial data has given rise to a class of models known as generalised auto-regressive conditional heteroskedasticity (GARCH) models, introduced in Bollerslev [1986], which remain popular with economists (see Shin Kim et al. [2010], for a recent application to option pricing).

- Observation 4: *The volatility smile: the Black-Scholes implied volatility for equity derivatives of expiry  $T$  is a non-linear as a function of strike price.*

The standard model of pricing European-style derivatives was devised in Black and Scholes [1973]; Merton [1973], and continues to be a reference model for the valuation of such securities today. The key result of Black, Scholes and Merton is that under the assumption of a Brownian motion representing the stock price process, the value

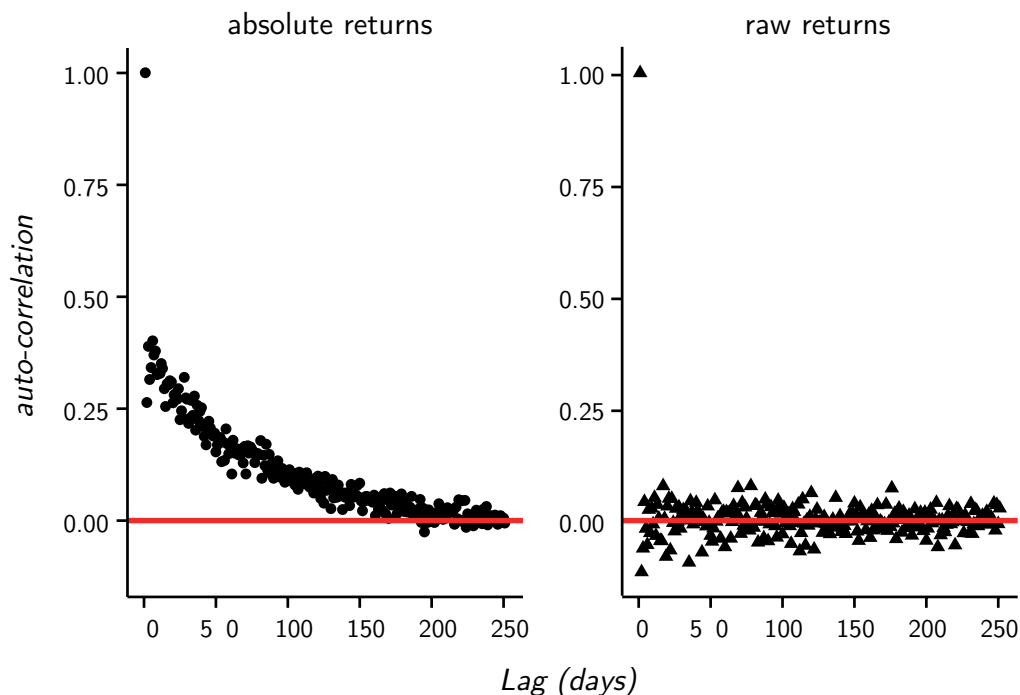


**Figure 2.7.** Volatility clustering of daily returns of the S & P 500 index. Significant auto-correlation persists for approximately 200 days, whereas raw returns exhibit no correlation. The data consists of daily data 2006 to 2014.

of a derivative can be found as a closed-form formula, Eqn.(2.25). Since one of the parameters in this formula is the volatility of the stock-price process, it can be inferred (implied) from market prices for a derivatives, by numerically inverting the Black-Scholes formula given by Eqn. (2.25).

Since the global crash of 1987, the implied volatility for most options exhibit a persistent non-linear shape, with implied volatility generally higher for strike prices both much less, and much greater, than the current market price (see Fig. 2.8). This persists for all maturities,  $T$ . One hypothesis for this feature is that that underlying assumption of a constant volatility Brownian motion process underestimates the frequency of tail events. Thus, volatility, and hence market prices, deviate from the Black-Scholes model.

In relation to the observed implied volatility smile, various models have been offered as alternatives to the underlying Brownian motion and Black-Scholes option pricing framework. In particular, stochastic volatility models, such as the seminal Heston [1993] model and more recently multivariate models [Muhle-Karbe et al., 2012; Da

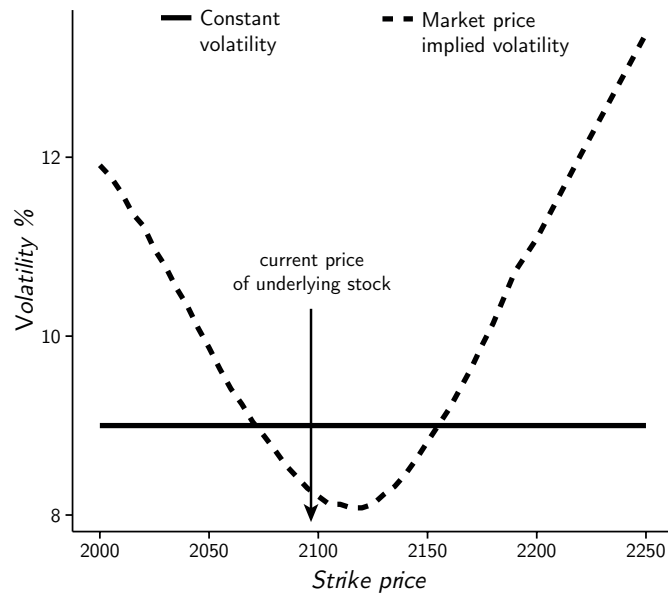


**Figure 2.8.** Volatility smile as of 26 November 2014 for options on the S & P500 index showing significant skew either side of the current market price.

Fonseca et al., 2014]. In chapter 5, another class of stochastic volatility models, known as multifractal models [Bacry et al., 2001; 2012], are discussed in the context of the new model presented there. Such models are able to reproduce so-called memory patterns often seen in asset return volatility.

Other popular class of models used in option pricing or asset price modelling include jump-diffusion models [Merton, 1976; Cai and Kou, 2011], asset pricing models employing Lévy processes [Brody et al., 2012], and non-Markovian option pricing models based upon GARCH dynamics [Heston and Nandi, 2000]. In addition to constructing option pricing models, researchers have developed models that focus specifically on modelled the volatility smile [Yan, 2011; Liu et al., 2014].

This chapter has described the mathematical background of the main modelling tools used throughout this thesis. The terminology and basic theory of networks have been introduced, due to the important role they play in analysing complex systems. In describing typical features of a complex system an overview of the various modelling approaches has been provided, and in particular, the circumstances in which a dynamical systems approach (the natural setting for bifurcation analysis) and a probabilistic approach, may yield useful results, are compared (see Table. 2.2). An important area of

analysis not fully covered here (but used in later chapters) is the combinatorial nature of systems with large numbers of interacting elements. In such systems, even rudimentary stochasticity can result in a wide array of different aggregate outcomes, reflecting the multiplicity of system states. Finally, an account of observed financial stylised facts has been provided and, importantly, how these remain unaccounted for by traditional economic and mathematical modelling. The next chapter presents a detailed analysis of a traditional, or equilibrium, economic model upon which much of modern mathematical financial analysis is based.

# **Chapter 3**

## **Standard economic theory and a socio-economic perspective**

### **3.1 Classical economic modelling: Dynamic stochastic general equilibrium models**

The prevalence of dynamic stochastic general equilibrium (DSGE) models used throughout major policy institutions is indisputable and, until recently, uncontroversial. Since the seminal work of Kydland and Prescott [1982] and Rotemberg and Woodford [1997], DSGE-based tools have successfully moved from academia to policy institutions, at an increasing pace over the last decade. A partial list of institutions known to incorporate DSGE modelling into forecasting, or policy, analysis is: the US Federal Reserve, International Monetary Fund, Bank of England, Bank of Canada, European Central Bank, Norges Bank, Sveriges Riksbank, as well as the central banks of Iceland, Peru, Chile, Nigeria and India. Tovar [2009] provides an overview of the use of DSGE models within central banks.

## 3.2 What are Dynamic Stochastic General Equilibrium models?

A DSGE model is an economic model that aims to describe aggregate economic variables (such as inflation, consumption, etc.) as a consequence of interactions between different agents within an economy (such as households and firms). As the name implies, such DSGE models are general equilibrium in nature, meaning that markets clear in each period. More formally, DSGE models attempt to describe aggregate economic behaviour via the (microeconomic) decisions of agents. In the economic lexicon, DSGE models are said to be microfounded, in contrast to the earlier and more traditional empirical forecasting models [see Lubik and Surico, 2010, on the Lucas critique] that are based upon observed historical relationships between macroeconomic variables. DSGE models derive their dynamism from considering agents as time-varying decision makers with the ability to formulate expectations of future outcomes, and to apply these to current decisions. Furthermore, the DSGE methodology considers the economy subject to fluctuations, and this is captured by taking into account exogenous driving processes, or so-called stochastic shocks. In addition to identifying which agents to include in a model, the modeller must specify an agents' preferences and technological endowments. Preferences determine the objectives of an agent (e.g. households as utility maximiser), and technology determines the productivity of an agent (e.g. how effective a firm is at using capital and labour to produce goods). Furthermore, constraints governing economic interaction between agents must also be specified (e.g. any market-clearing procedures and budget constraints). In this chapter an analysis of a DSGE model, and its assumptions, is presented.

In summary, DSGE models attempt to model the economy as a coherent and interacting whole, by identifying relevant agents and specifying their associated preferences, technology and interactions. Macroeconomic interaction equations and equilibrium conditions are then formulated from the aggregation of agents' microeconomic actions. Very often the rational expectations hypothesis, introduced by Muth [1961], is invoked

in empirical DSGE models as a simplifying mechanism for agents that are required to solve inter-temporal optimisations (dynamic utility maximisation) associated with their preferences. Moreover, the aggregation of agents' microeconomic decisions is simplified via the assumption of agent homogeneity, leading to the so-called representative agent simplification.

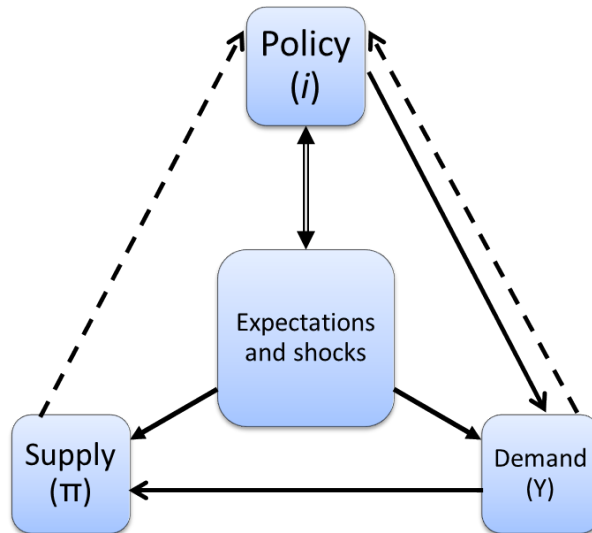


**Figure 3.1.** A diagram showing the relations between the basic components of a simple DSGE model. Economic variables belonging to a block are shown in brackets. Solid lines depict the direction of influence and dashed lines represent feedback.

### 3.2.1 A basic New-Keynesian DSGE model

Deciding whether a specific agent type, or exogenous shock, is to be included in a model is a judgement made by the economist constructing the model. In deciding these, the economist is likely to consider how relevant the activity of that agent is to the economic variables under analysis, and the potential explanatory power of the shock. With that said, many contemporary empirical DSGE models used for monetary policy analysis share a common framework based on the basic New-Keynesian model, or a variation thereof. A schematic of the interrelations between economic blocks of a simple model is shown in Fig. 3.1. The economic blocks (demand, supply and policy) provide a context in which the model equations are constructed. In the most simplistic case, each block can be associated with a single economic variable whilst links between

blocks represent parameter dependencies.

A basic DSGE model is derived for completeness, and the details can be found in appendix A.

### **3.2.2 Criticism of DSGE models and methodology**

The DSGE framework is said to lack realism due of the ubiquitous assumption of homogeneous (representative) agents that exercise rational expectations [see Milani and Rajbhandari, 2012]. Furthermore, modelling components used in early DSGE models often excluded financial sectors, international capital flows and economic sectors, and financial intermediaries (such as banks and loan providers). By excluding such items, the model is unable to capture the influence of shocks arising from these institutions and as a result, the impact such sectors may have on macroeconomic variables go untested. The inclusion of such items is becoming more frequent, and especially so post-financial crisis [Gerali et al., 2010]. Furthermore, the forecasting ability of DSGE models have been questioned [see Edge and Gürkaynak, 2010; Wickens, 2012].

Relevant to this thesis, the period post financial crisis has seen an increasing number of researchers and policy makers, both outside and within the economic academic community, dispute the benefits of such models [Arthur, 2014; Holt et al., 2011]. A central argument of this thesis is that while the intention to formulate a macroscopic model based upon the interaction of microscopic economic elements can yield useful results - the traditional modelling tools of economics require adverse simplifications and assumptions in order to yield tractable problems. Alternatively, a modelling approach based upon complex systems can allow for aggregate system states to emerge, rather than be predetermined by modelling constraints.

The limitation of realistic macroscopic system states produced by traditional analysis such as DSGE modelling, coupled with the central role such modelling plays in research programmes and policy making institutions, has resulted in negative feedback where the observed phenomena, in financial markets for instance, is judged against a

benchmark constructed from an economic model, rather than a firm understanding of the intrinsic dynamics underlying such systems. In the absence of a firm understanding of the dynamics of economic systems, a scientific observer might argue for an analysis driven by data, where this is available. Frankfurter and McGoun [2001] argue that while observed anomalies typically force a re-evaluation of a true scientific model, this has not been the case for traditional economic modelling, where “anomaly” appears synonymous with lacking scholarly content.

### **3.3 A socio-economic perspective**

The understanding of socio-economic systems is an important aim of social scientists (Helbing et al. [2011], Bouchaud [2013]). Collective human behaviour inherent in socio-economic systems includes many interesting and complex phenomena. For instance, the dynamics of crowds, mass panics and social movements [Shiwakoti and Sarvi, 2013] are examples of collective behaviour that cannot be understood as naïve aggregation of the interacting parts. In this regard, socio-economic systems present emergent behaviour, and represent a canonical example of a complex system.

In particular, herd behaviour (or herding) arises naturally (though not always expectedly) in a range of situations, and of particular interest to this study, has been discussed in the context of financial markets for some time [Kirman, 2010b]. Indeed, forums such as financial markets may even exacerbate herding tendencies [Helbing et al., 2011].

An analysis of the dynamic stochastic general equilibrium model, and its modelling assumptions, (in appendix A) reveals that some modern economic models have deviated from such considerations (by effectively making emergent behaviour inadmissible either as an input or output of the model) [Stiglitz, 2011]. While this thesis is not concerned about the motivations for this, it is useful to know in a modelling context, and places the comments of Trichet [2010] (I surmise), in their intended context.

In this chapter I argue that if tools based in complex system science are to aid economic policy makers, incorporating herding should be seen a priority. To achieve this, herding in financial markets needs to be seen - by financial market participants and policy

makers - as a source of systemic risk, rather than as an anomaly or market irregularity. The latter interpretation represents an intellectual dead-end, while the former frames herd behaviour as a natural consequence of collective behaviour, and encourages intellectual investigation. Secondly, I discuss a selection of existing agent-based herding models and motivate the models developed in this thesis.

### **3.3.1 Herding as a contributor to systemic risk**

As discussed in chapter 1, herd behaviour has been seen as responsible for (or played a significant part in) a number of financial crashes and asset bubbles [Sornette, 2003], and most recently the financial crisis [The Financial Crisis Inquiry Commission, 2011]. Although, due to the opacity of financial markets, and the assumed independence amongst market participants, the exact mechanisms that cause this are not fully understood. Herd behaviour in asset markets is not the only source of systemic risk. Historically, the prototypical model of systemic risk is that of a ‘bank run’, which describes the near simultaneous withdrawal of bank funds by depositors [Allen and Gale, 1998]; the use of leverage and complex derivatives has been cited as a potential source of market instability [Thurner and Poledna, 2013; Battiston et al., 2013], and systematic erroneous credit rating and asset price modelling decisions - such as not taking account of interconnectedness or relevant market factors in structural models [Eisenberg and Noe, 2001]. While there is no consensus on the exact definition of systemic risk as applied to financial markets, a significant volume of recent research has focussed on systemic risk associated with institutions; such as research concerning the default of banks, and interbank network stability (Haldane [2009], Gai and Kapadia [2010], Roukny et al. [2013], Anand et al. [2012]). While such research is immensely important, systemic risks can arise, or manifest, via other avenues as the most recent crisis demonstrates. By adopting the definition of systemic risk of Helbing [2012], herding can be categorised as systemic risk, via its ability to ‘trigger unexpected large-scale changes of a system or imply uncontrollable large-scale threats to it’ Helbing [2012].

### 3.3.2 Classes of agent-based models of herding

It has been observed that a colony of ants, when presented with two identical food sources, will not divide equally and utilise both sources of food - but a majority of them will herd on one source only. Moreover, the majority group of ants will, at random times, decide to herd on the other food source, before switching back. In a seminal article, Kirman [1993] presented a 1-step 2-state Markov switching model to describe this observed behaviour of ants. Kirman's model has been used as the basis for a plethora [see Alfarano and Milaković, 2009, for a discussion of this] of agent-based financial market models, (the paradigmatic example being Lux and Marchesi [1999]), with food-switching replaced with strategy-switching among heterogeneous agents. As this model is central to many of the agent-based models in the literature, a brief description is included here.

#### **Kirman's ant model - financial interpretation**

Assume a population of  $N$  traders, divided into two groups,  $A$  and  $B$  of size  $n$  and  $N - n$  respectively. The groups of traders are usually given labels such as chartists and fundamentalist. Then at each time step, the size of population  $A$  transitions according to

$$P(n \rightarrow n + 1) = (N - n) \left( \varepsilon + \delta \frac{n}{N} \right) \quad (3.1)$$

$$P(n \rightarrow n - 1) = n \left( \varepsilon + \delta \frac{N - n}{N} \right), \quad (3.2)$$

where  $\varepsilon$  represents random switches between groups, and  $\delta$  represents the herding effect. For  $N$  large, Kirman showed that this Markov chain has an equilibrium beta distribution [Kirman, 1993].

### 3.3.3 Lux's categorisation of behavioural agent-based models

Here, the standard categorisation of agent-based models, proposed by Lux [2006], is stated and example models from each category are listed. The key point of doing this is to demonstrate that agent-based models represent an important modelling paradigm

for financial markets, and to highlight the difficulty in constructing coherent financial models capable of generating realistic dynamics over a range of parameters. While much research has been published on producing agent-based, or herding based models of financial markets, many suffer from the lack of generality imposed by a restriction on the parameters of the model.

- **Dynamical systems with attractor switching.** Models of this type consist of heterogeneous agents, with a modified notion of economic rationality, such as adaptive or bounded. Communication between agents takes place globally, rather than locally reflecting in a realistic way how market participants limit direct interaction. A prototypical example is provided in Hommes [2006].
- **Statistical physics critical systems.** Models of this type utilise some aspect of an already well-known critical phenomena, such as percolation [Grimmett, 1999], which critically transitions between a connected macro state and an unconnected state (or vice-versa). Such models generally require parameter tuning to arrive at the critical dynamics. Moreover, the agent interaction structure is typically local, contravening how real markets operate. Examples include Cont and Bouchaud [2000]; Xiao and Wang [2012].
- **Herding models.** Such models directly include social interaction, and herd effects via local interaction. Critical dynamics result from finite size effects only (an agent population of size  $N$ ), formalised by Alfarano and Milaković [2009] as the ‘large  $N$  effect’, implying model dynamics revert to Gaussian as  $N$  increases. Prototypical examples are Alfarano and Lux [2007] and Kirman [1993].

Recent research using behavioural models have revealed important insights into financial markets. Kononovicius and Gontis [2014] reveal how herding may be controlled by a small number of individuals who are immune to herding effects. In chapter 5, I return to this point and detail how a hierarchy of herding may occur, and its relation to volatility clustering observed in financial markets.

In the next chapter, I present a new model of cascade on a stochastic pulse model, that has been constructed with the shortcomings of the above models in mind. In subsequent chapters this new model is further refined and developed into a financial market model, that does not rely on strategy switching, scales correctly with  $N$ , and a simple mechanism will be proposed that allows the model to be considered self-organising.

## **Chapter 4**

# **Stochastic pulse-coupled network: A threshold model of emergent behaviour**

In chapter 3, it was demonstrated that the standard economic framework of dynamic stochastic general equilibrium (DSGE) models rely upon a collection of assumptions and constraints that restrict agent behaviour. In particular, agents are endowed with so-called rational expectations that enforce internal model-consistent agent behaviour, and presupposes the existence of certain agent equilibria. As a direct result, DSGE models lack the ability to accommodate non-trivial emergent behaviour, and rely upon exogenous inputs (so-called shocks) to determine model dynamics. In chapter 3 section 3, examples of socio-economic systems exhibiting complex endogenous phenomena are provided, and a selection of behavioural agent-based models are discussed in order to demonstrate the viability of agent-based models as a modelling paradigm for emergent phenomena. This chapter acts a mathematical prelude to the presentation of a new financial market model incorporating herd behaviour in chapter 5, that aims to avoid some of the aforementioned weaknesses in standard economic modelling, and address some of the aforementioned shortcomings of existing agent-based models of financial markets.

In particular, this chapter presents a new model consisting of a network of stochastic pulse-coupled oscillators, and is systematically analysed using both numerical simulation and a mean field dynamical system [Wray and Bishop, 2014]. The proposed model, an extension of the neural network model presented by DeVille and Peskin [2008] (DP model), accounts for oscillators sending and receiving pulses of (binary) opposing influence. Pulse-coupling between oscillators is modelled as taking place on an all-to-all network where incoming pulses, from firing oscillators, are successfully received with coupling probability  $0 < p < 1$ , and ignored otherwise. The oscillators in the model interact in such a way that a pulse from a single firing oscillator probabilistically, and instantaneously, induces other oscillators to fire, which may result in a cascade of oscillator firings. Throughout this chapter, and the next, the cascade size is to be taken as the number of firing oscillators during a single pulse-coupling event.

For systems consisting of a finite number of oscillators, a critical range of coupling probability,  $p$ , is found that separates two distinct system regimes: asynchronous (corresponding to the case when all cascade sizes are small) and synchronous (when large cascade sizes appear). In this chapter, the use of the terms ‘synchronous’ and ‘asynchronous’ adheres to the usage of DeVille and Peskin [2008], and refers to the moments at which pulse-coupling takes place. If pulse-coupling results in more than one oscillator firing at a single instant, then those oscillators fire simultaneously (since pulse-coupling occurs instantaneously). At the system (macroscopic) level, when the dynamics consists of repeated simultaneous oscillator firings, then the system is said to be in the synchronous regime, and in the asynchronous regime otherwise.

Numerical confirmation of asynchronous and synchronous regimes of the stochastic system is presented, along with identification of the sparse-coupled fixed point of the associated mean field system. Furthermore, a closed-form expression for the cascade size of a low-dimensional mean field system is derived. The detailed specification of the model can be found in appendix B. Although this material is not standard bookwork, it is included as an appendix to aid the readability of the text.

While the extended model is not intended to serve the original problem-domain of neuronal dynamics it is, however, relevant for a slightly different class of problem concerning interacting elements subject to recurring opposing influences. This chapter serves as a prelude to the next, in which these ideas are formulated into a stylised model of a financial market.

## **4.1 Model motivation: Cascade phenomenon in the presence of opposing influences**

For many interconnected systems the propagation of constituent failure can represent a serious, and often irreversible, risk. Examples include corporate insolvencies in the real economy [Roukny et al., 2013; Tedeschi et al., 2012b; Arinaminpathy et al., 2012; Haldane and May, 2011], blackouts caused by mechanical failures in power grids [Dobson et al., 2007] and the spreading of fatal diseases [Kermack and McKendrick, 1932; Brauer, 1990]. When the propagation of failures amongst system components is fast, relative to the system lifetime, it is natural to characterise this spreading as a cascade. As a result, much research has focused on understanding the important phenomenon of cascades of an irreversible, or absorbing, state in networks [Watts, 2002; Crucitti et al., 2004; Gleeson and Cahalane, 2007; Hackett et al., 2011].

In contrast, many other systems exhibit persistent, yet transient, cascades of a specific non-absorbing state, interspersed with disordered behaviour. Such a system is said to display both asynchronous and synchronous behaviour. Examples of systems displaying bursts of synchronised behaviour include: neuronal activity in the brain during both normal, and abnormal, phases [Salinas and Sejnowski, 2001; Beggs, 2013; Vladimirski et al., 2008], and financial markets, where recurrent cascades of buying and selling may result in crashes and bubbles [Lux, 1995; Abreu and Brunnermeier, 2003; Sornette and Johansen, 1997; Khandani and Lo, 2011]. In the latter case, agents exerting both buying and selling influences are necessary for the proper functioning of markets, although large imbalances, especially over short timescales, can result in volatile price

dynamics [Easley et al., 2011]. In these systems, understanding cascades in a one-off, or static, context only provides partial understanding of the macroscopic behaviour. In this chapter, we investigate how transient synchronous behaviour, characterised by large cascades of state adoption, can arise as a result of many smaller cascades.

To model systems in which transient cascades of two distinct and opposing influences can form, the neural network DP model [DeVille and Peskin, 2012; DeVille et al., 2010; DeVille and Peskin, 2008] is extended, first, to allow each integrate-and-fire (IF) oscillator [Kuramoto, 1991; Maass and Bishop, 2001] to produce both positive and negative pulses that compel coupled oscillators to move closer to an upper or lower boundary (represented by distinct firing states), respectively. And second, by modelling the state variable as a symmetric diffusion process - that describes the oscillators' behaviour during the integrate phase.

Although deterministic pulse-coupled oscillator models have been successfully applied to a wide range of physiological and biological processes [Mirollo and Strogatz, 1990; Guardiola et al., 2000; Timme et al., 2002], for systems that exhibit multiple firing thresholds and uncertain state dynamics, stochastic models may be more appropriate.

## 4.2 Model description

The DP model of DeVille and Peskin [2008] describes the situation where the state of integrate-and-fire oscillators proceed monotonically towards a single firing threshold during the integrate phase. In the extended model presented here, oscillators may proceed towards, and recede away from, two firing thresholds during the integrate phase and, moreover, each firing threshold induces opposing pulse coupling (coupling originating from either firing state compels oscillators to move closer to that particular firing state and farther from the other firing state). The mechanics of the resulting cascades remains the same between both models (oscillators may be induced into a firing state instantaneously upon receiving pulse-coupling).

The model consists of  $N$  identical discrete-state IF oscillators,  $u$ , represented as the vertices of an all-to-all graph, with parameters  $K$  and  $p$  determining the number of states

and representing the coupling probability, respectively. Given  $K \geq 1$ , each oscillator is characterised by its discretised state variable

$$\theta_u(t) \in \{0, 1, \dots, 2K\}, \quad (4.1)$$

at time  $t$ . The system alternates between a diffusion phase (also called the integrate phase), during which each oscillator independently transitions between its two nearest-neighbour states, according to an unbiased continuous time one-dimensional random walk of step size 1, and an instantaneous cascade phase. The cascade phase begins when, at some time  $\tau$ , an oscillator first transitions into one of states 0 or  $2K$  (the firing states), and fires a negative (state 0), or positive (state  $2K$ ) pulse. The pulse is either received independently by the other nodes yet to fire, with probability  $p$ , or ignored, with probability  $(1 - p)$ . If an oscillator receives a positive pulse, its state is immediately increased by 1. Similarly, its state is immediately decreased by 1 upon receiving a negative pulse. A firing oscillator remains immune to all influences until the cascade phase ends, whereupon it is reset to state  $K$ . The cascade phase ends when there are no oscillators occupying either firing state, at which point the total number of oscillators that fired during the cascade is denoted  $m_R$ . When a cascade occurs at the upper boundary (initiated by an oscillator firing while occupying state  $2K$ ), then the cascade size,  $m$ , is set to  $m = m_R$ , while for cascades occurring at the lower boundary (initiated from state 0),  $m$  is set equal to  $-m_R$ . The diffusion phase restarts as soon as the cascade phase finishes.

As previously stated, while the dynamics of this extended system render it unsuitable as a model of neuronal interaction as it stands, it can be used to examine and interpret certain systems involving repeated binary choice and social influence. A pertinent example of this is a system of interacting agents in a financial market, repeatedly buying and selling an asset. In this case, the synchronous regime may be identified with herd behaviour [Banerjee, 1992] in financial markets, which occurs when investors mimic the decisions of other investors upon gaining knowledge of their actions. Re-

searchers addressing herd behaviour in financial markets have done so using a variety of techniques: percolation models [Cont and Bouchaud, 2000; Eguíluz and Zimmermann, 2000]; game theory [Challet et al., 2001a; Zheng et al., 2004; Zhao et al., 2011]; econometric modelling [Cipriani and Guarino, 2014; Chang, 2014], and agent-based modelling [Lux and Marchesi, 2000; Kim and Kim, 2014; Tedeschi et al., 2012a]. The advantage of a herd behaviour model based on the work presented here, is the availability of a mean field dynamical system which facilitates the identification of certain features of interest, such as phase transitions. As a result, the model provides a novel approach for investigating the so-called two-phase behaviour of financial markets [Zheng et al., 2004; Plerou et al., 2003], discussed in chapter 5.

Throughout this study the coupling probability  $p$  is parametrised as  $p = Kq/N$ , for  $0 \leq q \leq N/K$ ,  $N$  is taken to be large, but finite, with  $N \gg 2K + 1$ . For supplementary calculations concerning the model described, see appendix B.

### 4.3 Numerical Analysis of the stochastic system

The stochastic system displays a number of interesting phenomena, including asynchronous and synchronous behaviour, separated by a region where both behaviours co-exist. Presented in Fig. 4.1 the evolution of the cascade size,  $m$ , plotted against boundary hitting time,  $\tau$ , for a system of fixed  $N = 1000$ ,  $K = 3$  and  $q = 0.5, 0.9, 1.1, 1.5$ . In Fig. 4.1(a) and Fig. 4.1(b) ( $q < 1$ ), we observe an almost symmetric process, about  $m = 0$ , with cascades of comparable sizes representative of the asynchronous regime. In contrast, Fig. 4.1(c) depicts the system during what DeVille and Peskin [2008] call the bistable regime, in which both the asynchronous and synchronous regimes co-exist. Figure. 4.1(d) depicts the synchronous regime, where cycles consisting of long periods of successive small cascades result in spikes of large cascades. Furthermore, when  $K > 1$  the results suggest a symmetry-breaking pitchfork bifurcation exists [Lai, 1996] that coincides with the end of the asynchronous regime, which was not present in the original DP model. In Fig. 4.1(c) and Fig. 4.1(d), it is noted that the cascades persistently favour one firing state over another (which state is favoured depends upon

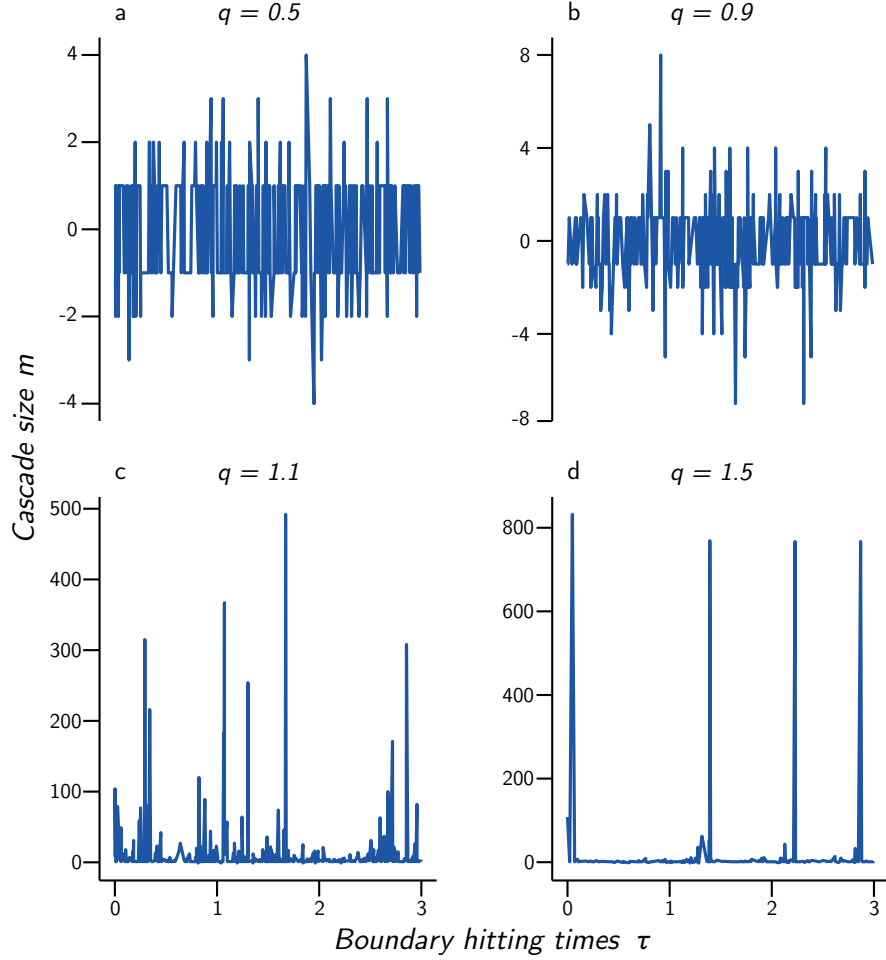


**Figure 4.1.** Cascade size propagation of the stochastic model. For a fixed network size  $N = 1000$  and  $K = 3$  the panels show the effect on the time series of cascade size for four values of  $q$ . (a)  $q = 0.5$  resulting in small cascades sizes occurring evenly at both boundaries. (b)  $q = 0.9$  resulting in small cascades sizes occurring evenly at both boundaries. (c)  $q = 1.1$  and the symmetry present in (a), (b) is broken with cascades occurring exclusively at a single boundary, dependent upon the initial conditions, and shown here occurring at the upper boundary. Both small and large cascade sizes are present, with no obvious periodic behaviour. (d)  $q = 1.5$  and the symmetry present in (a), (b) is broken with cascades occurring exclusively at a single boundary, dependent upon the initial conditions, and shown here to be occurring at the upper boundary. Cascade propagation appears almost periodic, with long periods of small cascades culminating in isolated large cascades of similar magnitude.

initial conditions), implying the symmetry seen for the system when  $q < 1$  is broken. Because the so-called bistable region represents the system switching randomly between the asynchronous and synchronous regimes, we expect to see this reflected in the cascade size output,  $m$ . To emphasise this effect, plotted in Fig. 4.2 is  $W_m$ , equal to the cumulative sum of absolute cascade sizes, against the boundary hitting time. For the case  $q = 1.1$ , corresponding to the bistable regime, the random duration of the

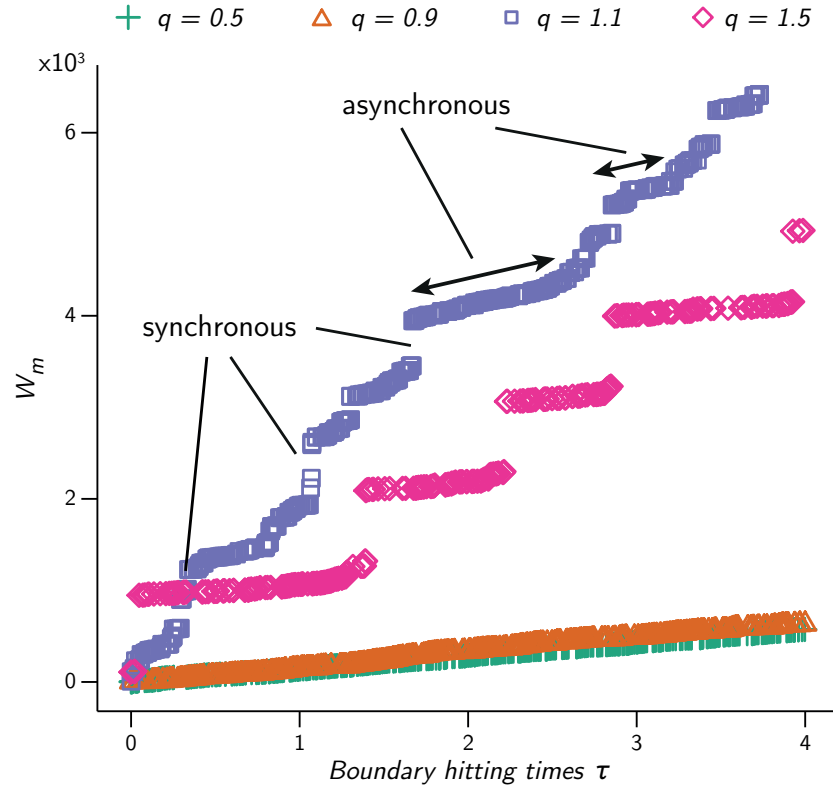


**Figure 4.2.** Cumulative absolute cascade size during different system regimes. Cumulative absolute cascade size,  $W_m$  is shown for the system  $N = 1000$ ,  $K = 3$  and  $q = 0.5, 0.9, 1.1, 1.5$ , based upon data shown for Fig. 4.1. Of particular note are the almost periodic large cascades present during the synchronous regime ( $q = 1.5$ ) and the linear, and almost identical, graphs for  $q = 0.5, 0.9$  representing the asynchronous regime. During the coexisting regime, the dynamics randomly switches between the asynchronous and synchronous regime, persisting in each for a random duration. Two such asynchronous regimes, of different durations, and three large cascade events, occurring during the synchronous regime, are labelled for the case  $q = 1.1$ .

asynchronous dynamics are highlighted along with the synchronous bursts.

The components of the extended stochastic model described here, while elementary, contribute two main sources of randomness to the system that complicate the analysis. The first is randomness from the coupling probability, controlled by  $p$ , and the second is via the (multiple) random walks used to represent the state dynamics during the diffusion phase of the system. A well-used tool for facilitating the analysis of systems of this type is the mean field approximation [see Stanley, 1988, for a summary], which is used to construct a deterministic approximation to the stochastic model.

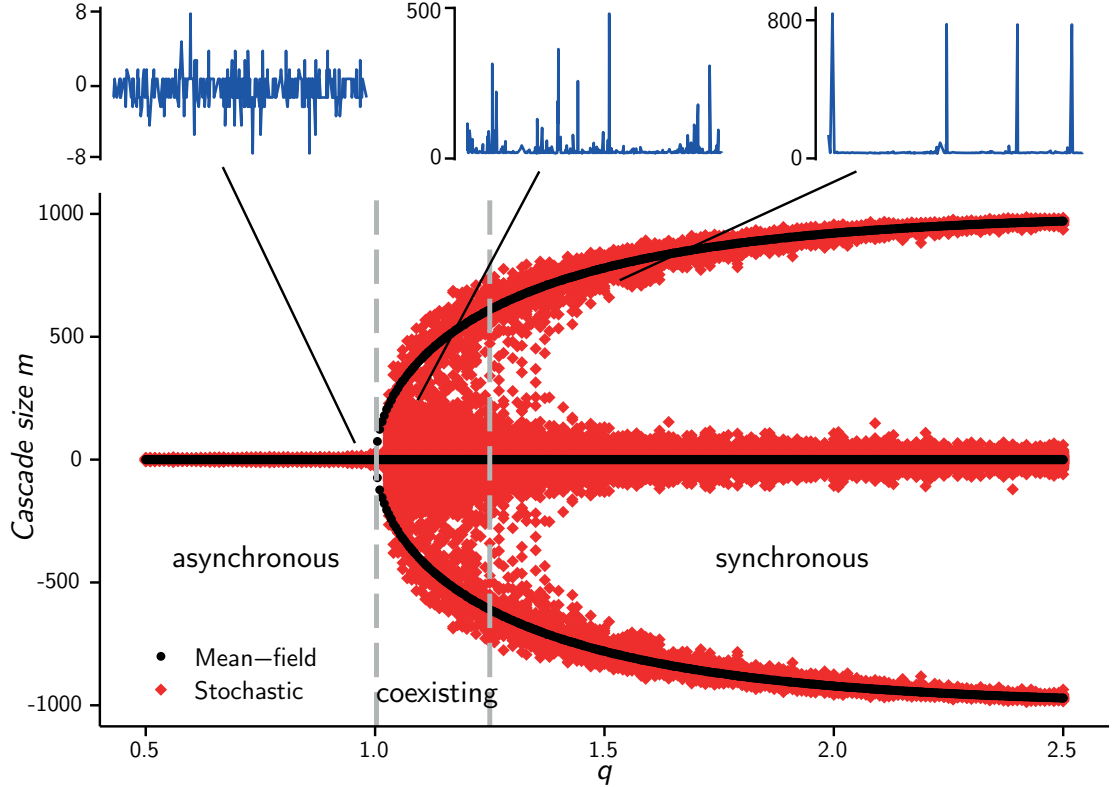


**Figure 4.3.** A bifurcation diagram representing the long-time behaviour of the mean field system superimposed over the same bifurcation diagram for the stochastic system. The system parameters are the same in both cases:  $N = 1000$  and  $K = 3$ . The bifurcation parameter is  $q$ , which forms part of the parameterised network coupling probability  $p = Kq/N$ . For  $q = q_c \approx 1$ , the cascade size suddenly increases in magnitude, denoting the end of the asynchronous regime. Panels (b), (c) and (d), from Fig. 4.1, corresponding to the cases  $q = 0.9, 1.1, 1.5$  respectively, are displayed emphasising the dynamics in each region. During the synchronous regime, the impact on the system of long periods of successive and relatively small cascades eventually accumulate, culminating in a large cascade, before the cycle is repeated (see Fig. 4.1(d)). As a result, both small and large cascades are evident during this regime.

## 4.4 Solution of the model in mean field approximation

By applying the method outlined by DeVille and Peskin [2008], a mean field approximation appropriate for our symmetric diffusion and binary firing states is constructed. The central quantity of the mean field approximation is the expected state occupation vector,  $\mathbf{x}(t)$ , given by

$$\mathbf{x}(t) = (x_0(t), x_1(t), \dots, x_{2K}(t)), \quad (4.2)$$

where  $x_s(t) > 0$  is the expected number of oscillators with state  $s$  in  $\{0, \dots, 2K\}$  at time  $t$ . Unless otherwise stated, the mean field system is normalised so that  $\sum_j x_j(t) = 1$ , and

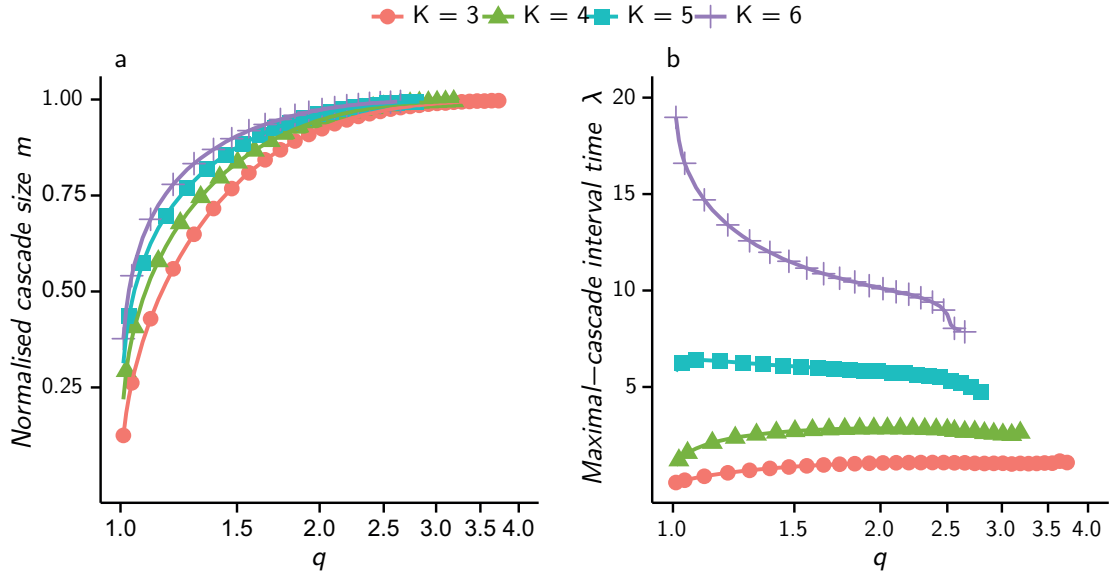


**Figure 4.4.** Maximal cascade size and interval between maximal cascades. (a) the absolute value of the normalised maximal-cascade size of the mean field system, of fixed size  $N = 1000$ , plotted against  $q$ , in log-scale, for  $K = 3, 4, 5, 6$ . (b) mean interval between successive maximal cascades for the same mean field systems used in (a), indicating a qualitative difference between the cases:  $K = 3, 4, 5$ , and  $K = 6$ . For the former case, the mean interval between large cascades initially increases as the parameter  $q$  is increased, while for the case  $K = 6$ , the reverse is true. This distinction holds for all cases  $K \leq 5$  and  $K \geq 6$  tested. In both (a), (b) the results for each mean field system are plotted up to the value of  $q$  that generates a cascade size equal to the total system (1000), and different random initial values are used for each value of  $q$ .

$\varepsilon = 1/N$  to facilitate the asymptotic analysis. All stochasticity is removed and replaced by a  $(2K + 1)$ -dimensional dynamical system which describes the dynamics of  $\mathbf{x}(t)$ .

Analogous to the results obtained by DeVille and Peskin [2008], the mean field system displays two distinct types of behaviour. The first, described as asynchronous, is characterised by isolated ( $m_R = 1$ ) oscillator firings originating from either firing state. The second corresponds to the synchronous regime, and is characterised by long periods of isolated firings (minimal cascades) leading to infrequent bursts of synchronised firing (maximal cascades). This is summarised in Fig. 4.3, which shows a bifurcation diagram of the long-time behaviour for the stochastic and mean field systems, plotting the range of  $m$  against  $q$ . The agreement between the mean field and stochastic systems at the critical value of  $q = q_c$ , marking the appearance of cascade sizes greater than 1 for the mean field system, is of particular note. Figure. 4.4 shows the normalised maximal cascade size and mean time interval,  $\lambda$ , between successive cascades as a function of  $q$ ,

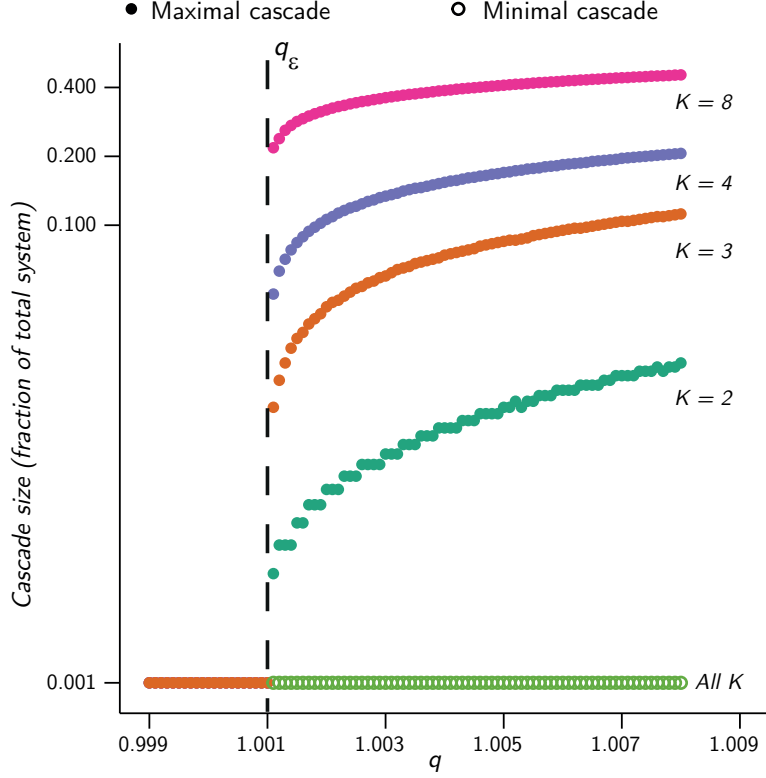


**Figure 4.5.** Transition from asynchronous to synchronous regimes. Maximal (solid circles) and minimum (open circles) cascade sizes occurring at the upper boundary obtained for each  $q$  value, suggesting  $q \approx 1/(1 - \varepsilon)$ , indicated by the dashed line and labelled  $q_\varepsilon$ , is a critical value of the finite  $N$  system for all  $K$  shown. Cascade sizes are shown as a proportion of  $N$  (normalised cascade size) and plotted on the vertical axis in log scale.

for mean field systems with  $K = 3, 4, 5, 6$ . Figure. 4.4(b) reveals qualitative differences between mean field systems in how increasingly synchronised behaviour (identified with increasing  $q$ ) affects the time interval between maximal cascades. While systems with  $1 < K < 5$  experience longer intervals between maximal cascades as synchronisation increases, for a significant range of  $q$ , systems with higher values of  $K$  (true for all  $K > 5$  tested) experience a monotonic decrease in the time interval between maximal cascades, for a significant range of  $q$ .

For the one-sided normalised mean field DP model, DeVille and Peskin [2008] obtain the value of  $\mathbf{x}(t)$ , (here, labelled  $\mathbf{x}_{DP}$ ) corresponding to behaviour in the asynchronous regime, as the solution to a fixed point equation using an asymptotic method, finding

$$\mathbf{x}_{DP} = (1/K, \dots, 1/K, O(\varepsilon)) \quad (4.3)$$

exists and is asymptotically stable for  $q < 1$ . A first order phase-transition representing the transition from asynchronous to synchronous behaviour was observed to occur at the critical value,  $q = q_c < 1$ , although little attention is given to actual value of  $q_c$ .

By applying the aforementioned asymptotic method to the system presented here, we solve a fixed point equation to obtain the steady-state behaviour of  $\mathbf{x}(t)$  when the system is in the asynchronous regime. It is sufficient to consider the case when the system exhibits isolated (size 1) cascades alternating between the two firing states  $2K$  and  $0$ . In particular, we compute the solution, up to  $O(\varepsilon)$ , of the fixed point equation  $G_0(\mathbf{x}) = \mathbf{x}$ , where the map  $G_0$  is given by (see appendix B.1 for a detailed description of the construction of  $G_0$ )

$$\begin{aligned} G_0(\mathbf{x}) &= (I + \varepsilon K q L_{C,-}) e^{\tau_2 L_D} \\ &\times \left[ (I + \varepsilon K q L_{C,+}) e^{\tau_1 L_D} \mathbf{x} - \varepsilon (\mathbf{v}_{2K} - \mathbf{v}_K) \right] \\ &- \varepsilon (\mathbf{v}_0 - \mathbf{v}_K). \end{aligned} \quad (4.4)$$

This gives the fixed point (up to  $O(\varepsilon)$ ) as

$$\begin{aligned} \mathbf{x}_0^* &= \left( O(\varepsilon), \frac{1}{K^2}, \frac{2}{K^2}, \dots, \frac{K-1}{K^2}, \frac{1}{K}, \frac{K-1}{K^2}, \dots, \frac{1}{K^2}, O(\varepsilon) \right) \\ &\in \mathbb{R}_+^{(2K+1) \times (2K+1)}. \end{aligned} \quad (4.5)$$

In Eqn. (4.4),  $\tau_1$  and  $\tau_2$  are the times spent in the diffusion phase before reaching the respective firing state,  $L_{C,-}, L_{C,+}$  are the pulse-coupling matrices for negative and positive pulses respectively, and  $\mathbf{v}_0, \mathbf{v}_{2K}$  are basis vectors. The fixed point  $\mathbf{x}_0^*$  exists for  $q < K$ , although to determine the exact range of  $q$  for which this solution is stable would require terms involving higher orders of  $\varepsilon$  to be taken in to account, and is not pursued here. Extensive numerical simulations strongly suggest that, for the finite systems tested, a transition takes place between the asynchronous and synchronous regimes, for  $q = q_c > \frac{1}{1-\varepsilon}$ . As  $q_c$  appears to be the same for all values of  $K$  tested, we infer, heuristically, a lower bound for  $q_c$  in the low-dimensional case  $K = 1$ , and obtain

$q_c > \frac{1}{1-\varepsilon}$  (see the next section titled ‘Path to synchronicity’). Figure. 4.5 presents a selection of the simulations performed, where the maximum and minimum cascade sizes, occurring at the upper boundary, are plotted against  $q$  for  $1 - \varepsilon < q < 1 + 8\varepsilon$ . Large cascades occur for values  $q > \frac{1}{1-\varepsilon}$ , in agreement with our calculation. As the system size  $N$  tends to infinity, and by taking the limit of  $\frac{1}{1-\varepsilon}$  as  $\varepsilon \rightarrow 0$ , we infer a phase transition takes place at  $q_c = 1$ .

Our final result for the normalised mean field system is a closed form expression for the cascade size  $m = m(\mathbf{x}(t))$ , which forms an essential part of the specification of the system dynamics given by equations given by Eqns. (B.11) - (B.12). This result is found for the case  $K = 1$  and stated in terms of the network coupling parameter  $p$  and the expected state occupation vector,  $\mathbf{x}$  given by Eqn. (4.2) (dropping the dependence on  $t$  as cascades occur instantaneously). For  $K \geq 1$ , during a cascade of (as yet undetermined) size  $m$  occurring at the upper boundary (and before firing oscillators are reset to state  $K$ ),  $\mathbf{x}$  is mapped to  $(I + pL_{C,+})^m \mathbf{x} - m\mathbf{v}_{2K}$ . By considering the  $2K$ -th row of the matrix  $(I + pL_{C,+})^m$ , the eventual cascade size can be written in terms of a vector inner product and computed as  $\min\{m : \langle \mathbf{z}(m), \mathbf{x} \rangle - m\varepsilon < \varepsilon\}$ , where the  $i$ -th component of  $\mathbf{z}(m)$  is given by

$$\mathbf{z}(m)_i = \begin{cases} 0 & \text{for } i < 2K - m, i = 0 \\ 1 & \text{for } i = 2K \\ p^{2K-i} \sum_{v=0}^{m-2K+i} \binom{2K-i}{v} (1-p)^v & \text{otherwise,} \end{cases} \quad (4.6)$$

and  $\binom{n}{r} = \frac{(n+r-1)!}{r!(n-1)!}$ . Since the cascade is assumed to occur at the upper boundary,  $x_{2K} = \varepsilon$ . Moreover, when  $K = 1$ , we note from Eqn. (4.6) that  $\mathbf{z}(m)_1 = p \sum_{v=0}^{m-1} (1-p)^v$  is the only non-trivial vector component. By treating  $m$  as a real-valued variable, and solving for the single solution of  $m$  satisfying

$$\langle \mathbf{z}(m), \mathbf{x} \rangle - \varepsilon(1+m) = 0, \quad (4.7)$$

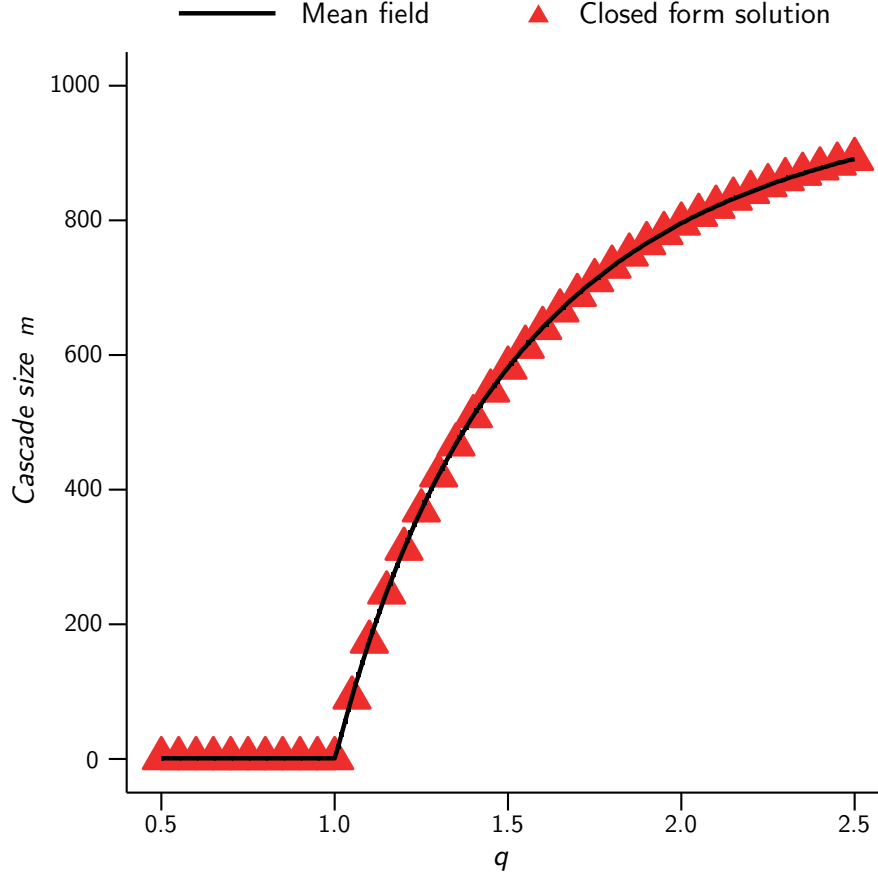


**Figure 4.6.** Comparison of  $K = 1$  mean field cascades size. Cascade size of the  $K = 1$  mean field system computed via direct simulation (solid line) and closed form expression (filled triangles), computed using Eqn. (4.8).

we obtain,

$$m = \max \left( 1, \left\lfloor \beta - \frac{W(\alpha\beta \exp(\alpha\beta))}{\alpha} \right\rfloor \right), \quad (4.8)$$

where the substitutions  $\alpha = \log(1 - p)$ ,  $\beta = x_1/\varepsilon$  have been made;  $\lfloor \cdot \rfloor$  the floor function [Iverson, 1962], and  $W$  the principle branch of the Lambert  $W$ -function [see Corless et al., 1996, for a discussion of the  $W$ -function]. The maximum function is used to make a correction for small cascades, while floor allows  $m$  to be reported as an integer. Figure. 4.6 compares cascade sizes obtained via direct simulation of the mean field system (solid line), and Eqn (4.8) (filled triangles), where  $p$  is parameterised as  $p = q\varepsilon$ . For each value of  $q$ , 50 values of  $x_1$ , equally spaced in the open interval  $(1 - 2\varepsilon, 1 - \varepsilon)$ , are used to compute and plot 50 values of  $m$  (in this case there is very little variation amongst these values). Obtaining similar closed form formulae for the cascade size when  $K > 1$  remains an open problem, and is not pursued here. This is due, in part, to

the difficulty associated with applying the direct calculation method (used for the case  $K = 1$  by solving Eqn. (4.7)) to the  $K > 1$  case, and as a result a new solution method would likely need to be devised.

While  $\mathbf{x}$  is a  $(2K + 1)$ -dimensional parameter, with  $2K - 1$  degrees of freedom, we note that in certain cases it may be sufficient to solve Eqn. (4.7) when  $\mathbf{x}$  is given by the asynchronous fixed point in Eqn. (4.5), and thereby reduce the number of parameters required in calculations.

## 4.5 Path to synchronicity

Within the asynchronous regime, the mean field DP model displays only one type of behaviour - a constant stream of isolated firings. In contrast, due to the extra degree of freedom of the mean field double threshold system presented here, there exists a multitude of behaviours during the asynchronous regime, each coinciding with a different firing pattern with respect to each of the firing states. The map  $G_0$  given by Eqn. (4.4) coincides with the infinite alternating sequence of firings:  $(\dots, +, -, +, -, \dots)$ , where “+” and “-” denote firing occurring at the upper and lower boundary, respectively. Via positive feedback, when an oscillator fires, it induces a proportion of the remaining oscillators to move closer to that firing state. Viewed from the perspective of the random walk, this feedback is equivalent to bias. By considering the indefinite sequence of isolated firings  $(\dots, +, +, +, +, \dots)$  represented by the map,  $G_1$

$$G_1(\mathbf{x}) = (I + \varepsilon K q L_{C,+}) e^{\tau_1 L_D} \mathbf{x} - \varepsilon(\mathbf{v}_{2K} - \mathbf{v}_K), \quad (4.9)$$

and the equivalent map,  $G_{-1}$  representing the indefinite sequence of isolated firings  $(\dots, -1, -1, -1, \dots)$ , it is clear that these cases inject the maximum amount of bias into the random walk process, and therefore represent a boundary of the asynchronous regime. Thus, by obtaining the fixed point of the maps,  $G_{-1}, G_1$ , given by  $\mathbf{x}_{-1}^*, \mathbf{x}_1^*$  respectively, and determining the range of  $q$  for which they exist, we claim to obtain bounds on the critical coupling parameter,  $q_c$  defining the asynchronous region.

For  $K = 1$ , and  $N$  finite, we use the asymptotic method, described previously, to determine that the solutions  $\mathbf{x}_{-1}^*, \mathbf{x}_1^*$  exist only when  $q$  satisfies  $1 < q < \frac{1}{1-\varepsilon}$ , while direct calculation demonstrates that the solution  $\mathbf{x}_0^*$  exists only for  $q$  satisfying  $0 < q < \frac{1}{1-\varepsilon}$ , suggesting that  $q_c > \frac{1}{1-\varepsilon}$ .

## 4.6 Analysis of the stochastic system: finite state-space

In order to derive and prove certain results presented in this, and subsequent, sections ideas from various branches of mathematics are used. In particular, deriving the probability distribution of cascade sizes requires notation and results from percolation theory [Grimmett, 1999] and enumerative combinatorics [Stanley, 2012]. In addition, the negative binomial approximation to the cascade size distribution, and Kolmogorov-Smirnov tests, assume a familiarity with basic results from mathematical statistics [Shao, 2007; Feller, 1968]. While these excursions are necessary (and not all such material represents trivial book work), many of the extended statements and proofs are placed in appendix B, to keep interference with the main text of this chapter to a minimum.

In this section the stochastic version of the  $(K, q)$  process presented in [Wray and Bishop, 2014], and earlier in this chapter, is analysed and briefly recounted in the context of an agent-based model (further details of the model in an economic agent-based context are contained in appendix C).

This and subsequent sections of this chapter act as a prelude to the financial market model developed in chapter 5. There, the stochastic cascade process, labelled  $(K, q)$  - generated by the probabilistic interaction of economic agents (traders) - is incorporated into a simple model of asset price returns. Using the new model presented in chapter 5, a number of empirical facts (see section 2.5.2 in chapter 2) concerning financial returns can be reproduced. Certain features of empirical data, such as truncated power-law distributed price returns, and volatility clustering, are exhibited, and the so-called (Black and Scholes [1973] implied) volatility smile [Derman and Kani, 1994], obtained from the price of index option contracts [Hull, 2011], is approximately recovered. In gen-

eral, from this point onwards the term ‘agents’ will be used in place of ‘oscillators’ - although both terms refer to the same underlying mathematical object.

The cascade size,  $m$ , is defined as the signed number of agents,  $m_A$ , that accumulate in the firing state, prior to being reset to state  $K$ . If the firing event of the agent whom initiated the cascade is positive (representing excess demand) we take  $m = |m_A|$  otherwise we take  $m = -|m_A|$ . After a reset, all agents resume stochastic accumulation of sentiment until the next transition into a firing state occurs, and the system repeats. The cascade process  $(K, q)$  is taken to refer to the sequence of cascade sizes,  $\{m_1, m_2, \dots\}$ , generated from such a system.

In the next section, an asymptotic expression for the cascade probability is derived in the case  $K = 1$ , while for  $K \geq 1$ , comparison with the negative binomial distribution enables the functional form of price return standard deviation (also known as volatility in the lexicon of financial markets) to be expressed in terms of  $q$ .

The  $K = 1$  system represents a special case as it can be most readily analysed using standard statistical methods. In this case, the system has three states: two firing states and a rest state. This implies that after each cascade event all agents will occupy the rest state, unconditional on their state prior to the cascade event. The system then repeats in this way. As a result, the cascade sizes can be considered to be independent and identically distributed statistical random variables. For  $K > 1$ , the system can be said to possess memory, because cascade sizes depend upon the outcome of previous cascades due, in part, to the distribution of agents among the system states generally differing after each cascade event.

#### **4.6.1 Cascade distribution of the $K = 1$ system**

When a cascade is initialised, the number of agents that are subsequently induced to fire is governed by a stochastic process. Furthermore, during the course of a single cascade, agents can only be induced to the firing state at which the cascade is initialised, as agents either transition closer to the firing state, or do not transition at all. We proceed by breaking the development of an arbitrary cascade into discrete levels. Let  $X_0 = 1$

represent the initial firing, and  $X_k$  represent the number of agents that fire at the  $k$ -th level. The total number of agents that have fired by level  $n$  is written as

$$m_n = \sum_{k=0}^n X_k. \quad (4.10)$$

Once agents are induced to the firing state, for a given level of the cascade, they fire serially and then enter a refractory state - reducing the number of nodes available to be induced to the firing state at the next level. Hence,

$$X_0 = 1, X_k = \sum_{i=1}^{X_{k-1}} Y_{i,k} \quad (4.11)$$

where  $Y_{i,k}$  is a binomial random variable given by

$$Y_{i,k} \sim \text{Bin}(N - m_{k-1} - \sum_{j=0}^{i-1} Y_{j,k}, q) \quad (4.12)$$

and  $Y_{0,k} = 0$ . The cascade stops at some level  $T < N$ , with

$$T = \min\{n \mid m_n = N \text{ or } X_n = 0\}$$

and the cascade size is taken to be  $m_T$ . The process defined by Eqns. (4.10)-(4.12) is similar to a Galton-Watson process [Watson and Galton, 1875], with the exception that our model is finite (meaning the process always stops) and “offspring” distributions do not satisfy the independence requirement ( $X_k$  for  $k > 1$  is the sum of dependent binomial random variables).

**Shrinking  $N$ -ary trees.** To obtain an asymptotic expression for the probability of a given cascade size, we apply combinatorial methods to a variant of rooted incomplete  $N$ -ary trees [Knuth, 1998]. A graphical interpretation of the tree-representation of an arbitrary cascade, described below, is presented in Fig. 4.7. Starting with a given single root node (level 0,  $X_0 = 1$ ), the evolution of a single cascade can be represented exactly by a tree consisting of two types of nodes: internal nodes and perimeter nodes

[Grimmett, 1999]. An internal node, at a given level of the tree, represents an agent induced to the firing state by an agent at the preceding level. A perimeter node represents an unsuccessful attempt, by an agent in a firing state at the previous level, to induce an agent to the firing state. Thus, perimeter nodes are connected to parent internal nodes, and do not produce any further branches. The collection of all perimeter nodes is called the perimeter of the tree, and the size of the perimeter,  $Q$ , is equal to the number of perimeter nodes. A cascade terminates when the firing state becomes unoccupied - which is represented in the tree as all nodes of a given level consisting of perimeter nodes (which means the tree stops growing). Therefore, a tree consisting of  $m$  internal nodes, and  $Q$  perimeter nodes, represents a cascade of size  $m$ . It follows the probability of a cascade of size  $m$  can be written in the form

$$P(m) = \sum_Q G(m, Q) p^{m-1} (1-p)^Q \quad (4.13)$$

where the summation is taken over different values of  $Q$  that correspond to a single value of  $m$ , and  $G(m, Q)$  is the number of trees consisting of  $m$  internal, and  $Q$  perimeter, nodes. When the number of agents remain constant at each level, for instance equal to  $(N-1)$ , an arbitrary cascade can be modelled using a standard (rooted, incomplete)  $(N-1)$ -ary tree. In this case the number  $G(m, Q)$  is given by the Fuss-Catalan numbers (also known as generalised Catalan numbers; see Hilton and Pedersen [1991] and Drmota [2009])

$$G(m, Q) = Q^{-1} \binom{(N-1)m}{m} \quad (4.14)$$

where  $Q$  is a 1-1 function of  $m$  given by

$$Q = m(N-2) + 1. \quad (4.15)$$

When dependence between levels of the tree is taken in to account, according to Eqns. (4.10)-(4.12), the arity of the tree representing a cascade shrinks monotonically

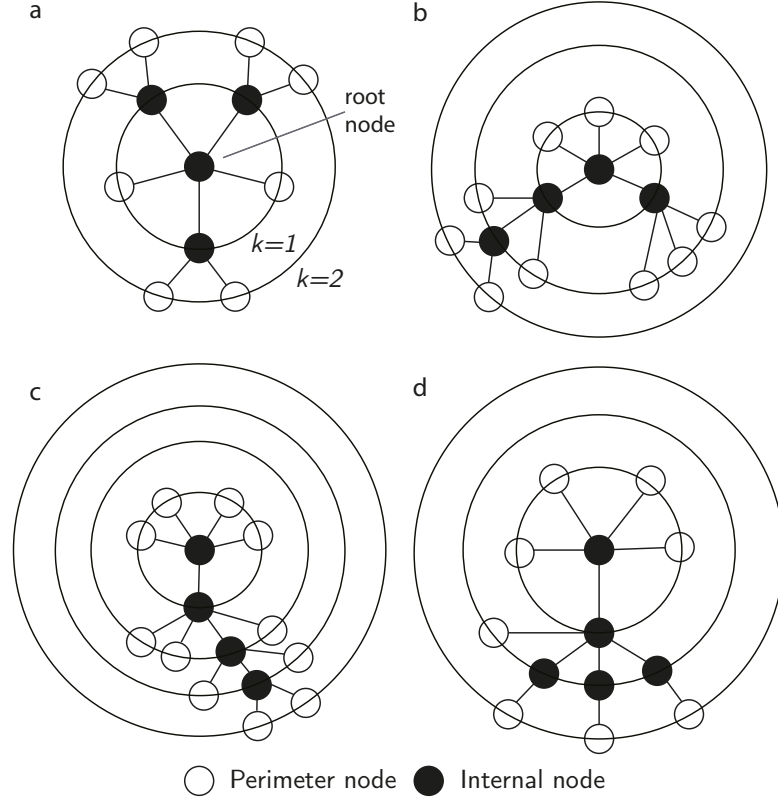


**Figure 4.7.** Filled nodes are internal nodes, representing agents induced to the firing state during the course of the cascade. Open nodes are perimeter nodes, representing the unsuccessful attempt of a connected parent node at the preceding level to induce an agent to the firing state. For all panels  $N = 6$ . a) depicts a cascade of size  $m = 4$ , with perimeter  $Q = 8$ , b)  $m = 4$  with  $Q = 10$ , c)  $m = 4$  with  $Q = 11$ , d)  $m = 5$  with  $Q = 8$ .

as the cascade progresses (see Fig. 4.7). For example, level 1 consists of a single-level  $(N - 1)$ -ary tree, while level 2 is a single-level tree, distributed over  $X_1$  root nodes, able to produce up to  $(N - 1 - X_1)$  internal nodes in total - and so on. For this tree structure we obtain the perimeter size, given the number of internal nodes  $m$ , as

$$Q = m(N - m) + \frac{1}{2}(m - 1)^2 - \frac{1}{2} \sum_{k \geq 1} X_k^2 \quad (4.16)$$

and asymptotically for large  $N$  the probability of cascade size reduces to,

$$P(m) \sim (2\pi)^{-\frac{1}{2}} m^{-\frac{3}{2}} e^{(1-q)m} q^{m-1}. \quad (4.17)$$

The details of the derivations of Eqns. (4.16) and (4.17) are presented in appendix B.

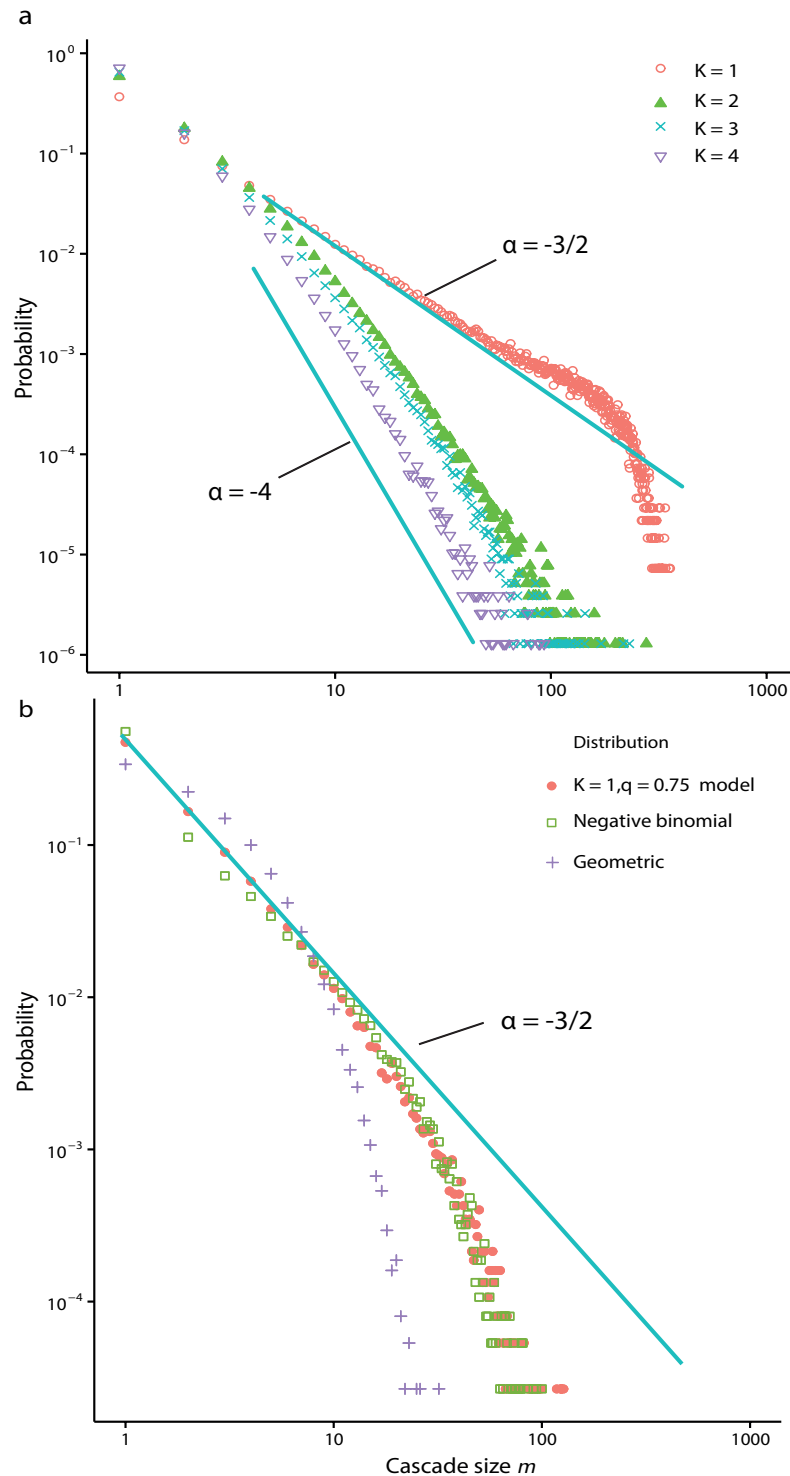


**Figure 4.8.** a) log-log probability plot of absolute cascade sizes when the system is near the transition value  $q = 1$  for  $K = 1, 2, 3, 4$  with  $N = 1000$ . The case  $K = 1$ , corresponding to the maximal coupling strength, displays an exponentially truncated tail due to finite size effects. b) log-log probability plot of cascade size for the system with parameters  $K = 1, q = 0.75$  and  $N = 1000$  (filled circles), compared to a geometric distribution (crosses) of equal mean, and a negative binomial (open squares) with both mean and variance matched.

When  $q = 1$  the asymptotic cascade distribution takes the form of a power law with exponent  $-3/2$ , consistent with the infinite sub-critical Galton-Watson process [Bouchaud, 2013], while for  $q \neq 1$ , Eqn. (4.17) represents a truncated power law. Figure. 4.8a displays the distribution of absolute cascade sizes for various  $K$  near the critical point of  $q = 1$ , obtained via simulation, reflecting these findings for  $K = 1$ .

#### 4.6.2 Analysis and approximation of systems with $K \geq 1$

When  $K > 1$  each agent requires more than one pulse to induce it to a firing threshold, from the rest state. As a result, this dampens the ability of cascades to sweep through the entire system. Figure. 4.8a displays the distributions of cascades sizes for  $K = 2, 3, 4$  when  $q = 1$ . The exponents are estimated via maximum likelihood estimation (MLE), and the distribution fit tested using the Kolmogorov-Smirnov test. Estimates of the exponent (with standard error in parenthesis) range from  $\alpha \approx -2.25(0.001)$  for  $K = 2$ , to  $\alpha \approx -3.5(0.06)$  for  $K = 4$ , although the quality of the power law fit decays rapidly as  $q$  deviates from the critical value  $q = 1$ . We leave the derivation of a closed-form expression for the cascade distribution (equivalent to Eqn. (4.17)) when  $K > 1$  for future research. Instead, the negative binomial approximation is sufficient for expressing the approximate moments of the cascade distribution in terms of  $q < 1$ .

#### 4.6.3 Fitting a negative binomial distribution.

Even though the mean and variance of the  $K = 1$  cascade distribution can be expressed in closed form using special functions, we provide numerical evidence for a range of  $K$  values showing that a negative binomial distribution [Feller, 1968] may be used as a good approximation to the cascade distribution, when  $q < 1$ . Figure. 4.8b shows the cascade distribution  $K = 1, q = 0.75$  compared to a moment-matched negative binomial distribution with good agreement. Figure. 4.9 shows how the parameters,  $r$  and  $p_{NB}$ , of moment matched negative binomial distributions vary with  $q$ . Except for the case of  $p_{NB}$  when  $K = 1$ , both sets of parameters can be well approximated as varying linearly with  $q$ , for all  $K$  tested. The benefit of this approach is that the moments of the cascade distribution are easily expressed in terms of  $q$ , the key parameter of interest.

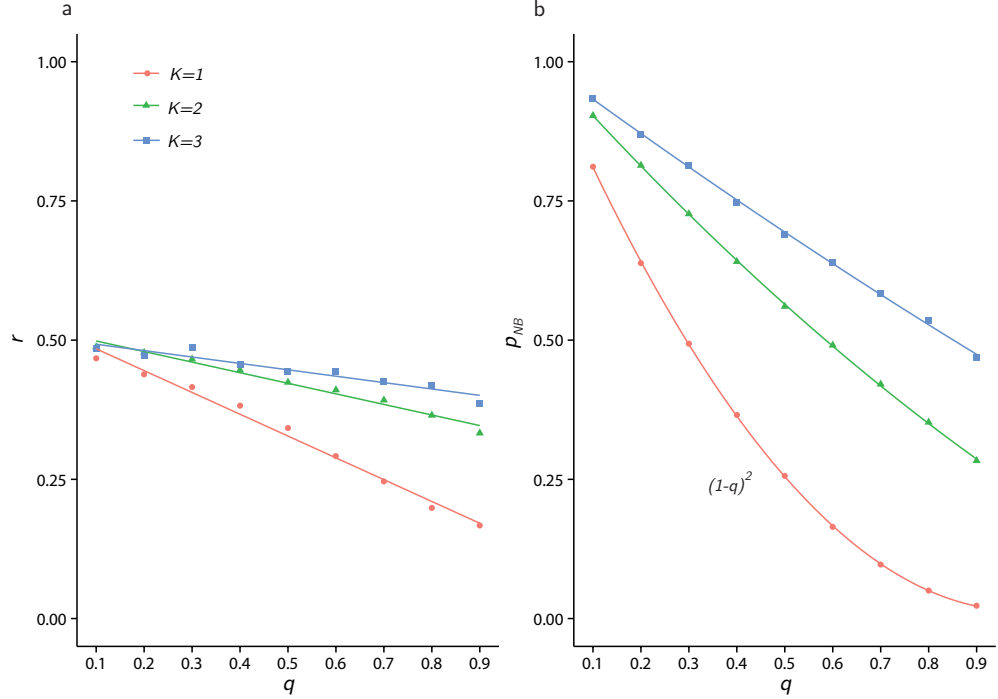


**Figure 4.9.** The parameters of moment matched negative binomial distributions as a function of  $q$ , for  $K = 1, 2, 3$ . a)  $r$  and b)  $p_{NB}$ .

In Figs. 4.10a and 4.10b, the Kolmogorov-Smirnov test statistic (see [Clauset et al., 2009] for methodological details) is reported for both a power law and negative binomial fit, and the regions of  $q$  in which each distribution provides the best relative fit to the distribution of  $(K, q)$  is highlighted (via filled shapes). In the case  $K = 1$ , the negative binomial provides a good fit for  $0 < q < 0.6$ , and the power law provides a better relative fit in the range  $0.79 \leq q \leq 1$ .

Cascades can occur in both the positive and negative directions, and in the case  $K = 1$  they occur with equal probability. As a result, the (approximate) full distribution of cascades sizes (both negative and positive) is obtained as a mixture distribution of two equally weighted negative binomial distributions, symmetric about 0. Using standard moment calculations (see appendix B) the variance of this full distribution may be written in terms of the negative binomial distribution parameters, considered as a function of  $q$

$$\sigma^2(q) = \frac{1}{p_{NB}(q)^2} \left( r(q)(1 - p_{NB}(q)) + [p_{NB}(q) + r(q)(1 - p_{NB}(q))]^2 \right) \quad (4.18)$$

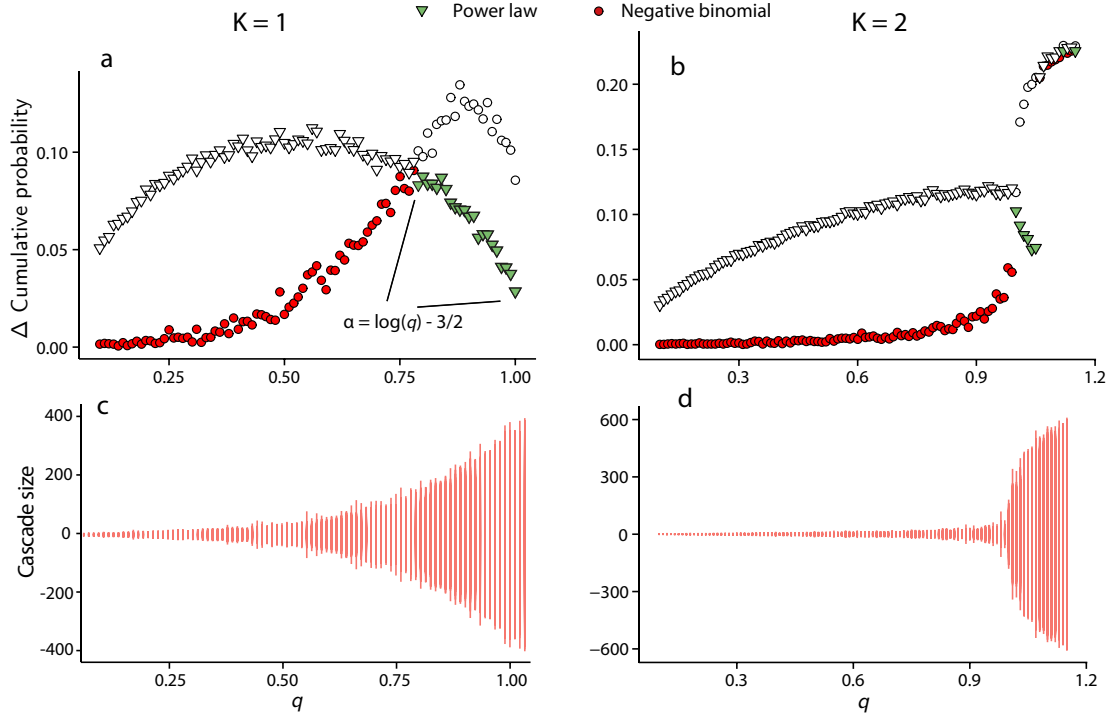


**Figure 4.10.** Filled shapes represent the minimum divergence of the two fits, calculated using the Kolmogorov-Smirnov statistic.  $N = 1000$  for all panels. a)  $K = 1$  and negative binomial fits well for  $q < 0.6$ , but power law (zeta distribution) is a better fit for  $q > 0.79$ , with exponent  $\alpha = \log(q) - \frac{3}{2}$  in this region. b)  $K = 2$  and negative binomial provides a good fit up to  $q < 0.85$ . c) and d) show the typical cascade sizes versus  $q$ .

where  $r(q) = a_1 + a_2q$ ,  $p_{NB}(q) = b_1 + b_2q + b_3q^2$  and the constants  $a_1, a_2, b_1, b_2, b_3$  vary with each value of  $K$  (see Fig. 4.9). For  $K = 1$ ,  $p_{NB}(q) = (1 - q)^2$  and mean values of  $a_1$  and  $a_2$  over 1000 observations are  $0.53(0.016)$  and  $-0.40(0.024)$ , respectively (standard deviation displayed in parenthesis). For  $K = 2$ ,  $a_1 = 0.52(0.03)$ ,  $a_2 = -0.19(0.04)$  and  $b_1 = 0.96(0.007)$ ,  $b_2 = -0.77(0.01)$ ,  $b_3 = 0$ .

When  $K = 1$ , the standard deviation can be written

$$\sigma(q) = \left[ \frac{(a_1 - a_2q)(1 - (1 - q)^2)}{(1 - q)^4} + \left( 1 + \frac{(a_1 - a_2q)(1 - (1 - q)^2)}{(1 - q)^2} \right)^2 \right]^{1/2}, \quad (4.19)$$

and a similar calculation can be performed for excess kurtosis, as presented in appendix B.

# Chapter 5

## Complexity model of herding in financial markets

In the previous chapter I introduced a model of a stochastic pulse-coupled network, incorporating two event boundaries, and established the existence of a critical pulse-coupling probability,  $p_c$ . The critical pulse-coupling probability separates the behaviour of the system into a small cascade-size regime (for  $0 < p < p_c$ , named asynchronous), and a regime in which large cascade sizes are repeatedly observed (for  $p \geq p_c$ , named synchronous). The aim of this chapter is two-fold. First, a detailed probabilistic analysis of the stochastic system is carried out, yielding an explicit asymptotic expression for the cascade-size probability distribution of the  $K = 1$  system. This analysis builds upon, and complements, the dynamical system (mean field) approach of the previous chapter. Second, the pulse-coupled network model is used to develop a new model of agent (or trader) interactions in a stylised financial market [Wray and Bishop, 2015].

The financial market model described here incorporates a number of important features (but not all) observed in real markets. In this regard, a pertinent property is its micro-foundedness, meaning dynamics produced by the model are derived directly from the economic interactions of market participants (rather than resulting from measured quantities or exogenous distributions and parameters). As well as accounting for

so-called fat-tailed, or leptokurtic, asset price return distributions (arising from a truncated power law derived directly from the interaction of agents), the model displays volatility clustering [Bollerslev et al., 1992] and evidence of long-memory volatility [Baillie, 1996]. The existence of a transition between system states, separated by the critical pulse-coupling probability, provides a mechanism accounting for both relative high and low return volatility regimes [the so-called two-phase behaviour, see Plerou et al., 2003; Zheng et al., 2004]. This is achieved in a coherent way, via identification with the synchronous and asynchronous regimes (respectively) of the underlying pulse-coupled network. A summary of so-called stylised facts in financial markets is provided by Cont [2001; 2007].

While the study of the empirical, or stylised, observations of financial markets can be traced back to the work of Mandelbrot [1963], research continues into the mathematical description of such phenomena [Muzy et al., 2013; Zheng et al., 2014; Xue and Gençay, 2012]. One reason for this persistent interest is that a universally accepted behavioural explanation of these phenomena is lacking, and although much progress has been made in this regard (pertinent examples are: investment strategy switching among agents [Lux and Marchesi, 2000; Bouchaud et al., 2001; Alfarano and Lux, 2007; LeBaron, 2012]; the development and application of minority games [Challet and Marsili, 1999; Ortisi and Zuccolo, 2013]; percolation and general Ising-like lattice interaction models [Cont and Bouchaud, 2000; Kaizoji et al., 2002; Sornette and Zhou, 2006; Bartolozzi and Thomas, 2004]; the development and application of bounded rationality to econometric models [Hommes, 2002] and models incorporating agent memory, evolutionary learning and multiple time scales [Brock et al., 2005; Zumbach and Lynch, 2001; Borland, 2006]), no clear consensus, favouring one behavioural mechanism over the others, has emerged. Indeed, in the case of financial markets, evidence of each of the different behavioural mechanisms can easily be found (or can be reasonably surmised).

For more than a decade, herd behaviour [Banerjee, 1992; Lux, 1995] in financial markets has been subject to much research [Bikhchandani and Sharma, 2000; Tedeschi et al., 2012a; Park and SgROI, 2012; Zheng et al., 2004; Eguíluz and Zimmermann,

2000; Cont and Bouchaud, 2000; D'Hulst and Rodgers, 2000], in parallel with research investigating the phenomenon of stock market crashes [Yalamova and McKelvey, 2011; Petersen et al., 2010; Levy, 2008; Johansen et al., 2000], and the identification of certain stylised features of financial market data (see the reviews by Cont [2001] and Bouchaud [2002]). Recent extraordinary market events [Khandani and Lo, 2007; Easley et al., 2011], reviewed by Cincotti et al. [2012], demonstrate that herd behaviour can have material consequences for investors, and regulators, alike. While identifying and estimating the impact of herd behaviour on financial markets remains a challenge, technological and market developments have increased the potential for herding to arise. For instance, investor sentiment via social media [Sprenger et al., 2014; Zhang et al., 2011; Bollen et al., 2011], and the availability of data sets quantifying collective behaviour [Preis et al., 2013; Curme et al., 2014], have the potential to facilitate both intentional and spurious herding, using the terminology of Bikhchandani and Sharma [Bikhchandani and Sharma, 2000]. Furthermore, in a report commissioned by the UK government [Sornette and Von der Becke, 2011], herd behaviour is identified as a possible consequence of high-frequency trading - although this is not a universally accepted conclusion amongst researchers. Indeed, the impact of high-frequency trading on financial markets is an active area of research with no clear consensus either for or against adverse market or regulatory impact [Hasbrouck and Saar, 2013; Brogaard et al., 2014].

Previous attempts at understanding the dynamics of financial markets have primarily focused on accurately describing the observed data using time-series, or purely statistical, methods. It is well-documented that price returns of financial assets exhibit significant deviations from the Gaussian model [Mandelbrot, 1963; Cont, 2001], which has resulted in a plethora of alternative representations. Models such as  $\alpha$ -stable distributions [Lévy, 1925], generalised hyperbolic models [Barndorff-Nielsen and Shephard, 2001], generalised autoregressive conditional heteroskedasticity (GARCH) models [Bollerslev, 1986] and stochastic volatility models [LeBaron, 2001; Heston, 1993] attempt to account for features, such as high kurtosis and volatility clustering which are

inconsistent with Gaussian behaviour.

More recently, a particular class of stochastic volatility models known as multifractal (or multi-affine) models, derived from multiplicative cascades studied in the context of fluid turbulence [Kolmogorov, 1962; Mandelbrot, 1974], and multifractal random walks [Arneodo et al., 1998] have successfully been applied to the modelling of financial time series [Bacry et al., 2001; Calvet and Fisher, 2004; Di Matteo, 2007; Barunik et al., 2012; Bacry et al., 2012]. Such statistical models explicitly capture multifractal anomalous scaling in higher statistical moments,  $M_b(L)$ . Explicitly,

$$M_b(L) = \mathbb{E}\{|X(t+L) - X(t)|^b\} \sim A_b L^{\zeta_b}, \quad (5.1)$$

where  $X(t)$  a stochastic process with stationary increments,  $b$  is the moment order,  $A_b$  is a constant, and the index  $\zeta_b$  is not equal to the Brownian motion value of  $b/2$ . An attractive feature of stochastic multifractal cascade models, as applied to financial markets, is the evolution of asset volatility is modelled as a multi-time scale process; an observation which is supported by empirical analysis [LeBaron, 2001; Zumbach and Lynch, 2001].

The financial market model described here contributes to the body of work that aims to combine agent-based modelling with traditional probabilistic analysis of financial markets [Feng et al., 2012; Gontis and Kononovicius, 2014]. In this endeavour, asset price returns are modelled using two variants of the stochastic version of a recent model [Wray and Bishop, 2014] describing cascades on a pulse-coupled network. In the first case, agents trade at two well-defined firing thresholds, that bound the state space in which information (both private and public) is considered to accrue. In the second case, a semi-infinite state space is considered by removing one of the firing thresholds and allowing agents to occupy states infinitely distant from the firing threshold. In both cases, for each agent the accumulation of private information is represented by random transitions between nearest-neighbour states (a random walk), thereby agents

are not endowed with any particular trading strategy. The agents preference to buy or sell is revealed only when a firing threshold is reached, at which point other agents may be induced (via observational herding) to imitate the decision of the initial agent, regardless of their own preference. In this regard both spurious and intentional herding [Bikhchandani and Sharma, 2000] may occur in the model, with equal probability. The inducing of agents towards the firing threshold is represented by stochastic pulse-coupling on a network, with  $N$  agents represented by  $N$  network vertices, with network edges able to successfully transmit a given pulse-coupling event with probability  $p = Kq/N$ , as described in the previous chapter.

### **Rationale for modelling approach.**

While this model may appear overly simplistic, empirical and theoretical financial economic justification for the modelling choices can be provided.

#### **i. Random walk/diffusion as a model for the accumulation of private agent information and sentiment.**

First, on theoretical grounds, the importance of noise traders [Kyle, 1985] has long been established as essential for the functioning of markets [Black, 1986; Shleifer and Summers, 1990]. Indeed, the conclusion of the no-trade theorem of Milgrom and Stokey [1982] states that in a market consisting entirely of economically rational traders, where common knowledge about the market structure exists, no exchange (trades) would take place - as it would be irrational to do so. Moreover, traders hedging existing positions or products, aiming to provide market liquidity, or trade on no information at all, can be classified as noise traders (Bloomfield et al. [2009], and for a recent literature review, see Ramiah et al. [2015]).

The relatively recent emergence of high and ultra-high frequency traders as significant market participants (numerous reports on participation rates in equity trades are broadly consistent, with approximately 35% in European markets [Menkveld, 2014], 74% for a 2010 sample of U.S. markets [Brogaard, 2010] and 77% in U.K. markets [Mizen and Rhode, 2011], while Easley et al. [2012] reports similar values) adds another dimension

to the continuing debate surrounding how noise traders contribute to the dynamics of market prices. While the question of whether high frequency traders represent true liquidity providers, as opposed to providers of phantom (or fleeting) liquidity [Golub et al., 2012] remains unresolved, the issue of whether such traders act upon solely fundamental news (and therefore not to be considered as noise traders) is easier to answer. Given trades and quotes are often placed at sub-millisecond intervals, which far exceeds the frequency with which fundamental corporate news is released (annual and quarterly reports, stock-split and dividend announcements, bankruptcies, mergers and acquisitions do not occur at sub-millisecond frequencies for a security issued by a single corporate entity) [Fricke and Gerig, 2015], it would appear high frequency traders are closer to noise traders than fundamental-based traders. Furthermore, in the case where agents are endowed with evolutionary competing strategies, simple trading rules may outlive (and even outperform), other so-called fundamental strategies [Hommes, 2001].

Finally, in a detailed study of U.S investment mutual fund performance Fama and French [2010] find only weak evidence in favour of investor skill, over investor luck. And using a similar data set, Barras et al. [2010] find that 25% of mutual funds are classified as unskilled, while 0.6% are classified as skilled using statistical tests on the distribution of cross-sectional returns.

Taking these arguments into account, at the aggregate market level, a random walk model of the accumulation of agent information is plausible.

## **ii. Separation of private agent information and public knowledge via a pulse-coupling model.**

Separating the accumulation of agent information, or sentiment, into a private phase and public phase (via the probabilistic observation of market prices) fundamentally reflects the expectations of investors (whom compensate agents for the use and application of their private knowledge for investing on their behalf) and financial regulators (whom encourage agents to act in accordance with their fiduciary duties). It is this observation that partly motivates the choice of an integrate-and-fire mechanism that forms

the basis of the model described in chapter 4. While consideration of the interaction (or communication) structure amongst economic agents is relevant (represented by the pulse-coupling mechanism used in the model presented in chapter 4), it is equally important to allow for agents to act in a seemingly independent capacity - and to study how the two modes of behaviour may interrelate. Indeed, lattice Ising-like models that assume direct or continuous agent coupling is an example of a modelling paradigm that does not demarcate between independent and dependent agent actions. It is noted, that although an argument has been put forward for a random walk model of the accumulation of private agent information - this does not preclude using a correlated random walk (for instance) to simulate a concentration of similar trading strategies.

### **iii. The preference for simple behavioural models over complicated ones.**

In accordance with the principle of parsimony, given that a multitude of behavioural mechanisms may be responsible for the same observed phenomena - and the difficulty associated with ruling certain mechanisms out (a falsification problem) - models that are simple enough to discern cause-and-effect between behavioural mechanisms and observed phenomena represent a viable way to approach modelling.

## **5.1 Financial market model**

As an application of the  $(K, q)$  process, we illustrate how it may be incorporated into a simple model of financial returns. Let the logarithmic price return,  $r_{t, \Delta t}$  over some interval  $\Delta t$  starting at time  $t$  be given by

$$r_{t, \Delta t} = \log P_{t+\Delta t} - \log P_t = \log \left( \frac{P_{t+\Delta t}}{P_t} \right) \quad (5.2)$$

where,  $P_t$  is the price of a traded asset - such as a stock, bond or commodity. We regard the cascade sizes  $m$ , generated by the actions of traders in our model, as excess demand for a financial asset. When the excess demand is positive, the price of the asset will increase and vice-versa it will decline when excess demand is negative (excess supply). Given an excess demand (cascade size) of  $m$ , the price impact function [Lillo et al.,

2003],  $F$ , dictates the magnitude of the price change by mapping  $m$  to a positive real variable, so that  $F(m) \in \mathbb{R}$ . In order to keep the model as simple as possible, we follow previous works [Cont and Bouchaud, 2000] and take  $F(m) = \lambda m$ , for some  $\lambda > 0$  referred to as the market depth parameter.

To summarise, by rearranging Eqn. (5.2) and setting  $\Delta t = 1$ , the 1-period price update can be formed as

$$P_{t+1} = P_t e^{\lambda m} \quad (5.3)$$

where  $\lambda m$  is identified with the 1-period return:  $r_{t,1}$ . More generally, let  $M$  be a variable representing observations  $\{m_1, m_2, \dots\}$  from the  $(K, q)$  cascade process. Then we can write the  $n$ -period price as

$$P_n = P_0 e^{\lambda \sum_{i=1}^n m_i}. \quad (5.4)$$

Recall that trades occur in continuous time with an exponentially distributed waiting time between trades. In order to fully specify the price process, we write this as a compound Poisson process

$$J(t) = \sum_{i=1}^{n(t)} M_i. \quad (5.5)$$

Each  $M_i$  follows the distribution of  $M$  and  $\{n(t)\}$  is a Poisson process with rate  $\theta$ , used to describe the time between trades (and any ensuing cascades). Finally, for time  $t > 0$  we write,

$$P_t = P_0 e^{\lambda J(t)} \implies r_{0,t} = \lambda J(t). \quad (5.6)$$

For the case  $K = 1$ , recall that cascades are statistically independent identically distributed events. As a result, using standard results of compound Poisson processes, and noting that the mean cascades size is zero due to symmetry, the variance of  $J(t)$  can be given as:  $\text{Var}(J(t)) = \theta t \mathbb{E}\{M^2\}$ . When  $M$  is approximated as a mixture distribution of two equally weighted negative binomial distributions symmetric about 0 we have

$$\text{Var}(J(t)) = \theta t \sigma^2(q) \quad (5.7)$$

where  $\sigma^2(q)$  is given by Eqn. (4.18). This connects the variance of model price returns, of all periods, to the network coupling probability.

A comparison between simulated values of  $\sqrt{\text{Var}(J(t))}$  (the standard deviation of period  $t$  returns  $r_{0,t}$  with  $\lambda = 1$ ) and  $\sqrt{\theta t} \sigma(q)$ , using Eqn. (4.18), is shown in Fig. 5.1. Parameter values used are  $N = 1000$  and  $q = 0.6$ . For each  $t$  shown, 100 values of  $\sqrt{\text{Var}(J(t))}$  are plotted, where the variance is taken over 200 period  $t$  returns. By appealing to standard results concerning random diffusion without drift between two symmetric absorbing barriers [Redner, 2001],  $\theta = N/K^2$ .

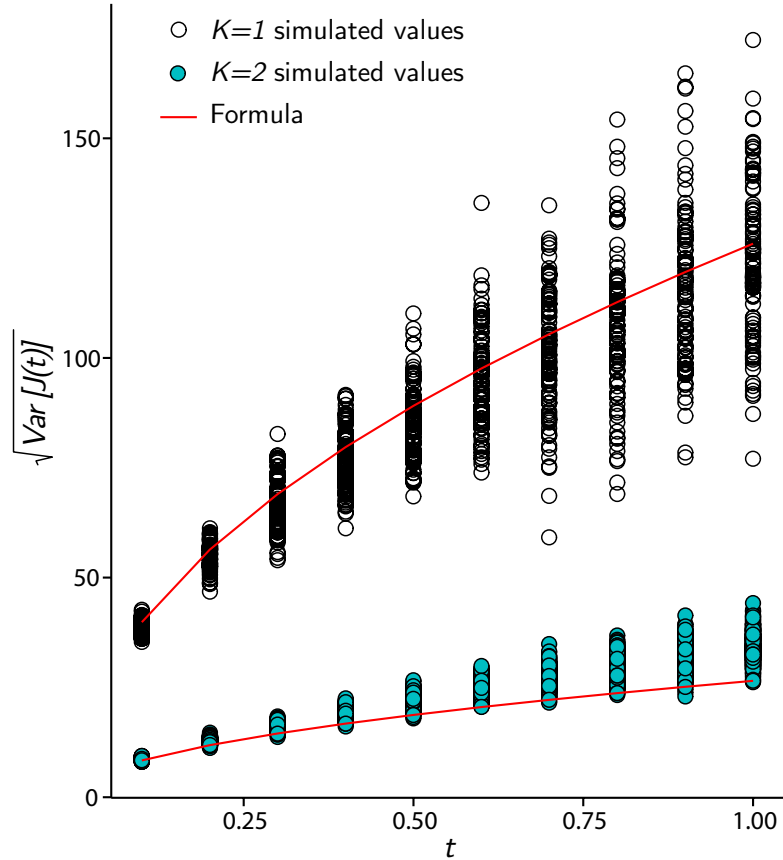


**Figure 5.1.** Simulated values of the standard deviation (volatility) of period  $t$  returns, for  $0 < t \leq 1$ , given by Eqn. (5.6) with  $\lambda = 1$ , compared to values given by Eqn. (4.18). Values for both  $K = 1$  (open circles) and  $K = 2$  (filled circles) are displayed. For  $K = 2$ , the formula underestimates the mean simulated value, due to dependence between returns.

## 5.2 Comparison to market data

**Equity returns.** As an example of the use of the  $(K, q)$  financial market model, indicative values of  $K$  and  $q$  are computed in order to estimate the distribution of market returns for a randomly selected instrument (General Electric equity stock) over two different time scales, and summarised in Fig. 5.2. To produce the plot shown in Fig. 5.2a, end of day closing prices from January 3 2003 to February 6 2015 are used to compute the daily log-return distribution, and this is compared with a  $K = 2$ ,  $q = 0.85$  distribution with market depth parameter,  $\lambda$ , of  $8.2 \times 10^{-3}$ . For Fig. 5.2b we use intraday data to compute non-zero log-returns, of approximately 1.5-second intervals, over a period of time capturing the so-called flash-crash of May 6 2010. In particular, we use data from May 6 2010 14:05 to 15:25 (EST), resulting in 3390 data points to compute the cumulative probability and compare this to a  $K = 2$ ,  $q = 1.05$  distribution with  $\lambda = 5.2 \times 10^{-5}$ . While these comparisons are provided as illustrative, rather than representing detailed statistical best-fits, it is of interest to note Fig. 5.2b showing  $q > 1$  during the extremely volatile period of the flash-crash, as one might expect.

### **Option on an equity index.**

One of the reasons for the persistence of Gaussian-based models of financial returns, is the body of knowledge accumulated to price derivative contracts [Hull, 2011] - and most notably the framework of Black, Scholes and Merton (BSM) [Black and Scholes, 1973; Merton, 1973], that enables a price of certain derivative contracts to be computed using closed form formulae. To account for the gap between real market characteristics and the Gaussian assumptions that underpin the BSM framework, traders make an adjustment to the volatility of returns (a parameter of the BSM pricing formula) to account for the observed heavy tails of financial returns [Derman and Kani, 1994; Pan, 2002]. As a result, when the volatility used to price derivative contracts is plotted against the strike price of option contracts, the resulting implied volatility curve is known as the volatility smile, due to its curved appearance, indicating larger values at the extremes of strike price.

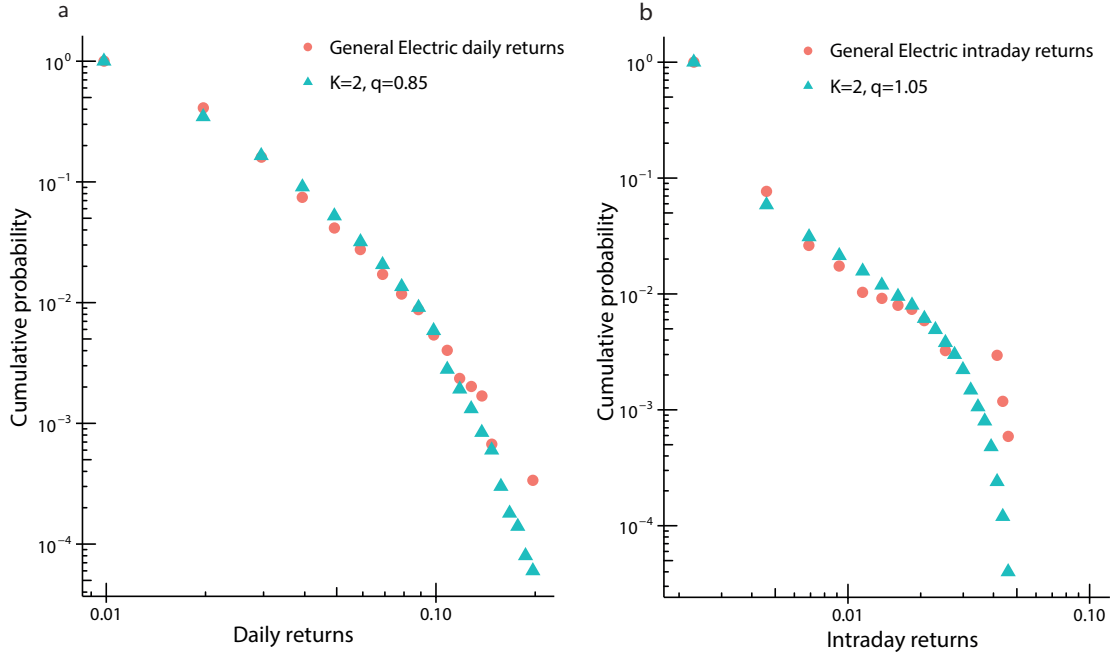


**Figure 5.2.** a) The cumulative probability distribution of daily non-zero returns for a randomly selected stock, General Electric, computed using data for the period January 3 2003 to Feb 6 2015 (3045 points) (filled circles). Overlaid is the distribution of  $K = 2$ ,  $q = 0.85$  using market depth  $\lambda = 8.2 \times 10^{-3}$ . b) The cumulative probability plot of the same stock as in a), but using intraday price returns computed at, on average, 1.5 second intervals over the period May 6 2010 (flash crash), 14:05 to 15:25 (3390 data points) (filled circles). Overlaid is the distribution of  $K = 2$ ,  $q = 1.05$  using market depth  $\lambda = 5.2 \times 10^{-5}$ .

I demonstrate that the  $(K, q)$  model is able to recover approximate market prices of European options (see appendix C) by matching the market price implied volatility smile. Data consisting of European call options written on the afternoon-settled S&P 500 (SPXpm) index as of November 25 2014, with an expiry of December 20 2014, is used. Options have a strike price between 2000 to 2250, with the SPXpm index level at 2067.03 at the close of November 25 2014. For a model comparison, the recovered implied volatility from a simulation of the Cont-Bouchaud percolation model [Cont and Bouchaud, 2000] is also shown. While the  $(K, q)$  model compares favourably to the Cont-Bouchaud model (parametrised by  $q_{\text{Cont}}$ ), the latter possesses one less effective parameter compared to the  $(K, q)$  model. Indeed, since the Cont-Bouchaud model is a static bond percolation model, it is most similar to the  $(K, q)$  when  $K = 1$ . Figure. 5.3 demonstrates the recovered volatility smile for these data. The fit, while not perfect, does match the general shape of the smile (although it must be taken into account that

volatility smile modelling is not a principle aim of either the  $(K, q)$  or Cont-Bouchaud models). To obtain the volatility smile, a large number of draws from the simulated asset return distributions derived from both models is taken, and the empirical option pricing procedure outlined in Bouchaud and Sornette [1994] is applied to obtain prices for call options for the given expiry and strike prices. The implied volatility is then recovered by using a simple numerical root-search. The recovered implied volatilities are compared to those obtained via market data, and the process is repeated with different values of  $K$ ,  $q$  and  $q_{\text{Cont}}$  until suitable fits are found.

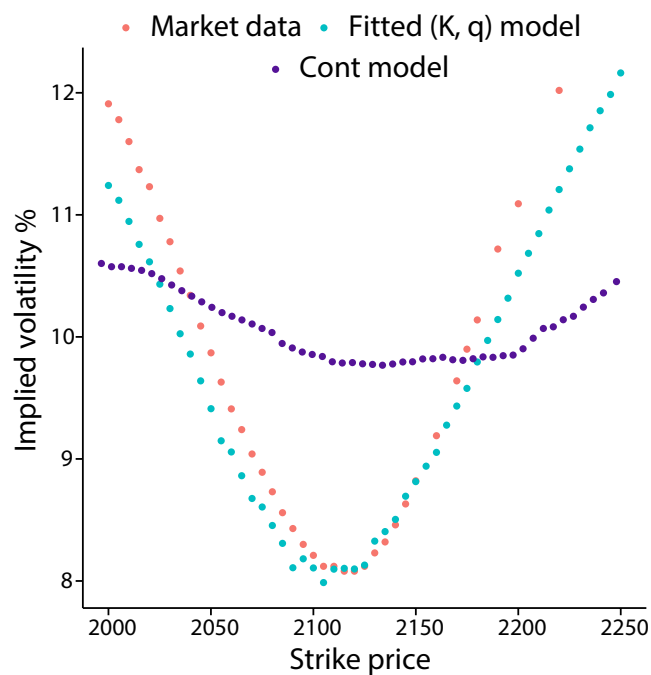


**Figure 5.3.** The Black-Scholes implied volatility smile obtained from market data of European call options on the SPXpm index is compared with the implied volatility obtained from empirical option prices, generated using a  $K = 2$ ,  $q = 0.78$  model, and the Cont-Bouchaud percolation model (with  $q_{\text{Cont}} = 1.01$ ), described in the main text. While the  $(K, q)$  model compares favourably with the Cont model, it must be remembered that the Cont-Bouchaud model has 1 less effective parameter compared to the  $(K, q)$  model.

In this section, a detailed probabilistic analysis of the stochastic pulse-coupled network model [Wray and Bishop, 2014] was carried out, yielding an asymptotic expression for the probability distribution of cascade size for the case  $K = 1$ , given by Eqn. (4.17). In general, the cascade size distribution takes the form of truncated power law, and reduces to a pure power law at the critical coupling parameter value  $q = 1$ . This result

is consistent with similar processes, such as the sub-critical Galton-Watson process. For the case  $K \geq 1$ , I demonstrated how a mixture of negative binomial distributions may be used to approximate the cascade size distribution when  $0 < q < 1$ .

Lastly, the stochastic pulse-coupled model is incorporated in to a new model of a stylised financial market, similar in character to the financial market models of Eguíluz and Zimmermann [2000] and Cont and Bouchaud [2000] and variants thereof. The model presented here differs from those previous network-based financial models in a number of critical ways. Firstly, our model is inherently dynamic - with the diffusion phase of the pulse-coupling controlling the time interval between pulse-coupling (and therefore cascade) events. The Cont and Bouchaud model, in contrast, is effectively a static bond-percolation on an Erdős-Rényi network, where ‘clusters’ on a network are formed simultaneously, and each assigned a random designation of buy, sell or hold. Excess demand or supply in this framework is therefore determined by the relative cluster sizes. In this regard, the  $K = 1$  model presented here results in a similar probability distribution for the simulated asset returns because the cascade sizes, induced by pulse-coupling, is equivalent to cluster size in standard bond-percolation on an Erdős-Rényi network.

Secondly, for  $K > 1$ , the cascade sizes are similar to so-called explosive percolation [Achlioptas and Spencer, 2009; Bohman, 2009; Chen et al., 2013], reviewed by Ziff [2013], in which the percolation transition becomes increasingly abrupt (although continuous [Da Costa et al., 2010]) and occurs, delayed, at a higher value of bond occupation probability. In the pulse-coupled model, as  $K$  increases, the transition to the large-cascade regime occurs at increasingly larger values of network coupling probability (see Fig. 4.4 of the previous chapter, noting the parametrisation  $p = Kq/N$ ). The model presented here, then, differs from the Cont-Bouchaud model in the types of percolation present in the system. Explosive percolation is covered in more detail in the next chapter.

It is of interest to note that the  $K = 2$  model is favoured over the  $K = 1$  model, when

model output is fit to the various stock market data shown in Figs. 5.2 and 5.3.

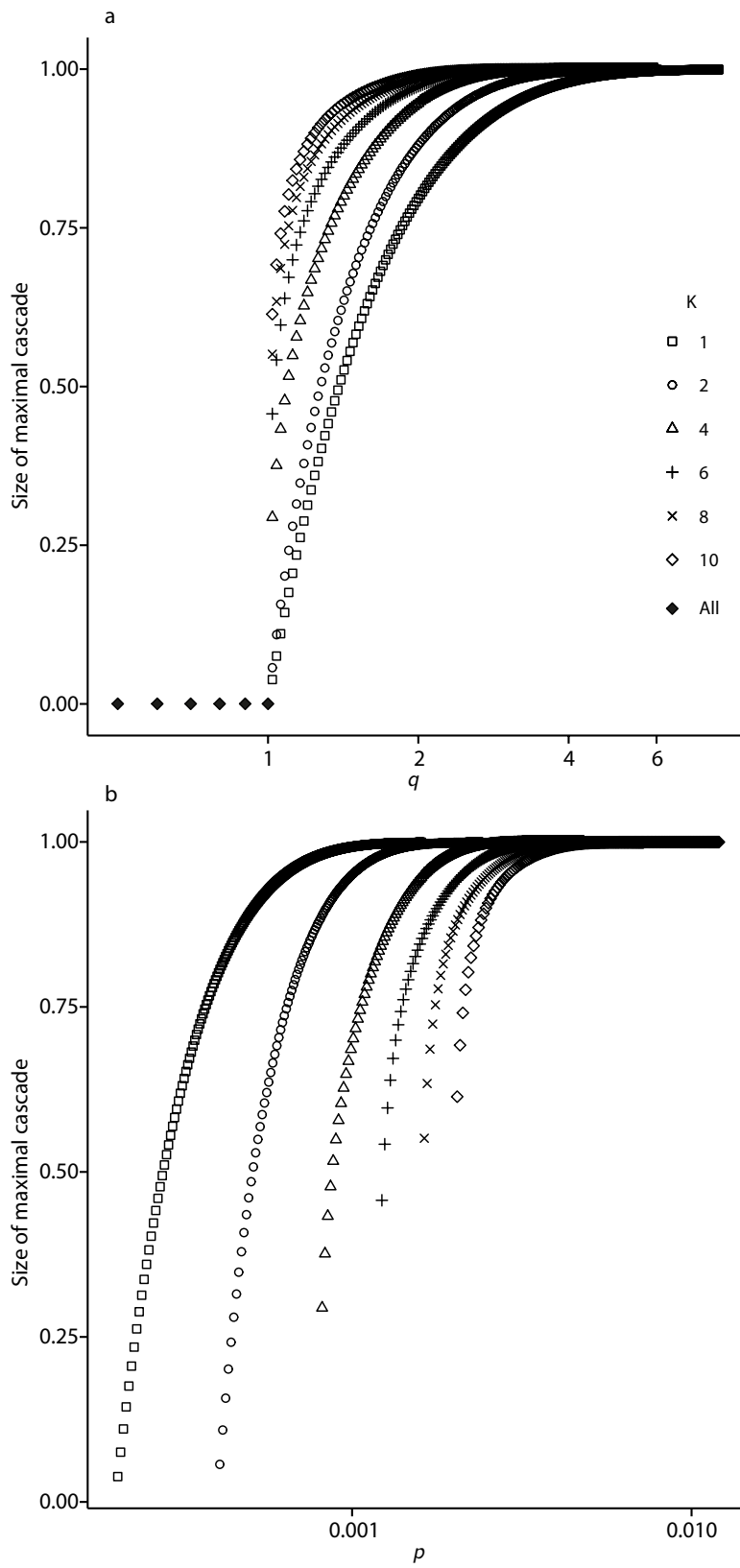


**Figure 5.4.** Log-linear plot of maximal cascade size for various  $K$  in a)  $q$ -space and b)  $p$ -space

### 5.2.1 Volatility clustering and long-memory

Zumbach [2011] details three functional forms of volatility autocorrelation,  $C(L, d)$ , given by Eqn. (2.26), each characterised by the rate of decay (exponential, logarithmic and hyperbolic), and provides evidence supporting the logarithmic decay of volatility autocorrelation. For ease of reference, the definitions of  $C(L, d)$  and the form of hyperbolic decay (a hallmark of long memory) are repeated here as Eqns. (5.8) - (5.9)

$$C(L, d) = \text{Corr}(|r_{t+L, d}|, |r_{t, d}|), \quad (5.8)$$

where  $L$  is the lag,  $r$  is the log-return and  $d$  is the horizon over which the return is calculated. Volatility is said to possess long memory [Baillie, 1996; Zumbach, 2004] when autocorrelation remains positive and, in particular, decays hyperbolically over large time-lags. Formally,

$$C(L, d) \sim AL^\gamma \text{ as } L \rightarrow \infty, \quad A > 0, \gamma < 0. \quad (5.9)$$

While volatility clustering is a much studied phenomenon, the behavioural causes of this effect remain only partially understood. In particular, two major behavioural mechanisms capable of generating volatility clustering have been identified in the literature. First, strategy switching amongst a group of agents, originating from ideas presented by Kirman [1993], and subsequently utilised in a number of studies [Lux and Marchesi, 2000; Alfarano and Lux, 2007; Xue and Gençay, 2012; Tseng and Li, 2011]. Second, is heterogeneity in agent time scales [Feng et al., 2012; Lynch and Zumbach, 2003; Giardinà and Bouchaud, 2003; Zumbach and Lynch, 2001], where more attention has been given to purely statistical models incorporating the heterogeneity of agent time-scales in models of market volatility and price dynamics [Bacry et al., 2001; Di Matteo, 2007; Bacry et al., 2012] (reviewed in Borland et al. [2005]). While such models are able to produce many of the observed features of financial time series, they lack behavioural explanations or interpretations for their dynamics.

Aside from behavioural models, other important classes of models that aim to capture volatility clustering effects include, stochastic volatility models (LeBaron [2001], and see Shephard and Andersen for an overview), GARCH-family of models [Bauwens et al., 2012], and regime-switching models [Liu, 2000; Liu et al., 2012]. While an in-depth study of these models is outside the scope of this thesis, they occupy a large and important proportion of the relevant literature.

In order to test for volatility clustering, substantial simulations, and a battery of statistical tests, are carried out and the results presented in the next section.

### **Simulation details**

In both the finite state-space and semi-infinite state-space case, simulations are performed (see Figs. 5.5-5.11) according to the following specification. Together the parameters  $N$  and the threshold distribution amongst the agents, which may be constant or vary, determine the speed of the simulation, which is measured by average trade arrival rate,  $j$ . For each of the simulations, the average trade arrival rate time is standardised. Returns are standardised, and the generated time-series are of equal length,  $X$ . The returns are taken over a unit of time equal to  $\delta t = \frac{5}{60}T = 0.083T$ , which equates to 5-minutes returns, when a unit of simulation time,  $T$ , is taken to be an hour. For these parameter values to reflect realistic market activity, with the unit of time  $T$  is fixed (at say one hour, or one minute or one day),  $N$  would need to be varied accordingly, to make the arrival rate of trades in the unit of time,  $T$ , realistic. In summary, although the threshold values, or distribution, varies along with  $N$ , in the simulations below, the average arrival rate of trades is constant. With the understanding above,  $\delta t = 0.083$ , Other than adhering to those common sense rules, the parameters were chosen arbitrarily and not tweaked.

Parameter	Value (if set)	Function
$\delta t$	$\frac{5}{60}T$	Return period
$j$	$10^{-3}T$	Average trade arrival rate
N	Variable	Number of distinct agents
X	$10^4$	Length of returns time series
T	1 (unit unset)	Determines the unit of 1 simulation time unit

**Table 5.1.** Parameter values of simulation corresponding to Figs. 5.5-5.11

For each simulation figure, the following statistical tests are run:

1. MLE estimate of the power-law exponent is computed for models returns (upper right panel).
2. Functions, exponential ( $Ae^{-\gamma L}$ ), logarithmic ( $A + B\log(L)$ ) and hyperbolic ( $AL^{-\gamma}$ ) are fit to the volatility auto correlation via non-linear least squares (lower left panel).

For Figs. 5.5 - 5.11, panel **a** depicts a sample of the generated time series arising from the particular simulated model. Panel **b** shows the distribution of the absolute value of log-returns from the particular simulated model, and a moment matched Gaussian distribution for comparison. In panel **c**, the coloured bands surrounding the volatility autocorrelation represent the one standard deviation limits and a non-linear least squares fit of the mean volatility autocorrelation. Panel **d** shows three samples of the volatility correlation, that is computed each time the simulation is replicated. Note for all of Figs. 5.5 - 5.11, panel **c** shows zero serial correlation in log-returns, in agreement with empirical observations (see chapter 2).

It is noted that the features observed have been tested over many parameter combinations  $N = 1$  to  $N = 10000$ , and over various values and distributions of  $K$  - suggesting the results, in particular long-memory patterns, are robust.

### **5.2.2 Volatility clustering in the finite state space case**

The numerical results of three scenarios are presented and discussed.

#### **Homogeneous model: Agents with identical firing thresholds. Fig.5.5**

This scenario consists of all agents having a single firing threshold equal to  $K = 1$ . In this case, agent time scale are homogeneous, and the probability coupling parameter is fixed. As might be expected, no evidence of volatility clustering is found, and no evidence of long memory in volatility is found. The estimated power-law exponent for the distribution of model returns is 7.0.

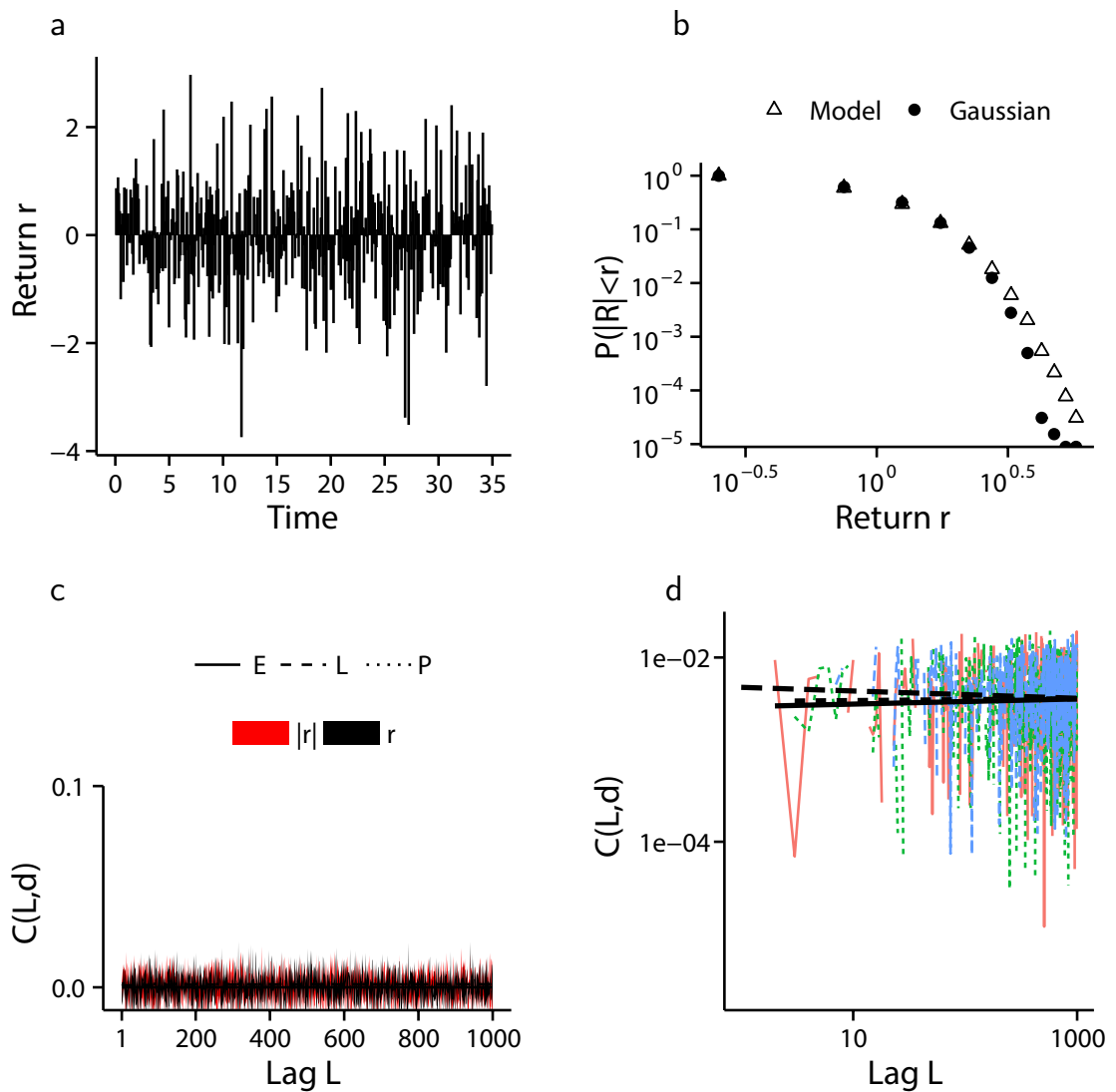


**Figure 5.5.** The results from ten independent simulations each of 150,000 cascades for  $N = 200$ ,  $K = 1$  and  $q = 1$  is presented. (a) A sample from one of the ten simulated log-returns series. (b) Comparison of the distribution of log-returns arising from the model ( $\triangle$ ) with a moment matched Gaussian distribution ( $\bullet$ ), shown in log-log scale showing fat-tails. MLE estimate of the power law exponent of model returns is 7.0. All simulated data used. (c) one standard deviation envelope around the mean volatility autocorrelation of log-returns ( $r$  and black) and absolute log-returns ( $|r|$  and red) with lag  $L$ , together with the non-linear least squares fit of exponential (labelled E - solid line), logarithmic (labelled L - dashed line) and hyperbolic (labelled P - dotted line) decay functions, with exponential decay providing the best fit. The correlation exponent is not computed as  $C \sim 0$ . All simulated data used. (d) a random sample of three out of ten volatility autocorrelation computations with hyperbolic decay lines of best fit, shown in log-log scale.

**Inhomogeneous model: Agents non-identical firing thresholds. Fig. 5.6**

Surprisingly, no evidence of volatility clustering or long memory is found, even though agents act over inhomogeneous time scales.

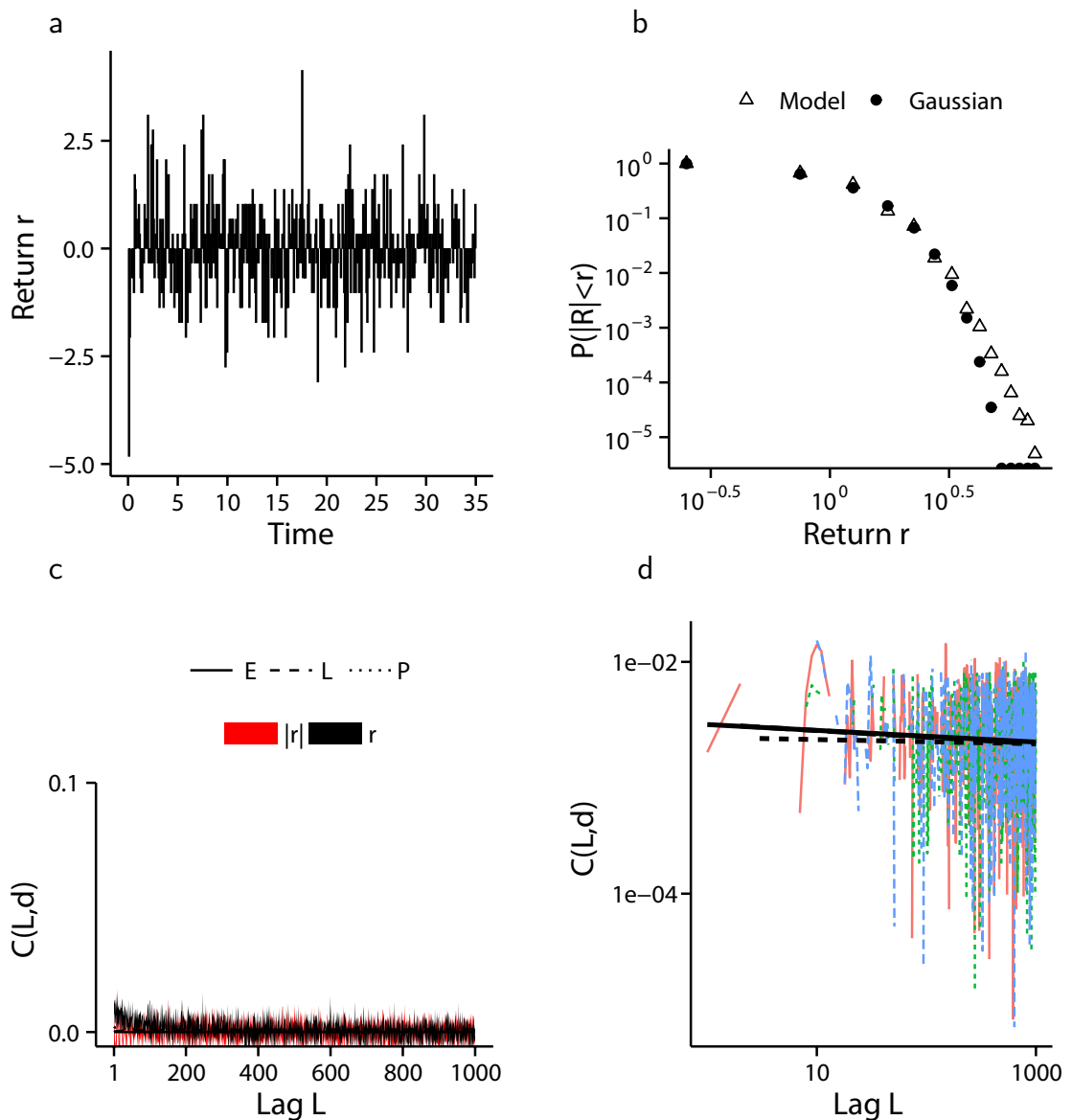


**Figure 5.6.** The results from ten independent simulations each of 150,000 cascades for  $N = 700$ ,  $K \sim U[1, 20]$  and  $q = 1$  is presented. (a) A sample from one of the ten simulated log-returns series. (b) Comparison of the distribution of log-returns arising from the model ( $\triangle$ ) with a moment matched Gaussian distribution ( $\bullet$ ), shown in log-log scale showing fat-tails. MLE estimate of the power law exponent of model returns is 6.5. All simulated data used. (c) one standard deviation envelope around the mean volatility autocorrelation of log-returns ( $r$  and black) and absolute log-returns ( $|r|$  and red) with lag  $L$ , together with the non-linear least squares fit of exponential (labelled E - solid line), logarithmic (labelled L - dashed line) and hyperbolic (labelled P - dotted line) decay functions, with exponential decay providing the best fit. The correlation exponent is not computed as  $C \sim 0$ . All simulated data used. (d) a random sample of three out of ten volatility autocorrelation computations with hyperbolic decay lines of best fit, shown in log-log scale.

**Homogeneous model: Agents identical threshold  $K$  and time varying coupling probability parameter. Fig.5.7**

In this case,  $K = 1$  for all agents, and the network coupling parameter,  $q$ , is made to vary according to an exponential Ornstein-Uhlenbeck mean reverting process around  $q = 1$  [Karatzas and Shreve, 1991]. In this case volatility clustering is expected due to the system fluctuating across the critical coupling parameter value of  $q = 1$ . Figure.5.7 shows that volatility clustering with exponential decay is recovered. The parameters of the Ornstein-Uhlenbeck (OU) process were set at  $\sigma_{OU} = 0.035$  and mean reversion  $\theta_{OU} = 0.02$ . It is noted that the volatility for of the return is given by Eqn. (4.19).

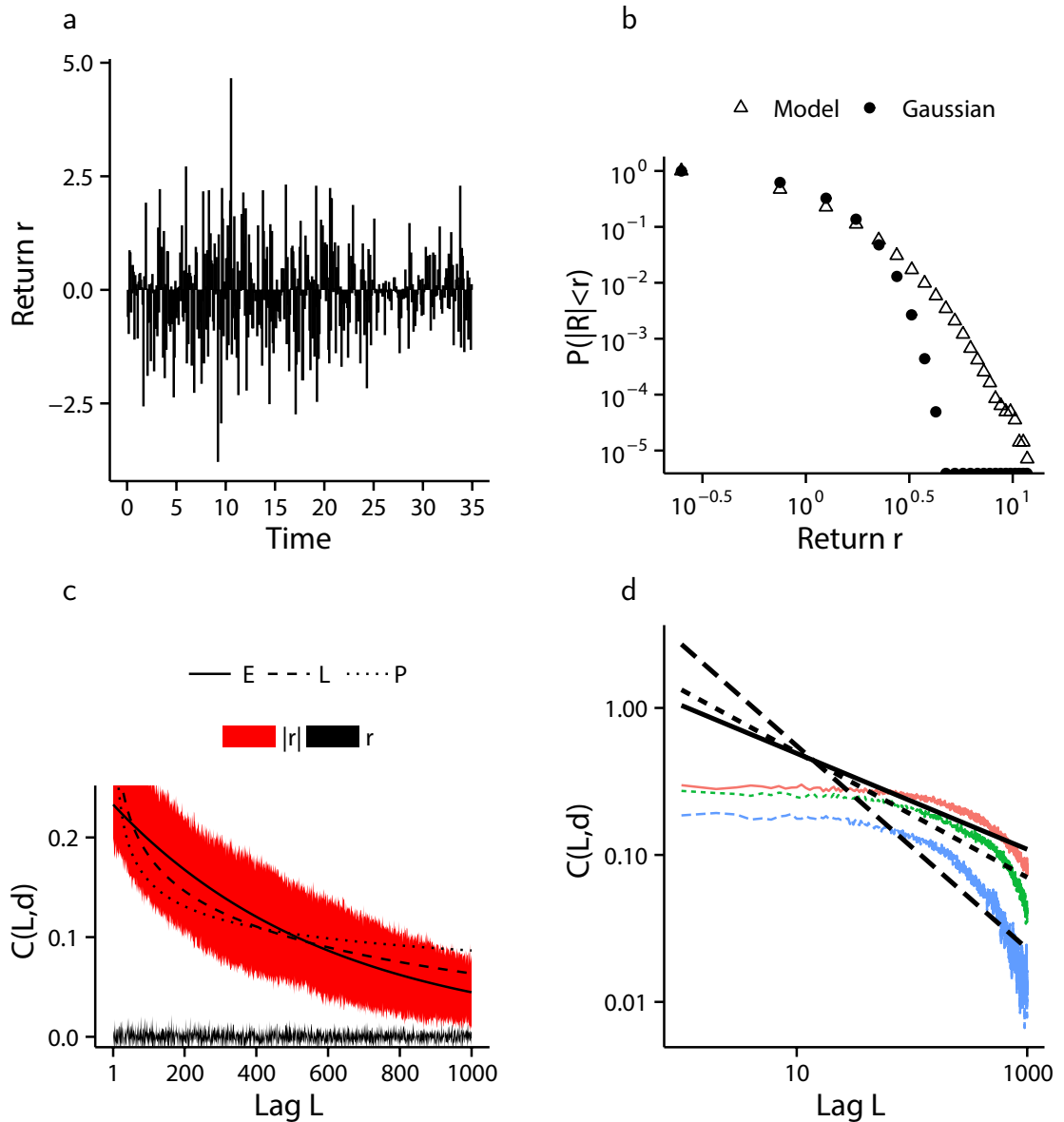


**Figure 5.7.** The results from ten independent simulations each of 150,000 cascades for  $N = 90$ ,  $K = 1$  and  $q$  time-varying according to an OU process with  $\sigma_{OU} = 0.035$ ,  $\theta_{OU} = 0.02$  is presented. (a) A sample from one of the ten simulated log-returns series. (b) Comparison of the distribution of log-returns arising from the model ( $\triangle$ ) with a moment matched Gaussian distribution ( $\bullet$ ), shown in log-log scale showing fat-tails. MLE estimate of the power law exponent of model returns is 6.2. All simulated data used. (c) one standard deviation envelope around the mean volatility autocorrelation of log-returns ( $r$  and black) and absolute log-returns ( $|r|$  and red) with lag  $L$ , together with the non-linear least squares fit of exponential (labelled E - solid line), logarithmic (labelled L - dashed line) and hyperbolic (labelled P - dotted line) decay functions, with exponential decay providing the best fit. The correlation exponent is obtained by non-linear least squares to give  $C \sim \exp(-0.0016L)$ . All simulated data used. (d) a random sample of three out of ten volatility autocorrelation computations with hyperbolic decay lines of best fit, shown in log-log scale.

### 5.3 Analysis of the stochastic system: semi-infinite state-space

Here, one of the firing thresholds is removed (the lower boundary is removed, without loss of generality) allowing the state-space defining the accumulation of private agent information to be replaced with the semi-infinite region (compare Eqn. (4.1) in chapter 4). In numerical results, a distribution of thresholds  $D$ , is incorporated, so that agents with different thresholds coexist. Numerical results presented below suggest that when  $D$  is left skewed, as a power law in Eqn. (5.10) long-memory patterns generically appear in asset return volatility (see Figs.5.10-5.11).

$$D(K) \sim (1 + K_{\max} - K)^{-\alpha}, \quad (5.10)$$

$$\theta_u(t) \in \mathbb{Z}_{\leq K}, \quad (5.11)$$

with  $u \in [1, 2, \dots, N]$  an index for each agent. While this represents a relatively minor amendment to the model, the system dynamics are altered quite considerably, in comparison to the bounded state-space case. In this section, I demonstrate using substantial numerical simulation, how the system with this amendment generically reproduces many of the observed features of financial time series, including evidence of long memory in volatility.

Initially, this model may appear to represent a physically infeasible situation with regards to participants in a financial market, because the mean first passage time for a single unbiased random walk in a semi-infinite region to reach a fixed boundary is known to be infinite [Redner, 1982]. Although, for a random walk biased towards the fixed boundary, the mean first passage time,  $\tau$ , is finite and given by

$$\tau(\hat{p}, K) = \frac{x_0 + K}{2\hat{p} - 1}, \quad \frac{1}{2} < \hat{p} \leq 1, \quad K > 0, \quad (5.12)$$

where  $\hat{p}$  is the biased probability, starting at position  $x_0$ , at each time step, of moving towards the fixed boundary  $K$  (see Fig. 5.8). Due to the network effect of pulse-coupling, agents are induced towards the firing threshold, and since there is only a single firing threshold, the unbiased random walk of agent information accumulation - in the unconnected case - behaves more like a biased random walk, as coupling probability increases. It follows from Eqn. (5.12), that when the coupling probability  $p = qK/N > 0$ , agents will have finite mean first passage times.

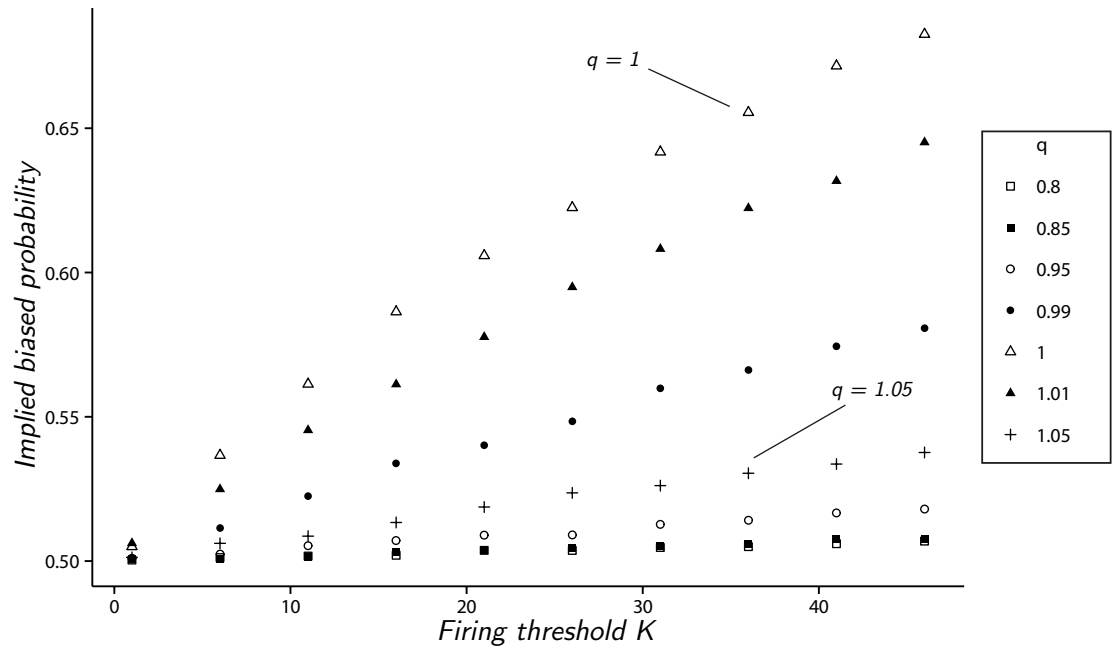


**Figure 5.8.** A randomly selected agent, one for each threshold, is followed by the simulation and mean hitting time is computed and compared with Eqn. (5.12), to infer the implied bias probability.

It is noted that for some categories of financial market participants, long durations between trading events may accurately describe their intrinsic trading frequency. For instance, so-called buy-and-hold long-term fundamental investors may hold the same security for years [Cella et al., 2013].

An economic basis for considering a semi-infinite state-space can be developed by first noting that the mean time to reach the firing threshold for a single uncoupled agent is approximately Lévy distributed, and in the presence of pulse-coupling the same passage time is approximately distributed as inverse Gaussian [Barndorff-Nielsen, 1997]

(by identification of the biased random walk described above with Brownian motion with drift in the continuous limit). In both cases the distribution of sojourn times is heavy-tailed with power law tails of exponent  $\frac{3}{2}$ . Reboredo et al. [2014] presents a statistical analysis showing the time duration between large returns in European equity indices are well-fitted by heavy-tailed distributions, while Liu [2000] develops a statistical regime switching model, where the distribution of the in-regime time duration is heavy-tailed, that displays long-memory patterns in volatility correlation. While these studies do not directly corroborate the modelling assumptions made here, they are evidence that heavy-tailed intra-event durations are not implausible as a model for agent behaviour. Furthermore, investors may withdraw their participation at any given time, depending upon both their sentiment and the prevailing market conditions [Easley et al., 2012, report high frequency traders withdrawing liquidity during the flash-crash of May 2010].

While different market participants undeniably have different investment horizons, holding periods and motivations for participating in financial markets, a consequence of the model developed in this chapter is the idea that the observed investor time scale is the result of two effects. The first, an internal private sentiment process such as cognitive reasoning (knowledge gathering, or risk-aversion), algorithmic, random or imitative. And the second effect comes from indirectly and probabilistically observing the actions of others, via market prices. The conclusion of the sentiment process is modelled as coinciding with an agent reaching a fixed threshold. While the second effect is modelled as instantaneous stochastic pulse-coupling between agents.

While the long-memory patterns appear only when  $q \geq 1$ , I argue, with reference to Fig. 5.12 which shows for a range of threshold distributions over the agents, that when  $q \approx 1$ , the agents minimise their intra-trading times. In contrast to models that keep the agents investment holding period fixed, here it can vary in accordance with the behaviour of other agents.

### **A heuristic argument for self-organised behaviour**

The above can be rephrased as saying there is a stable fixed point in the neighbourhood of  $q = 1$ . A simple heuristic argument for this can be given. Take an agent whom has threshold  $K_1$  and let  $q < 1$  initially. Assume our agent desires to accumulate her knowledge, or sentiment, as fast as possible. The probability that an agent accepts a pulse from another agent is  $K_1 q / N$ , so she would like to make  $q$  as large as possible. On an all-to-all network, in mean field she can be considered to have up to  $K_1$  neighbours, who are assumed fixed. There are two effects that this agent experiences, the first is increased implied bias from receiving pulse-coupling events from her neighbours, allowing her to accumulate sentiment more quickly. But she also gains no bias from her neighbours that reset with her, as they are just as likely to reach the firing threshold after she does, than before. Recall that in the semi-infinite state-space, the mean time to reach the firing threshold without pulse-coupling effects is unbounded. The other effect is, if our agent increases  $q$  without bound, then there is no reason to assume all other will not do the same. But clearly, not all agents can do this, otherwise a macroscopic cascade occurs and all agents are left at the reset, equidistant from the firing threshold. Thus it is highly likely the fixed point, if it exists, is on the boundary of the critical coupling parameter value. As this is when cascade sizes are microscopic compared to the system size and, almost surely, no agent will reset with a neighbour - gaining maximum bias from her neighbours, any deviation from this fixed point will result in an adverse effect, hence the fixed point will be stable.

#### **5.3.1 Volatility clustering in the semi-infinite state-space case**

As for the finite state-space, numerical simulation of the financial market model is performed. In the case where all agents have the same threshold, exponential decay volatility clustering can clearly be seen (Figs. 5.9-5.10). In the case where thresholds are distributed according to an inverse power-law (with many agents with large thresholds and a few with small thresholds) volatility clustering is seen with hyperbolic decay (Fig. 5.11). This together with the slow convergence to Gaussian behaviour (Fig. 5.14),

and the fat-tailed model returns replicate important stylised facts of financial asset markets, using a minimalistic model.

Volatility clustering is generated which decays exponentially in the homogeneous case, and hyperbolically when agent pulse-coupling thresholds are inhomogeneous and distributed according to Eqn. (5.10). The hyperbolic decay visible in Fig. 5.11c is exhibited for all  $\alpha$  tested in the range  $\alpha = 1.5$  to  $\alpha = 5$ , and  $K_{\max} \in [10, 100]$ , although the hyperbolic nature of the decay becomes less pronounced as the distribution  $D$  deviates from the power-law form given by Eqn. (5.10), and becomes virtually non-existent when  $D$  is changed so as to produce a market consisting of many relatively influential (low  $K$ ) agents together with fewer easily influenced (large  $K$ ) agents.

In Fig. 5.13 the average time to threshold is shown when  $D$  is given by a power law with  $\alpha = 2$  in Eqn. 5.10. In Fig. 5.14, a log-log plot showing slow convergence to a Gaussian when the period of returns is increased. In the same figure, the Kolmogorov-Smirnov two sample test statistic and excess kurtosis is plotted, showing the tests for normality are unable to be rejected only after approximately 2 simulation years.

In Fig. 5.12, average time to threshold (hit) time is computed for a range of  $q$ , about  $q = 1$ , and for a range of distributions  $D$ : in order of figure key 1: Power-law(2), 2 : Power-law(3), 3 : Uniform[1,50], 4 : Triangular with mode at  $K = 1$ . A minimum hit time occurs around  $q \approx 1$ , for nearly all threshold distributions.

In terms of economic implications, these results are consistent with previous studies that incorporate heterogeneity of agent time-scales into statistical models of market volatility Bacry et al. [2012; 2001]; Xue and Gençay [2012], although in the models presented here, an explicit trader interaction mechanism is responsible for patterns in asset volatility autocorrelation. Moreover, this model shows how hyperbolic decay of volatility autocorrelation, associated with statistical long-memory, may be the result of a leadership effect [Kononovicius and Gontis, 2014] resulting from the structure and composition of markets with agents of differing trading, or informational, thresholds. Kononovicius and Gontis [2014] detail how a small number of herd-immune agents

can influence and control a larger number of agents whom have a higher propensity to herd. With regards to agents in the model presented here, agents with threshold  $K$  have a probability proportional to  $Kq$  of receiving an incoming pulse-coupling, therefore agents with low- $K$  thresholds are less likely to receive pulse-coupling than an agent with a higher threshold. When the threshold distribution over the agents is then left-skewed (a few agents with low  $K$  thresholds and relatively more with high  $K$  thresholds) as is the case in Eqn. (5.10), the herding conditions are similar to what is studied by Kononovicius and Gontis [2014]. Such an understanding may aid investors in determining appropriate trading strategies for a given market, or in examining if a particular trade or market is crowded, with an abundance of either influential, or easily influenced, traders.

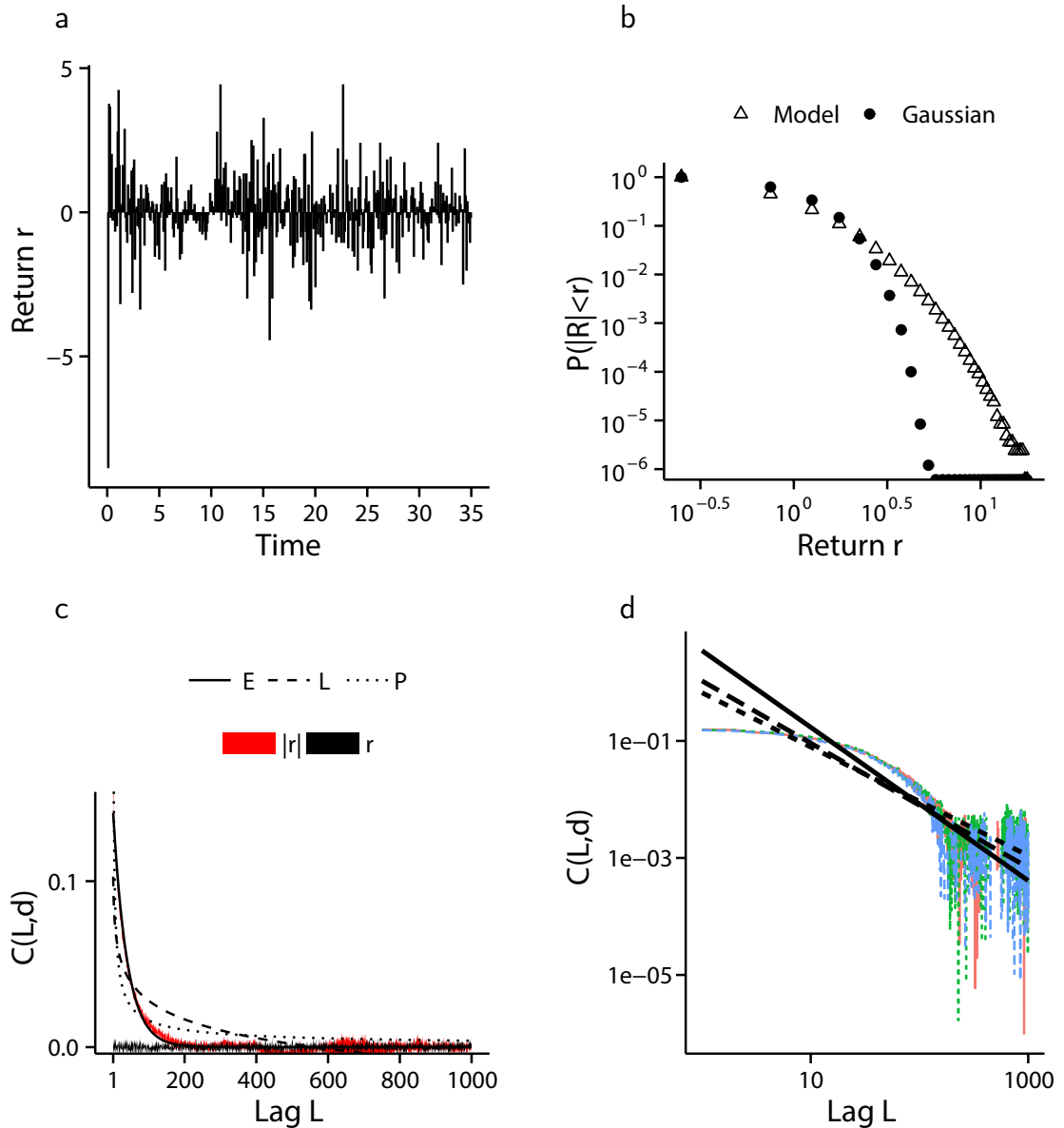


**Figure 5.9.** The results from ten independent simulations each of 150,000 cascades for  $N = 200$ ,  $q = 1$  and  $K = 1$  is presented (a) A sample from one of the ten simulated log-returns series. (b) Comparison of the distribution of log-returns arising from the model ( $\Delta$ ) with a moment matched Gaussian distribution ( $\bullet$ ), shown in log-log scale clearly showing fat-tails. MLE estimate of the power law exponent of model returns is 5.8. All simulated data used. (c) one standard deviation envelope around the mean volatility autocorrelation of log-returns ( $r$  and black) and absolute log-returns ( $|r|$  and red) with lag  $L$ , together with the non-linear least squares fit of exponential (labelled E - solid line), logarithmic (labelled L - dashed line) and hyperbolic (labelled P - dotted line) decay functions, with exponential decay providing the best fit. The correlation exponent is obtained by non-linear least squares to give  $C \sim \exp(-0.25L)$ . All simulated data used. (d) a random sample of three out of ten volatility autocorrelation computations with hyperbolic decay lines of best fit, shown in log-log scale.

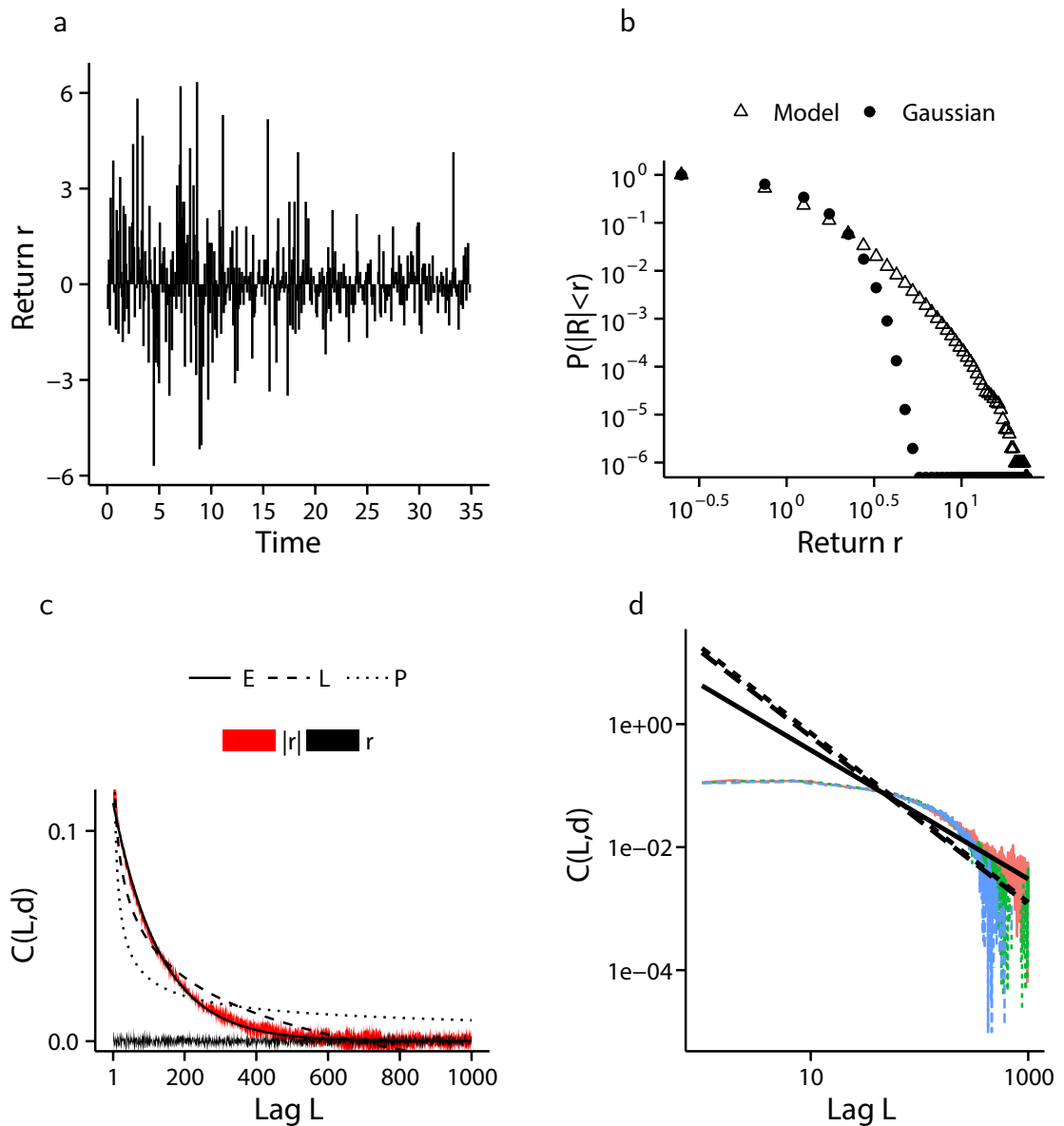


**Figure 5.10.** The results from ten independent simulations each of 150,000 cascades for  $N = 325$ ,  $q = 1$  and  $K = 2$  is presented (a) A sample from one of the ten simulated log-returns series. (b) Comparison of the distribution of log-returns arising from the model ( $\Delta$ ) with a moment matched Gaussian distribution ( $\bullet$ ), shown in log-log scale clearly showing fat-tails. MLE estimate of the power law exponent of model returns is 5.5. All simulated data used. (c) one standard deviation envelope around the mean volatility autocorrelation of log-returns ( $r$  and black) and absolute log-returns ( $|r|$  and red) with lag  $L$ , together with the non-linear least squares fit of exponential (labelled E - solid line), logarithmic (labelled L - dashed line) and hyperbolic (labelled P - dotted line) decay functions, with exponential decay providing the best fit. The correlation exponent is obtained by non-linear least squares to give  $C \sim \exp(7.6 \times 10^{-3}L)$ . All simulated data used. (d) a random sample of three out of ten volatility autocorrelation computations with hyperbolic decay lines of best fit, shown in log-log scale.

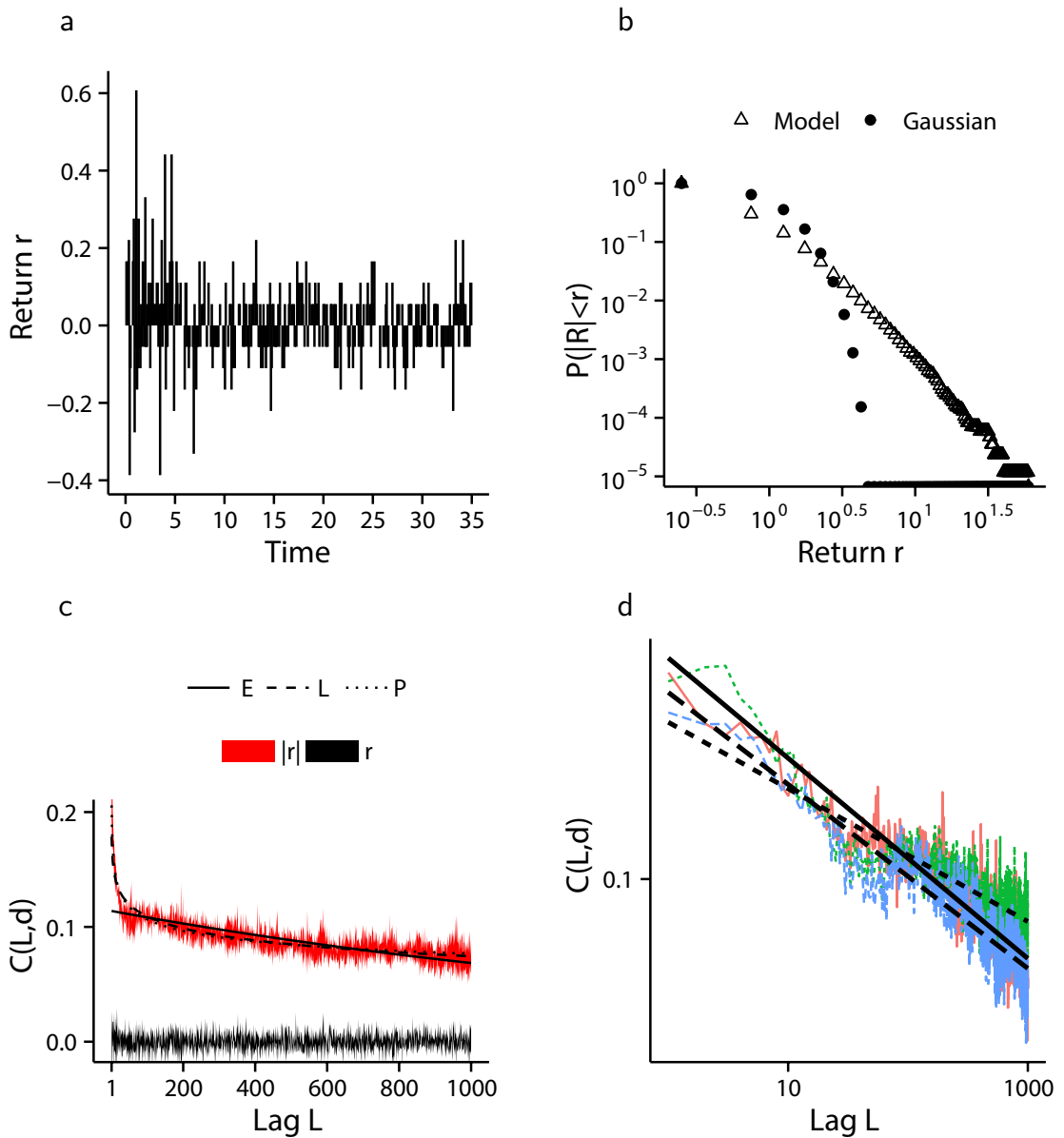


**Figure 5.11.** The results from ten independent simulations each of 150,000 cascades for  $N = 300$ ,  $q = 1$  is presented where firing thresholds are distributed according to Eqn. 5.10 with  $\alpha = 2$  and  $K_{\max} = 20$ . (a) A sample from one of the ten simulated log-returns series. (b) Comparison of the distribution of log-returns arising from the model ( $\Delta$ ) with a moment matched Gaussian distribution ( $\bullet$ ), shown in log-log scale clearly showing fat-tails. MLE estimate of the power law exponent of model returns is 3.5. All simulated data used. (c) one standard deviation envelope around the mean volatility autocorrelation of log-returns ( $r$  and black) and absolute log-returns ( $|r|$  and red) with lag  $L$ , together with the non-linear least squares fit of exponential (labelled E - solid line), logarithmic (labelled L - dashed line) and hyperbolic (labelled P - dotted line) decay functions, with hyperbolic decay providing the best fit. The correlation exponent is obtained by non-linear least squares to give  $C \sim L^{-0.15}$ . All simulated data used. (d) a random sample of three out of ten volatility autocorrelation computations with hyperbolic decay lines of best fit, shown in log-log scale.

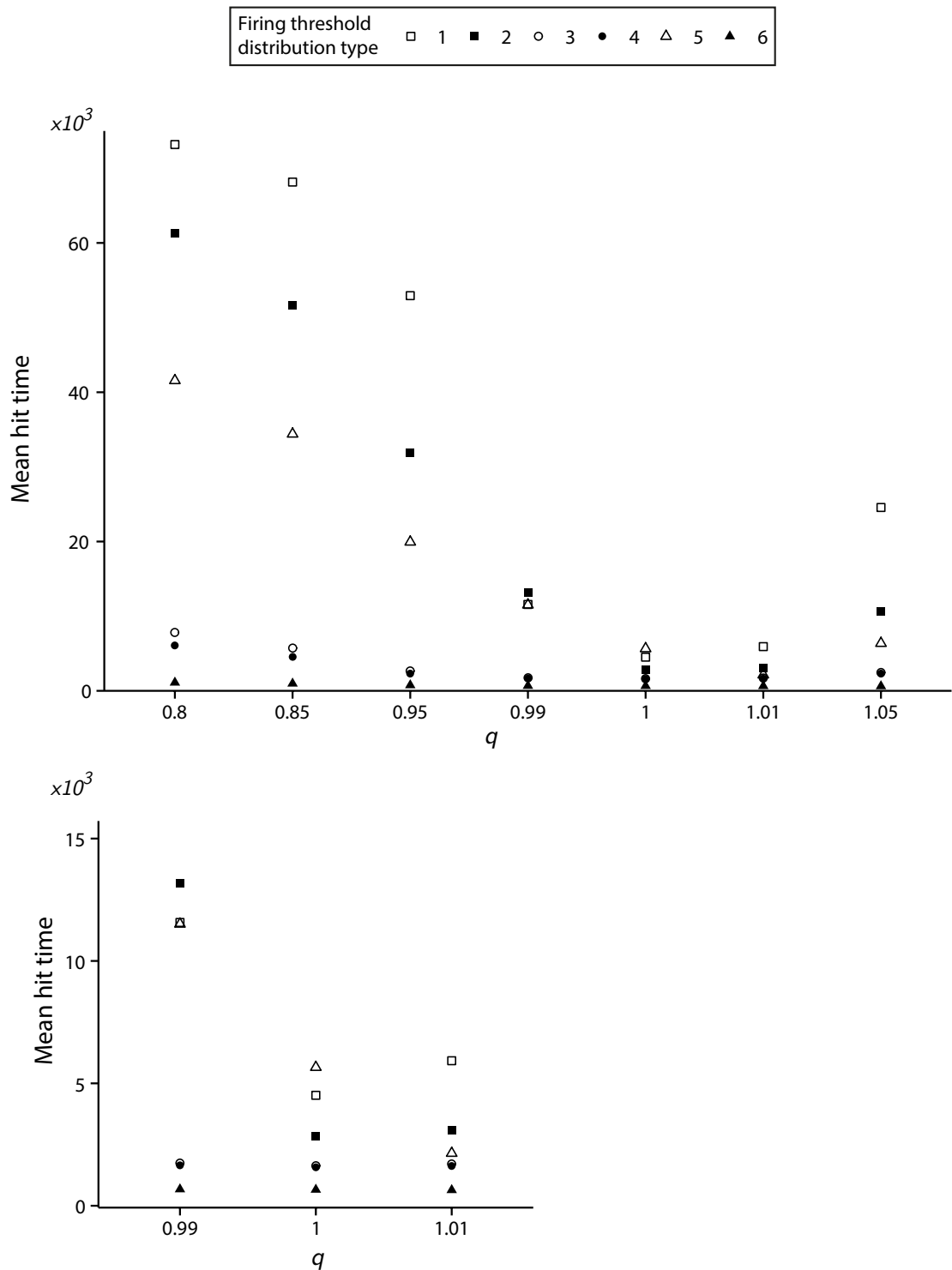


**Figure 5.12.** Distribution  $D$  in order 1: Power-law(2), 2 : Power-law(3), 3 : Uniform[1,50], 4 : Triangular with mode at  $K = 1$ , 5 : Poisson(25), 6 : Geometric( $\frac{1}{6}$ ). Results of  $N = 2000$ , with the distribution of thresholds ( $K$ ) specified by  $D$ , for various  $q \in [0.8, 1.05]$ . Taking  $q = 1$  minimises the average time to reach threshold of a random agent for a range of threshold distributions of both left-skew, no skew and right-skew.

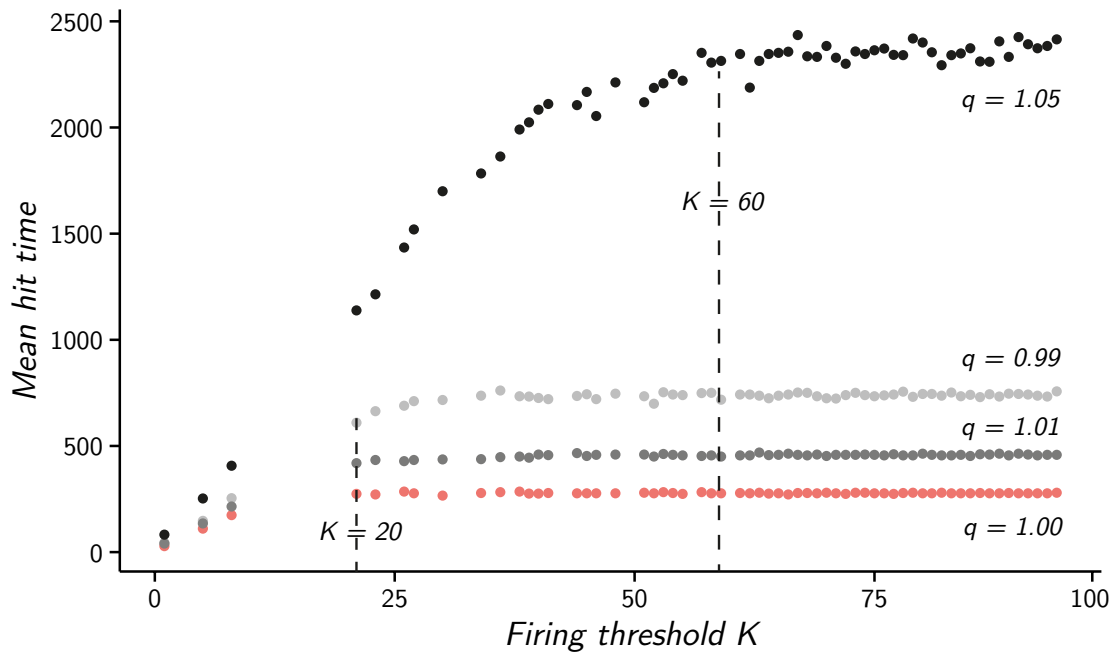


**Figure 5.13.** Results of  $N = 2000$ ,  $q \in \{0.99, 1, 1.01, 1.05\}$  shown. The mean hit time (equivalently, mean trade time) for a single agent of each threshold. For  $q \in \{0.99, 1, 1.01\}$ , agents with  $K > 20$  have very similar mean intra-trade time. In the case  $q = 1.05$ , this effect occurs for agents with  $K > 60$ . The threshold distribution  $D$  is taken as the inverse power law in Eqn. (5.10), with  $\alpha = 2$  and  $K_{\max} = 100$ .

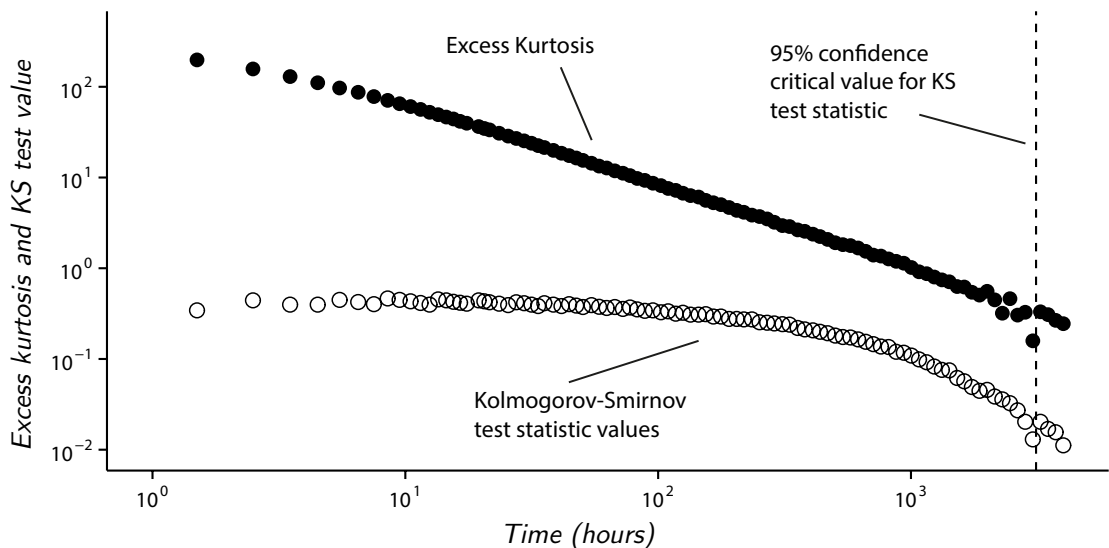


**Figure 5.14.** Log-log plot showing slow convergence to a Gaussian. The Kolmogorov-Smirnov two sample test statistic and excess kurtosis of the financial market model, plotted against increasing price return interval. The results show the tests for normality are unable to be rejected only after approximately 2 simulation years.

## **Chapter 6**

# **Financial complexity and its use in policy scenarios**

Here, the research reported in previous chapters (in particular 4 and 5) is framed in the context of economic policy and regulation. While the financial crisis of 2007-2008 has provided an opportunity for researchers from the wider scientific community to engage with problems originating from the socio-economic domain, how (and where) such theories and models are used in relation to the management of an economy is an important consideration for policymakers, distinct from the particular problem itself.

As is true for many applied science disciplines, a community of expert practitioners may consume and apply results established by a community of researchers (and vice versa), via a knowledge transfer process [Rynes et al., 2001]. The extent to which members belong to both communities, interact and share knowledge are the subjects of knowledge transfer theories that aim to explain the gap between theory and practice [see Van De Ven and Johnson, 2006, in the context of organisational management], otherwise known as the academic-practitioner gap [Bartunek and Rynes, 2014].

While research of knowledge transfer, in relation to applying complex systems modelling to already established disciplines, is beyond the bounds of this thesis; ascertaining and formalising pertinent factors relevant to the application a body of knowledge from one discipline to another [Carlile, 2004] is an important context for this chapter,

and the conclusion of this thesis. Furthermore, the perspective of knowledge transfer offers researchers a simple framework in which to classify and contextualise existing cross-discipline literature, and identify potential areas of future endeavour discussed in the conclusion of this thesis.

Using the example of economic policy in particular, knowledge transfer between policy makers and complexity-theoretic research conducted outside the domain of economics, must traverse an economic discipline barrier since policy makers, and especially so their advisers, are likely trained in classical economics, and may be unable, or unwilling, to fully engage with research external to their specialisation. In addition to the academic-practitioner gap and the discipline barrier mentioned above, the application of complex systems research to economic policy faces a third barrier to knowledge transfer, arising from the long established interdependence between economic policy and the political and institutional objectives of the incumbent administration (see Hibbs Jr [1977] and chapter 3 of Persson and Tabellini [1999]). In particular, institutional objectives may influence research agendas in such a way that impacts (either advantageously or adversely) knowledge transfer between particular domains [see The European Commission, 2007, for example].

## **6.1 A brief outline of broad UK economic policy before and after the financial crisis**

During the period 1979-2007, the UK was firmly committed to economic policies aimed at maintaining low inflation, via consumer price stability, and maintaining international competitiveness of the financial sector via light-touch regulation [Hodson and Mabbett, 2009]. Financial regulation during this period was conducted in a micro-prudential fashion, meaning the objective of financial stability is pursued by ensuring the solvency of individual institutions. With the arrival of the 2008 financial crisis, a radical change in policy occurred starting with the reduction of the Bank of England base interest rate, which stood at 5.75% in July 2007, to 0.5% by March 2009. Policy

action continued with the unconventional measure of internationally coordinated quantitative easing, via the creation of an Asset Purchase Facility [see Joyce et al., 2011, for a summary of quantitative easing carried out by the Bank of England], designed to stimulate the economy and improve market liquidity.

Subsequent to the UK policy decisions taken shortly after the start of the financial crisis, a consensus emerged amongst policymakers and researchers [Hanson et al., 2011; Bernanke, 2009; Sap, 2009] advocating a macroprudential approach to financial regulation and policy. In contrast to a microprudential approach, macroprudential frameworks approach the objective of financial stability [Allen and Wood, 2006; Schinasi, 2005] via the soundness of the entire system [Borio, 2003]. A key concept relevant to macroprudential frameworks is systemic risk [Acharya, 2009], defined simply as the risk of system-wide failure of financial institutions. Galati and Moessner [2013] provide a review of the literature surrounding macroprudential economic policy and, in particular, discuss the difficulties policymakers have in agreeing how macroprudential regulation should be implemented.

As part of international efforts to make financial systems (more) robust to the failures of connected institutions (either other banks via the interbank market, or firms in the real economy defaulting on loans), a range of suggested (and some already finalised) policy measures have emerged that aim to improve the soundness of individual financial institutions, and to curtail the propagation of systemic risks, or contagion. In the following sections, a selection of these policies are discussed, in light of the findings of this thesis.

## **6.2 Bank capital adequacy and delayed transitions**

Since 2008, the literature concerning failures in financial networks has grown to a large extent, with many researchers, and policymakers, carrying out both analytical and experimental analysis of financial networks. In particular, research has focused on interbank networks, given the central role such markets play in facilitating orderly day-to-day banking activities. For instance, when banks require liquidity (typically a

short term loan) to meet requirements originating from their own activities (or more accurately, their balance sheet) they attempt to obtain such liquidity from other banks, via the interbank market. As a last resort, the central bank may provide such liquidity.

When banks experience losses on their assets (which might occur when a bank makes a loan to another bank, who subsequently defaults before repaying the loan), as occurred during the recent financial crisis, the capital of the creditor bank is diminished (see Fig. 1 of Arinaminpathy and May [2010] for a stylised bank balance sheet). When the capital of a bank is totally depleted, below that of mandatory regulatory requirements, the bank either requires a so-called bail-out from a central bank or government agency, or defaults. In a bid to make banks, and the financial system as a whole, more resilient to network risks, increasing the amount of capital that banks are required to hold (as prescribed by the Third Basel Accord [Basel Committee on Banking Supervision, 2010], colloquially known as BASEL III), has become the central policy response of banking regulators in the aftermath of the 2008 financial crisis. In accordance with the updated accord, banks will be required to hold 2.5% of assets as capital (known as the mandatory capital conservation buffer) in addition to the 4.5% capital buffer, already in effect, prescribed by the Second Basel Accord [Bank for International Settlements, 2004]. Additional variable capital requirements may be imposed by regulators of up to 3.5% for institutions deemed to be systemically important [Basel Committee, 2011] (also known as systemically important financial institutions (SIFIs)).

In chapter 4 of this thesis, a pulse-coupled dual-threshold cascade model is presented that exhibits a transition from a small-cascade regime to that of a large (macroscopic) cascade size regime, as coupling probability is increased, and surpasses a critical coupling value [Wray and Bishop, 2014]. In addition, it was demonstrated that as the threshold ( $K$ ) determining the onset of pulse-coupling is increased, the capacity of the system to accommodate connectivity amongst its components, prior to the onset of the large-cascade regime, is increased (see Fig. 6.1). Moreover, for  $K > 1$  tested, when the transition does occur, at  $p_c$ , it does so according to  $\Delta m = (m(p_c + \varepsilon) - m(p_c)) \propto K$ , where  $m(p)$  symbolically represents the maximal cascade size (as a fraction of the total

system) obtained at the corresponding value of  $p$ . Figure. 6.2 depicts this relationship for  $1 \leq K \leq 9$  using a value of  $\Delta p = \varepsilon \approx 10^{-5}$ . These general observations continue to hold when the model is restricted to a single threshold, and components do not recover as is the case for a network of banks. In this scenario, the threshold  $K$  can be identified with the capital buffer of the banks and pulse-coupling, initiated when the capital buffer is depleted, representing an insolvent bank defaulting on interbank loans.

Transitions of a similar nature have been documented to occur in other network systems. For example, in telephony communication networks dynamic routing [Gibbens, 1988] of calls is known to increase the working capacity of the system without dynamic routing, measured as the total number of calls the system can successfully simultaneously connect, and induce instabilities in the form of sharp transitions to a congested regime [Gibbens et al., 1990; Kelly, 1996]. More recently, so-called explosive percolation [Achlioptas and Spencer, 2009; Da Costa et al., 2014] is documented to occur in network bond percolation models, where bond formation is determined by an Achlioptas process [Achlioptas and Spencer, 2009]. Achlioptas processes permit a limited amount of choice in the formation of network bonds. Instead of adding a single bond randomly (as in standard bond percolation), two candidate bonds are randomly selected, and the bond that minimises the subsequent connected component is chosen. In both of the examples just described the optimisation of some key quantity delays the transition of the system to an undesirable regime, but at the cost of a more abrupt and comprehensive transition.

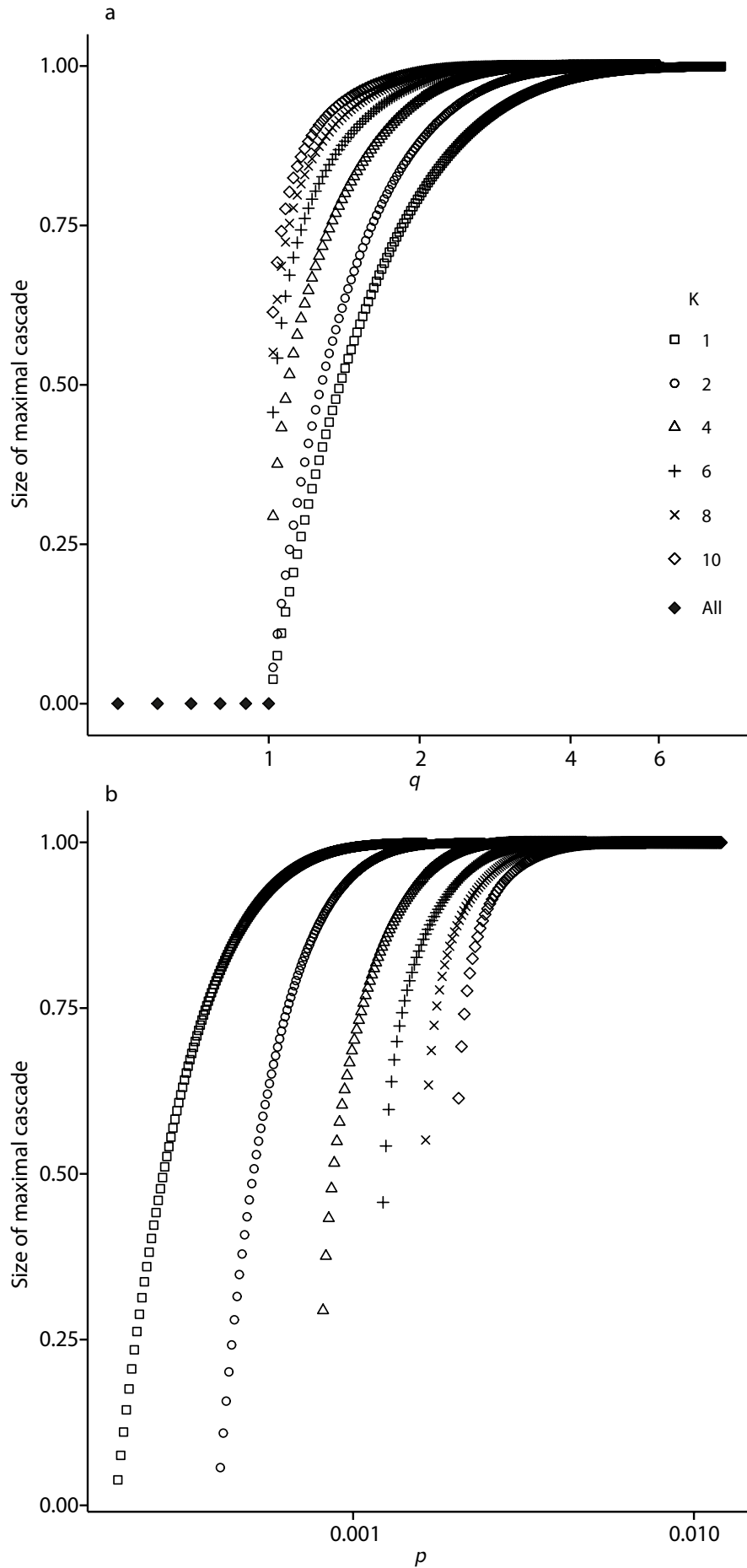


**Figure 6.1.** a) Transition from small cascade regime to large cascade size regime shown against  $q$  for  $K=1, 2, 3, 5, 8, 10$  b) as in a) plotted against  $p$ , where  $p = Kq/N$  124 and  $N$  is system size.

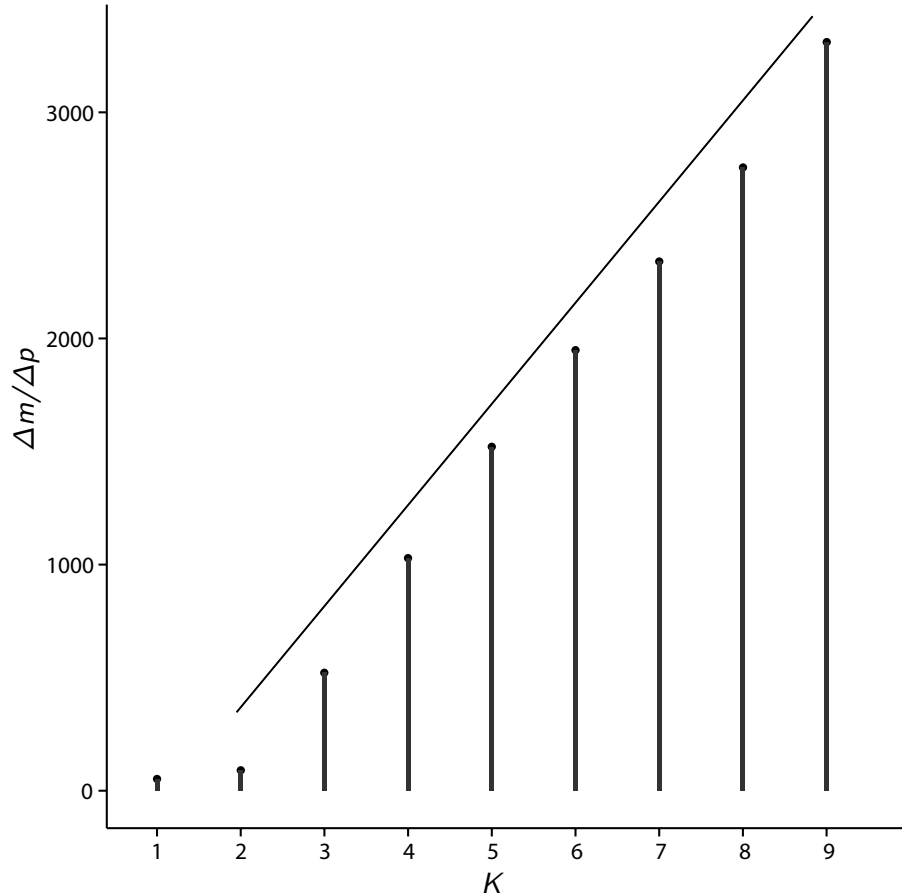


**Figure 6.2.** The rate of change in the size of the maximal cascade as coupling probability is perturbed slightly beyond the transition value:  $p_c + \varepsilon$ , for all  $1 \leq K \leq 9$  and  $\varepsilon = 10^{-5}$ .

Recent empirical studies conclude that higher capital buffers for individual banks promote stability [Gai and Kapadia, 2010; Anand et al., 2012], and reduce the frequency of contagious defaults. By drawing parallels with known results from communications networks and explosive percolation, coupled with the results of chapter 3 of this thesis, such a conclusion, while not incorrect, may represent only a partial description of the effect of increasing capital buffers. From a policy perspective, there are two main implications. The first is a need to understand more fully how optimising characteristics over a network impact the dynamics of the system, and the second relates to how monitoring, or the composition of early-warning metrics [Scheffer et al., 2009; Scheffer, 2010; Lade and Gross, 2012] should be performed, if the observable evidence of systemic events is subdued.

### **6.3 Asset bubbles and herding as a precursor to systemic risk**

The inflation stabilising policies of the UK during 1979 to 2007 viewed consumer prices as centrally important quantities, while asset prices (of financial assets such as real estate and housing market loans) were considered to be of secondary concern. Indeed, the collection and reporting of financial soundness indicators, instigated and organised by the International Monetary Fund [2006], lists real estate markets as a non-essential (but encouraged) indicator of macroeconomic soundness. Although this non-core view of asset markets and prices has been challenged and debated by economists and policymakers for some time [Cecchetti et al., 2000; Bean, 2004; Detken and Smets, 2004], the pre-crisis consensus was that macroeconomic policy should not react to asset markets [Bernanke and Gertler, 2001].

The leading report in to the financial crisis carried out by The Financial Crisis Inquiry Commission [2011] highlights the central role played by the American housing bubble (see Fig. 6.3), defined as a systematic deviation in price from economic fundamentals [Blanchard and Watson, 1982; Tirole, 1985; Lux, 1995; Abreu and Brunnermeier, 2003], and the market for home loans (as well as other markets), in the crisis. This suggests a re-evaluation of asset markets, and asset prices, as indicators of (and catalysts for) potential macroeconomic instability and systemic risk.

While the economic theories of efficient markets [Fama, 1970] and rational expectations [Muth, 1961] virtually preclude the existence of phenomena such as bubbles, a complexity-theoretic approach has much to offer policymakers in this regard. Being unconstrained by the supposition of steady-states, or equilibrium dynamics, a complex system may operate over a multitude of regimes, each of which may cause the system to produce potentially distinct qualitative output. In such a framework an extreme phenomenon, such as asset price bubbles, may be modelled as emerging from the underlying dynamics, rather than via an exogenously imposed mechanism. Behavioural economists, using a less stringent form of economic rationality [Thaler, 1994] com-

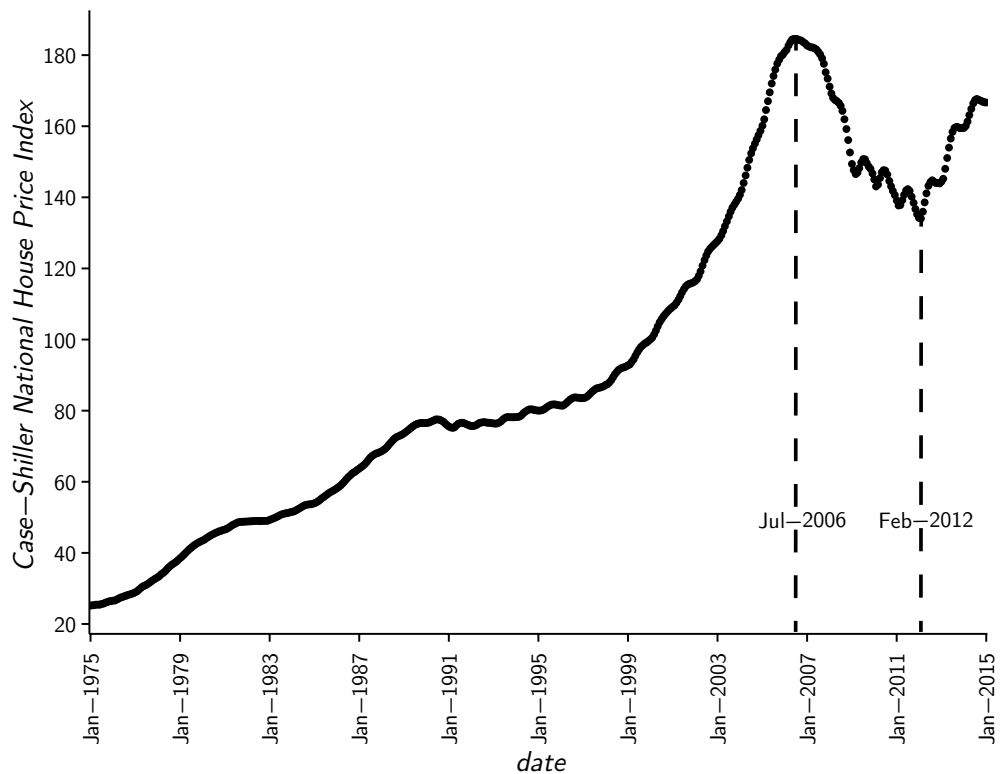


**Figure 6.3.** Monthly index values of the Case-Shiller United States National House Price Index. The maximal value occurs during July 2006, marking the end of over thirty years consistent growth. The subsequent downtrend persists for over five years. Data source: S&P Dow Jones Indices LLC.

pared to the rational expectations theory, have begun to explore emergence in financial markets [Hommes, 2001; Hommes and Wagener, 2009], finding that many of the observed features of price dynamics can be reproduced by market models composed of heterogeneous agents utilising competing trading strategies [Hommes, 2002; Brock et al., 2005].

One route to improve the detection of market instability, or asset price bubbles, may be to have alternative theories of the determinants of asset price fluctuations. As a starting point, Robert Shiller’s definition of an asset bubble is recounted [Shiller, 2015; 2014]:

A situation in which news of price increases spurs investor enthusiasm which spreads by psychological contagion from person to person, in the process amplifying stories that might justify the price increase and bringing in a larger and larger class of investors, who, despite doubts about the real value of the investment, are drawn to it partly through envy of others

successes and partly through a gamblers excitement.

In chapter 5 of this thesis, and in the spirit of Shiller's asset bubble definition, the stochastic pulse-coupled model (of chapter 4) is used to produce a stylised model of asset price dynamics in a financial market. The model utilises the concept of informational cascades defined, at the simplest level, as the situation that occurs when personal preference is subordinated by information obtained from others, or their actions [Shiller, 1995; Bikhchandani et al., 1998; Hirshleifer and Hong Teoh, 2003]. In the model, price bubbles form as the result of a symmetry-breaking bifurcation that occurs when coupling probability surpasses a critical value.

The problems asset bubbles pose for policy makers, and regulators of financial markets, include the identification of bubble onset, on one hand, and the onset of bubble collapse on the other. Even though the extent to which bubble onset and bubble collapse are produced by similar (or even the same) mechanisms is unknown, the objectives of policy makers may be different in each scenario. If macroprudential policy is to react efficaciously to asset markets, detection of bubbles must be coupled with an assessment of the risks posed to the wider economy, which in turn depends upon forecasting both the size and duration of such an episode. Instigating policy interventions aimed at curtailing bubbles that dissipate (presenting minimal implications for systemic risk) before policies come in to effect would be costly, erode public confidence in regulators and deter investors. On the other hand, when a bubble collapses (or market crashes), it may not be possible, or beneficial, for policy makers to avoid entirely a fall in asset prices, although a gradual decline in asset values may be preferable to a sudden crash.

In a complex systems approach, transitions between different regimes of the system may be accompanied by certain bifurcations [Kuehn, 2011] (such as the fold and cusp catastrophe). In the case of a bubble collapse, identified with sudden market crashes, such a transition may be considered analogous to a tipping point. Researchers studying systems in which such transitions occur (the extinction of an ecological population [Scheffer et al., 2001], changes in opinion dynamics [Brock, 2006] and climate [Dakos

et al., 2008], for example) have developed methods, and leading indicators, that aim to detect the onset of tipping points. Such research recognises that systems very near to a bifurcation may take a long time to recover from perturbations (so-called critical slowing down [see Scheffer, 2010, for a review]) and changes to the variance of fluctuations may result, enabling statistical indicators of tipping points to be produced [Carpenter and Brock, 2006; Drake and Griffen, 2010; Lade and Gross, 2012]. The dynamic behaviour of system fluctuations near a critical point appears to be general. For instance, Podobnik et al. [2015] study the time to network collapse when nodes undergo random attack and recovery, and show the approach to collapse is marked by rising variance of fluctuations.

By augmenting the network model of Podobnik et al. [2015] with a simple dynamic edge-rewiring rule as node failures occur, the abrupt network collapse can be delayed, and in certain instances totally avoided (see Fig. 6.4). In the context of a financial network, the edge rewiring mechanism described here, could represent the novation of transactions away from unsound counterparts, to those perceived as safer.

While detecting asset bubbles, and avoiding the abrupt market crash that so often follows may be notoriously difficult tasks, a complexity-theoretic tipping point approach may provide policymakers, and regulators, with tools and models where such abrupt behaviour can be studied in detail greater than that available using standard economic analysis. A policy implication is then a complex systems model may provide useful indicators of instability and augment the financial soundness indicators [International Monetary Fund, 2006] currently used.

## **6.4 General comments on the use of complexity models by policymakers**

As financial markets become more integrated, and financial innovation introduces ever more complicated products to markets and ways to create markets, it is plausible that future financial crises may be even more comprehensive and harder to detect, than

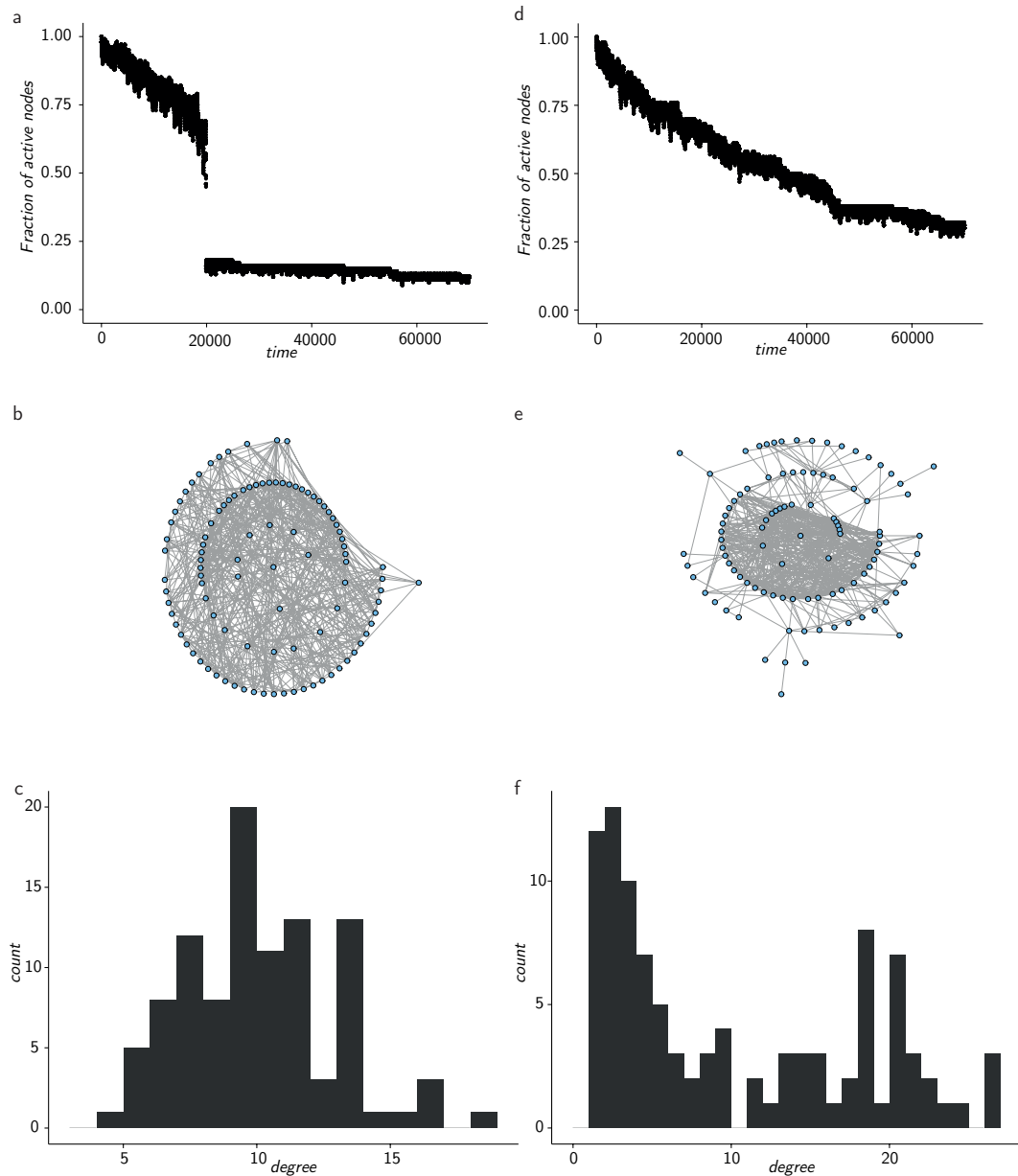


**Figure 6.4.** Smoothing an abrupt tipping point in a 100 node network of average degree 10, undergoing systematic node failure. a) the proportion of active nodes while network nodes experience intermittent and permanent failure. b) the initial random network. c) the degree distribution of the network in b). d) the proportion of active nodes when the network in b) undergoes the same failure process in a) with the addition of dynamic edge rewiring. e) the network in b) with all edges that have been rewired taken into account. f) the degree distribution of the network in e).

that of 2008. For example, many markets remain opaque, such as so-called over-the-counter markets where a significant proportion of trades in interest rate, currency and commodity products take place, and they appear to be growing [Bank for International Settlements, 2013].

While policymakers, and some economists, advocate the need to make more use of unorthodox tools and different methodologies [Trichet, 2010], this need not supplant existing tools. On the contrary, in recognition of the difficulties modelling socio-economic complex systems pose, Helbing [2010] suggests a pluralistic modelling approach may offer many benefits. In particular, such a framework does not require models and tools adhere to a single theory or methodology; favouring collaboration over conformity [see Helbing et al., 2011; Helbing, 2013, for a more detailed account of this].

# Chapter 7

## Conclusions

### 7.1 Summary of results

This thesis set out to understand and explore the use of complexity theoretic concepts, tools and techniques in the study of financial systemic risk. The catalyst for this endeavour was in part an external one - arising from the public admission by a policy maker of a fundamental epistemological gap in how to manage, and navigate, a financial crisis.

The study sought to answer the following question:

- How can mathematical models provide a context in which complex systems, and financial systemic risk, come together in a coherent way to aid policy makers?

I will return to the answer after describing the main body of the thesis.

Before I could begin to answer that question, an analysis of the dynamic stochastic general equilibrium approach was performed, in order to better understand why such models failed to serve policy makers during the financial crisis of 2007-2008. In this regard, the work in chapter 3 (and appendix A) was an attempt to understand why the incumbent body of knowledge had failed to provide the useful tools that policy makers sought. A key insight gleaned from this exploratory work, is that the general equilibrium theory which underpins the DSGE model is firstly, too constrained by the various requirements which components of the model must meet (households as utility

maximisers, economic agents as rational), to the point where pertinent questions cannot be asked of it.

Secondly, the presumption of exogenous shocks, coupled with the assumed constrained behaviour of model components suggests, a priori, that forecasts have limited range (which is not the same as inaccurate forecast - but there is ample evidence to suggest DSGE forecast accuracy prior to the financial crisis was not high [Wickens, 2012]). Moreover, prior to the financial crash, many DSGE models [Gerali et al., 2010] did not contain financial sectors, seriously limiting what insight they could offer during a financial crisis.

The primary aim of a DSGE model is to inform policy makers, rather than predict or forecast. In this regard, it is difficult to draw a sharp conclusion as to whether they failed or not. It would be disingenuous to suggest DSGE models have failed because they did not predict a financial crisis - but it does raise the question of whether policy makers should rely on a single model, or modelling framework, to stay informed.

In conclusion, an ensemble of models, or adapting a pluralistic approach [Helbing, 2010], would bring informational and model diversification benefits. Indeed complexity science has much to offer a policy maker in this regard - for instance, an agent based model could incorporate multiple information sources (and other models) in a coherent way.

The latter part of chapter 3 introduced the modelling rationale that underpinned the rest of this thesis. A broad version [Helbing, 2012] of systemic risk [compared to Fouque and Langsam, 2013, p. xxi], incorporating herding in asset markets, was identified as linking together collective behaviour and systemic risk, via complex systems.

I will briefly describe the results of chapters 4 to 6, and what has been gained from each of the chapters.

In chapter 4 a stochastic pulse-coupled network [Wray and Bishop, 2014] was constructed, that extends the work of DeVille and Peskin [2008] and DeVille et al. [2010], by allowing for pulse-coupling to occur at two boundaries. This adaptation enables cas-

cade phenomena to be studied in the presence of opposing influences; a situation that occurs predominately in socio-economic systems. The model is inherently dynamic - which is something that has been overlooked in previous percolation type models. As a special case, the model recovers standard bond percolation, and can generate sharper percolation transitions by making use of the parametrised thresholds.

From a complexity science perspective, the techniques of phase transitions and networks have been used in the analysis of both models. In addition, by framing herding as a systemic risk, coupled with the view of financial markets as a complex system in which systemic risk arises endogenously, I identify herd behaviour as an emergent feature. This is in contrast to the treatment of herd behaviour (and associated asset bubbles and market crashes) by the dominant classical economic theory, as irrational or anomalous.

In relation to the stylised financial market model developed in chapter 5 [Wray and Bishop, 2015], a novel feature of my findings is that long-memory patterns observed in financial time series may be explained by a simple threshold model. In the model, thresholds represent economic agents' decision making process. The model as described in chapter 4, is extended to allow for a semi-infinite state space, and for a distribution of thresholds over the agents. Numerical results arising from simulations, suggest that by taking a left skewed distribution of thresholds,  $D$  (many agents with a high threshold, and few agents with low thresholds) of the form

$$D(K) \sim (1 + K_{\max} - K)^{-\alpha} \quad (7.1)$$

volatility clustering can be generically induced. This is related to recent research detailing how a small number of herd-immune agents can influence and control a larger number of agents whom have a higher propensity to herd [Kononovicius and Gontis, 2014]. This analogy can be drawn since agents with threshold  $K$  have a probability proportional to  $Kq$  of receiving an incoming pulse-coupling.

This analysis contributes to the literature of agent-based, or multi-agent, herding mod-

els that aim to describe the stylised facts observed in the price returns of financial assets using simple behavioural mechanisms. In contrast to previous studies, which predominantly utilise strategy switching amongst agents, or consider agents to operate over fixed heterogeneous time scales, the model developed in this thesis utilises a minimalistic threshold model, which can be furnished with an economic context. In the model, numerical analysis reveals that the simple optimising mechanism of minimising the time spent decision making, over multiple epoch, may drive agents to self-organise to a critical regime of the system, where long-memory patterns, emerge. In mathematical terms, this optimising mechanism translates into the minimisation of the first passage time to a fixed boundary in a semi-infinite domain.

Lastly, by phrasing the model thresholds, not as zones to traverse but as capital buffers to deplete, the model can be adapted to the context of default cascades of banks.

In chapter 6, I applied my findings to the two policy areas. First, to bank capital adequacy buffers, and connected an increase in buffers to how the transition in the pulse coupled model increases in sharpness as thresholds are increased. I further linked this resource pooling in telephony networks, where stress can build up in the system unrecognised. Second, I argued that stability measure of the macro-economy would benefit by incorporating asset markets and the associated herding and bubbles that can result in systemic risk events.

In conclusion I have found mathematical models can contribute to the understanding of systemic risk by utilising complexity science. In particular, by constructing models that present emergent behaviour (in line with complex systems emergent behaviour), plausible behavioural mechanisms for systemic risk events in asset markets can be investigated.

## **7.2 Extensions and future research and limitations**

With regards to the numerical results of chapter 5 on left-skewed distributions of agent thresholds, an interesting inference not covered by Kononovicius and Gontis [2014] (and in line with what my numerical results suggest), is how a hierarchical structure of

herd behaviour may generically generate long-memory patterns in asset return volatility. This would be an interesting result, and offer a very simple behavioural mechanism under which long-memory patterns in volatility can arise.

Another direction would be to allow for a more satisfying network structure in the pulse-coupled model. By generalising the model to multiplex networks a multi-asset version could be developed, possibly offering richer phase transitions and correlations.

On a different theme, endogenous economic growth could be studied, in a similar way to how agent interactions have been modelled in this thesis. Growth is then transmitted between firms, much like orders for business.

A limitation of my work is that more empirical data analysis could have been performed - this would have added more weight to some of my conclusions, and permitted different analyses to be carried out.

# Appendix A

## A New Keynesian DSGE model - for chapter 3

The details presented here largely follow that of Galí [2009], and estimate a model fitted to US economic data using Bayesian methods [for a review of Bayesian techniques related to DSGE modelling, see An and Schorfheide, 2007].

After describing the model, the log-linearised model equilibrium equations and the graphs of input-response functions (IRF) are presented. The details of standard derivations can be found in Galí [2009, chapter 3].

Following convention, lower-case variables denote log-linearised versions of upper-case variables. This means for a given and sufficiently well-behaved variable  $H_t$ , we define  $h_t = \log(H_t) - \log(H)$ , where  $H$  is the so-called steady-state of the variable  $H_t$ . It follows that

$$H_t = H \exp(h_t) \approx H(1 + h_t). \quad (\text{A.1})$$

The DSGE model can be decomposed into the following parts, each one is described separately.

- Agents: households, firms (final and intermediate goods) and a monetary authority.
- Blocks: demand, supply and policy.

- Variables: output ( $Y_t$ ), aggregate price ( $P_t$ ) and consumption ( $C_t$ ) index, inflation ( $\Pi_t$ ), one-period bond ( $B_t$ ) and its associated price ( $Q_t$ ), nominal short term interest rate ( $i_t = -\log Q_t$ ), hours worked ( $N_t$ ), nominal wage ( $W_t$ ), lump sum component of income ( $T_t$ ).
- Constants:  $\alpha, \beta, \varepsilon, \varphi, \sigma, \sigma_a, \sigma_v$ .
- Exogenous variables: firm technology ( $A_t$ ), exogenous interest rate process ( $v_t$ ).

The preferences and technology of agents are specified as

- Households: maximise expected lifetime utility subject to budget constraints.
- Firms: intermediate good firms are monopolistically competitive and maximise expected profit, subject to demand constraints. Each firm is subject to the same time-varying production function.
- Monetary authority: sets a nominal interest rate, according to a specified policy rule.

### A.0.1 Exogenous variables

The basic model contains two exogenous auto-regressive AR(1) processes (known as *shocks* or *driving processes* in the literature) describing technology ( $v_t$ ) and policy ( $a_t$ )

$$v_t = \rho_v v_{t-1} + \eta_{v,t}, \quad (\text{A.2})$$

$$a_t = \rho_a a_{t-1} + \eta_{a,t}, \quad (\text{A.3})$$

$$\eta_{v,t} \sim N(0, \sigma_v^2), \eta_{a,t} \sim N(0, \sigma_a^2), \quad (\text{A.4})$$

where  $\rho_a$  and  $\rho_v$  are constants and  $\eta_{v,t}$ ,  $\eta_{a,t}$  are zero-mean normally distributed random numbers. These processes provide the fluctuations around steady-state observed in the economic variables of the DSGE model.

## A.0.2 Households

Households supply labour to firms, and plan when to consume the products produced in the economy, or to defer consumption by holding bonds (savings). The preferences of households is described by the utility function  $U(C_t, N_t) = \frac{C_t^{1-\sigma}}{1-\sigma} - \frac{N_t^{1+\varphi}}{1+\varphi}$ . A representative, infinitely lived, household is assumed to maximise

$$\mathbb{E}_0 \sum_{t=0}^{\infty} \beta^t U(C_t, N_t) = \sum_{t=0}^{\infty} \beta^t \mathbb{E}_0 \left\{ \frac{C_t^{1-\sigma}}{1-\sigma} - \frac{N_t^{1+\varphi}}{1+\varphi} \right\}, \quad (\text{A.5})$$

subject to the budget constraint

$$P_t C_t + Q_t B_t \leq B_{t-1} + W_t N_t + T_t. \quad (\text{A.6})$$

The aggregate consumption index is given by  $C_t = \left( \int_0^1 C_t(i)^{1-1/\varepsilon} di \right)^{\frac{\varepsilon}{\varepsilon-1}}$ , and similarly the aggregate price index is  $P_t = \left( \int_0^1 P_t(i)^{1-\varepsilon} di \right)^{\frac{1}{1-\varepsilon}}$ . The quantity  $C_t(i)$  represents the amount of good  $i$  consumed by the household in period  $t$ , and  $P_t(i)$  is the price of good  $i$ . As will be confirmed in the firms section, we assume here the existence of a continuum of goods represented by the interval  $[0, 1]$ . The log-linearised optimality condition, under rational expectations, is given by the consumer Euler equation

$$c_t = \mathbb{E}_t \{ c_{t+1} \} - \frac{1}{\sigma} (i_t - \mathbb{E}_t \{ \pi_{t+1} \}), \quad (\text{A.7})$$

where  $\mathbb{E}_t$  is the conditional (time- $t$ ) expectation. Under market clearing for goods,  $c_t = y_t$ . Combining this condition with Eq. (A.7) results in the so-called forward investment and savings (IS) equation

$$y_t = \mathbb{E}_t \{ y_{t+1} \} - \frac{1}{\sigma} (i_t - \mathbb{E}_t \{ \pi_{t+1} \}), \quad (\text{A.8})$$

where  $\mathbb{E}_t \{ \pi_{t+1} \} = \mathbb{E}_t \{ p_{t+1} - p_t \}$ .

### A.0.3 Firms

There exists a continuum of firms, indexed by  $i \in [0, 1]$ , each producing a differentiated good, and all using identical technology. The production function for firm  $i$  is given by

$$Y_t(i) = A_t N_t^{1-\alpha}. \quad (\text{A.9})$$

Each firm restates its price with a probability  $1 - \theta$ , in any given period and independently of previous update times. A firm that does not update its price in period  $t$  continues to use the price of the previous period. With  $Y_{t+k|t}$  denoting the output of a firm in period  $t + k$ , that last updated its price in period  $t$ ;  $Q_{t,t+k}$  a stochastic discount factor and  $\Psi_{t+k}$  a cost function, a firm updating its price,  $X_t$ , in period  $t$  will select the price that maximises the current market value of profit, subject to the demand constraints. Formally,

$$\max_{X_t} \sum_{k=0}^{\infty} \theta^k \mathbb{E}_t \{ Q_{t,t+k} (X_t Y_{t+k|t} - \Psi_{t+k}(Y_{t+k|t})) \}, \quad (\text{A.10})$$

subject to demand constraints

$$Y_{t+k|t} = \left( \frac{X_t}{P_{t+k}} \right) C_{t+k}, \text{ for } k = 0, 1, 2, \dots \quad (\text{A.11})$$

The result of considering the optimal price setting of firms in equilibrium provide a model equation for inflation, in terms of the output-gap ( $y^g$ )

$$y^g = y_t - \frac{1/\sigma(1+\varphi)}{1-\alpha+1/\sigma(\varphi+\alpha)} a_t, \quad (\text{A.12})$$

$$\pi_t = \beta \mathbb{E}_t \{ \pi_{t+1} \} + \kappa y_t^g. \quad (\text{A.13})$$

Where  $\kappa = \frac{(1-\theta)(1-\beta\theta)}{\theta} \frac{1-\alpha}{1-\alpha+\alpha\varepsilon} \left( \sigma + \frac{\varphi+\alpha}{1-\alpha} \right)$ . It is also possible to rewrite Eq. (A.8) as

$$y_t^g = \mathbb{E}_t \{ y_{t+1}^g \} - \frac{1}{\sigma} (i_t - \mathbb{E}_t \{ \pi_{t+1} \} - r_t^n), \quad (\text{A.14})$$

with  $r_t^n$  the natural rate of interest

$$r_t^n = \sigma \frac{1 + \varphi}{\sigma(1 - \alpha) + \varphi + \alpha} \mathbb{E}_t \{a_{t+1} - a_t\} \quad (\text{A.15})$$

$$= \sigma \frac{1 + \varphi}{\sigma(1 - \alpha) + \varphi + \alpha} (\rho_a - 1) a_t, \quad (\text{A.16})$$

with the last equality following from Eq. (A.3). By consider market clearing in the goods and labour market, we establish a relationship between output, technology and labour supply (employment)

$$y_t = a_t + (1 - \alpha)n_t \Rightarrow n_t = \frac{y_t - a_t}{1 - \alpha}. \quad (\text{A.17})$$

#### A.0.4 Monetary policy

The monetary policy block of the model encapsulates the interest rate setting agent and any policy equations. This often takes the form of a central bank that sets the short term interest rate for the economy via the so-called Taylor rule [see Galí, 2009]

$$i_t = \phi_\pi \pi_t + \phi_y y_t^g + v_t. \quad (\text{A.18})$$

### A.1 Estimating the model and fitting data

The method of undetermined coefficients, described by Uhlig [1995], can be used to obtain a reduced-form recursive solution of the linear rational expectations system formed from equations (A.12), (A.13), (A.13), (A.14), (A.16), (A.17), (A.18), the total number of which is  $M_d$ , and the equations for exogenous variables, (A.2) and (A.3), of which there are  $M_e$  in total. Applying the method determines the values of matrices  $A, B, C$  in the reduced form solution

$$\zeta_t = A \zeta_{t-1} + B z_t, \quad \zeta_t \in \mathbb{R}^{M_d}, A \in \mathbb{R}^{M_d \times M_d}, B \in \mathbb{R}^{M_d \times M_e} \quad (\text{A.19})$$

$$z_t = C z_{t-1} + \eta_t, \quad C \in \mathbb{R}^{M_e \times M_e}, \eta_t, z_t \in \mathbb{R}^{M_e}. \quad (\text{A.20})$$

Where,  $\zeta_t = [y_t^g, y_t, \pi_t, r_t^m, i_t, n_t]^T$  and  $z_t = [a_t, v_t]^T$ . In order to facilitate Bayesian parameter estimation, when fitting the model to economic data, a state-space representation of the reduced-form recursive solution is used.

$$\gamma_t = \Phi\gamma_{t-1} + \Theta\eta_t, \quad \gamma_t = [\zeta_t, z_t]^T. \quad (\text{A.21})$$

The matrices  $\Phi, \Theta \in \mathbb{R}^{M \times M}$  (for  $M = M_d + M_e$ ) are functions of the matrices  $A, B, C$  above. As an illustration, the model is fitted to two observable economic time series, together with shocks to production ( $a_t$ ) and technology ( $v_t$ ):

- $\pi_t$ : UK Consumer Price Inflation (UK CPI).
- $i_t$ : UK Sterling Overnight Index Average (SONIA).

Quarterly data from March 1997 to June 2013, publicly available from Office of National Statistics-UK [2013], is used. Once a parameter fit is obtained plots of IRFs are produced that visualise how an isolated one standard deviation shock in an exogenous variable (either  $a_t$  or  $v_t$ ) evolve the endogenous variables through time.

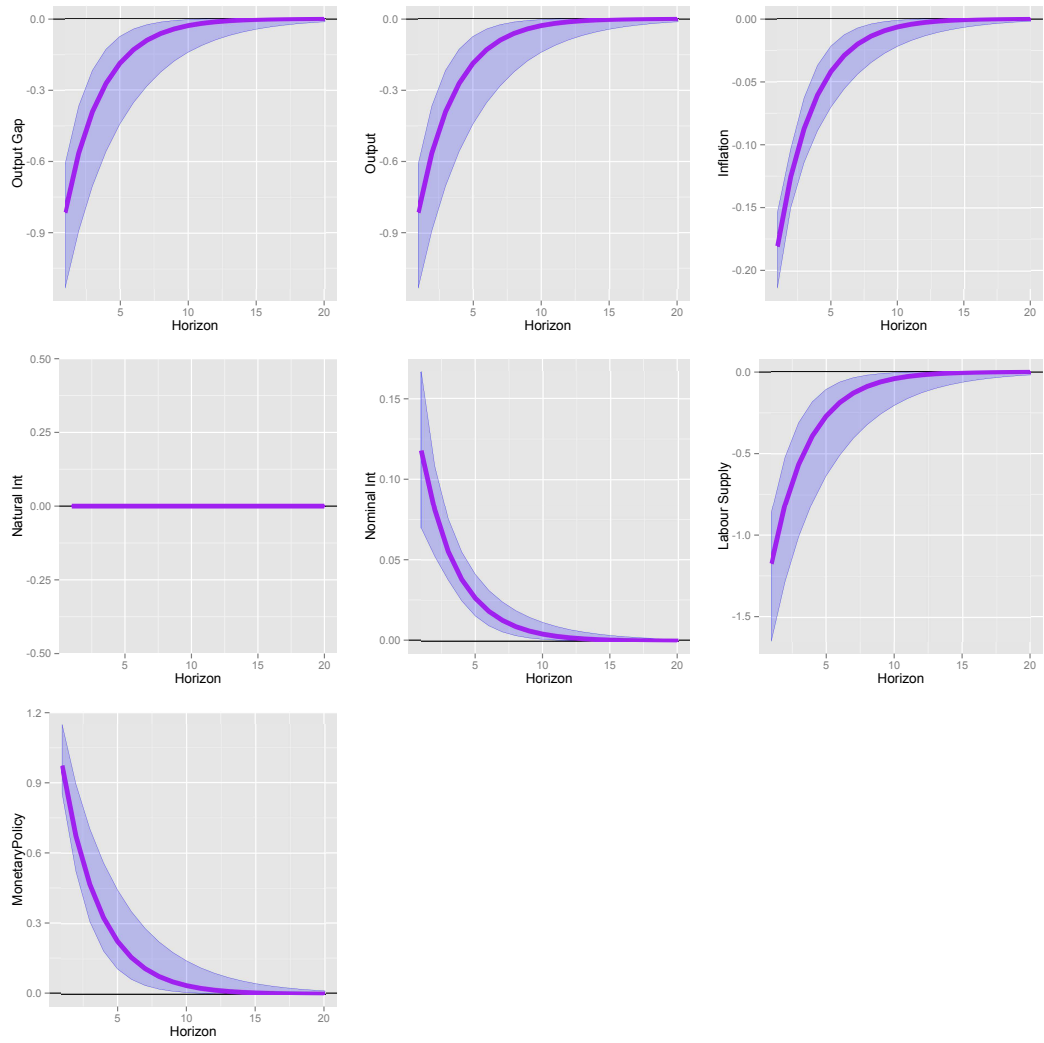


**Figure A.1.** An input-response function diagram showing the relations to policy shock.

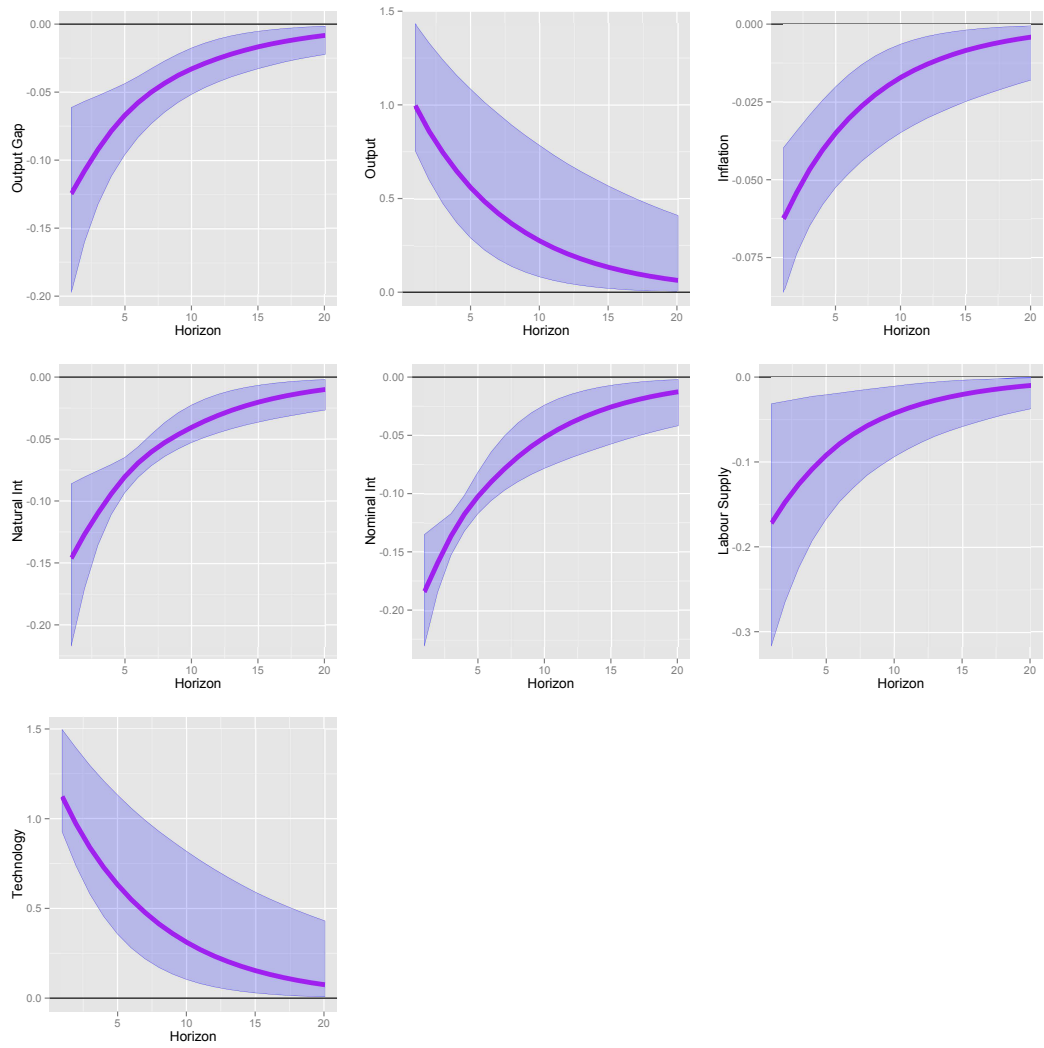


**Figure A.2.** An input-response function diagram showing the relations to technology shock.

# Appendix B

## Pulse-coupled model details and proofs - for chapter 4

### Description of the stochastic model

During the diffusion phase, at time  $t$ , the state variables  $\theta_u(t)$  update according to a simple unbiased continuous-time random walk between nearest neighbour states, satisfying

$$\begin{aligned} \frac{1}{2} &= \mathbb{P}\{\theta_u(t + \delta_u) = s + 1 \mid \theta_u(t) = s\} \\ &= 1 - \mathbb{P}\{\theta_u(t + \delta_u) = s - 1 \mid \theta_u(t) = s\}, \end{aligned} \quad (\text{B.1})$$

where  $s \in \{1, \dots, 2K - 1\}$ ,  $\theta_u(t)$  is the current oscillator state and  $\delta_u$  are independent exponentially distributed random variables,  $\text{Exp}(\Lambda)$  with mean  $1/\Lambda$ , representing the passage of time until the next state transition. Without loss of generality, throughout this study we set  $\Lambda = 1$ . The first oscillator to transition to either of the firing states occurs at the boundary hitting time,

$$\tau = \min_u \{t : \theta_u(t) = 0, \text{ or } \theta_u(t) = 2K\}, \quad (\text{B.2})$$

at which time the diffusion process ends and the cascade phase begins. The existence of finite hitting times, for this random walk between two boundaries, is guaranteed by standard results Redner [2001]. The cascade process continues as described for the original one sided model DeVille et al. [2010]; DeVille and Peskin [2008], with the difference being oscillators reset to state  $K$  after firing and the cascade ending, before the diffusion phase restarts.

## Mean field model.

Let  $\mathbf{v}_i \in \mathbb{R}_+^{2K+1}$  denote the  $i$ -th standard basis vector, with 1 in position  $i$  and 0 elsewhere, and let  $S_0, S_+, S_-$  be subsets of phase space, defined by

$$\begin{aligned} S_0 &= \{\mathbf{y} \in \mathbb{R}_+^{2K+1} : \langle \mathbf{y}, \mathbf{v}_0 \rangle < 1, \langle \mathbf{y}, \mathbf{v}_{2K} \rangle < 1\}, \\ S_+ &= \{\mathbf{y} \in \mathbb{R}_+^{2K+1} : \langle \mathbf{y}, \mathbf{v}_{2K} \rangle \geq 1\}, \\ S_- &= \{\mathbf{y} \in \mathbb{R}_+^{2K+1} : \langle \mathbf{y}, \mathbf{v}_0 \rangle \geq 1\}, \end{aligned} \tag{B.3}$$

where  $\mathbb{R}_+ = \{r \in \mathbb{R} : r \geq 0\}$ , and  $\langle \dots \rangle$  denotes the standard inner product on  $\mathbb{R}^{2K+1}$ . The set  $S_0$  represents the system state during the integrate (or diffusion) phase - that is, between firing (pulse-coupling) events. The sets  $S_+$  and  $S_-$  represent the state of the system during a cascade phase originating from either the positive pulse-coupling firing state ( $S_+$ ), or the negative pulse-coupling firing state ( $S_-$ ). Throughout this section, all vectors and matrices are indexed with component labels ranging from 0 to  $2K$ .

The basis of the mean field model, is the vector of expected state occupation, which encodes the macroscopic state of the system. Let  $x_s(t) \geq 0$  be the expected number of oscillators in state  $s$  at time  $t$ , then  $\mathbf{x}(t)$  is given by

$$\mathbf{x}(t) = (x_0(t), \dots, x_{2K}(t)) \in \mathbb{R}_+^{2K+1}. \tag{B.4}$$

Our aim is to use the MF system to solve for the vector  $\mathbf{x}(t)$ , in specific cases. For instance, equation (4.5) shows the solution for  $\mathbf{x}(t)$  when the MF system produces singleton firings that alternating indefinitely between the upper and lower boundaries.

Although the mean field model is deterministic, the dynamics still occur in two phases: a continuous-time diffusion phase and instantaneous cascade phase. Since the diffusion of each oscillator state evolves according to equation (B.1), during the diffusion phase  $x_s(t)$  evolves according to

$$\begin{aligned}
\frac{dx_0(t)}{dt} &= \frac{1}{2}x_1(t), \\
\frac{dx_1(t)}{dt} &= \frac{1}{2}x_2(t) - x_1(t), \\
\frac{dx_j(t)}{dt} &= \frac{1}{2}x_{j-1}(t) + \frac{1}{2}x_{j+1}(t) - x_j(t), \\
\frac{dx_{2K-1}(t)}{dt} &= \frac{1}{2}x_{2K-2}(t) - x_{2K-1}(t), \\
\frac{dx_{2K}(t)}{dt} &= \frac{1}{2}x_{2K-1}(t),
\end{aligned} \tag{B.5}$$

where  $j \in \{2, \dots, 2K-1\}$ . We can write the linear equations (B.5) in the more compact form  $\dot{\mathbf{x}}(t) = L_D \mathbf{x}(t)$ , with solution  $\mathbf{x}(t) = e^{tL_D} \mathbf{x}(0)$  where the matrix  $L_D \in \mathbb{R}^{(2K+1) \times (2K+1)}$ , indexed from  $i, j = 0, \dots, 2K$ , has entries

$$(L_D)_{ij} = \begin{cases} \frac{1}{2} & \text{for } i = j-1, j = 1, 2, \dots, 2K-1, \\ \frac{1}{2} & \text{for } i = j+1, j = 1, 2, \dots, 2K-1, \\ -1 & \text{for } j = i, j = 1, \dots, 2K-1, \end{cases} \tag{B.6}$$

with all other entries zero. Recall that the diffusion phase ceases as soon as an oscillator transitions to either of the firing states. For the non-normalised mean field system, this condition is encoded as  $x_0(t) \geq 1$  or  $x_{2K}(t) \geq 1$ , or equivalently as

$$\begin{aligned}
\langle \mathbf{x}(t), \mathbf{v}_0 \rangle &\geq 1 \text{ (negative pulse condition),} \\
\langle \mathbf{x}(t), \mathbf{v}_{2K} \rangle &\geq 1 \text{ (positive pulse condition),}
\end{aligned} \tag{B.7}$$

We say the equations  $\langle \mathbf{x}(t), \mathbf{v}_0 \rangle = 1$  and  $\langle \mathbf{x}(t), \mathbf{v}_{2K} \rangle = 1$  define discontinuity boundaries Casini and Vestroni [2004]; di Bernardo et al. [2001], in the context of piecewise-smooth dynamical systems, of which the mean field model is a simple example. As

soon as one of the conditions in equation (B.7) is satisfied, the cascade phase begins, with the appropriate pulse-coupling.

The action of a single oscillator firing is encoded using the pulse-coupling matrix,  $L_C$ , and the map  $F_p$  given by

$$F_p(\mathbf{x}(t)) = (I + pL_C)\mathbf{x}(t) - \mathbf{v}, \quad (\text{B.8})$$

where the term  $-\mathbf{v}$  removes the firing oscillator from the system, after it has fired, to satisfy the requirement that it enters a refractory state. The matrix  $L_C$  describes the effect of pulse-coupling on the remaining oscillators in the system, and can take one of two values. For an initial positive pulse  $L_C = L_{C,+}$  and  $\mathbf{v} = \mathbf{v}_{2K}$  are used, while for an initial negative pulse  $L_C = L_{C,-}$  and  $\mathbf{v} = \mathbf{v}_0$ , where

$$(L_{C,+})_{ij} = \begin{cases} 1 & \text{for } i = j + 1, \quad j = 1, \dots, 2K - 1 \\ -1 & \text{for } i = j, \quad j = 1, \dots, 2K - 1 \end{cases} \quad (\text{B.9})$$

$$(L_{C,-})_{ij} = \begin{cases} 1 & \text{for } i = j - 1, \quad j = 1, \dots, 2K - 1 \\ -1 & \text{for } i = j, \quad j = 1, \dots, 2K - 1, \end{cases} \quad (\text{B.10})$$

with all other entries zero, for both matrices. The cascade, refractory and resetting processes continue in the same way as for the original model DeVille et al. [2010]; DeVille and Peskin [2008], with the exception that oscillators reset to state  $K$  after firing

In order to correctly encode the cascade procedure involving multiple oscillators, the map given by equation (B.8) must be applied to the state vector  $\mathbf{x}(t)$  each time an oscillator fires. To do this, we use functional composition defined as follows: for an arbitrary function  $f$ , and arbitrary integer  $a$ , the  $a$ -fold composition is denoted via an exponent  $\overbrace{f \circ f \circ \dots \circ f}^{\text{a times}} = f^a$ . Applying the map in equation (B.8) to  $\mathbf{x}(t)$   $a$  times, we obtain  $F_p^a(\mathbf{x}(t)) = (I + pL_C)^a \mathbf{x}(t) - a\mathbf{v}$ , because  $\mathbf{v}_{2K} \in \ker(L_{C,+})$  and  $\mathbf{v}_0 \in \ker(L_{C,-})$ . The cascade size,  $m$ , is defined as  $m = m(\mathbf{x}(t)) = \inf\{a : F_p^a(\mathbf{x}(t)) \in S_0\}$ , given appro-

appropriate values of  $L_C$  and  $\mathbf{v}$ , and  $S_0$  defined by equation (B.3). Finally, the  $m$  oscillators that fired during the cascade, and subsequently removed from the system, are added back in and reset to level  $K$ . Hence, we can define a map

$$\begin{aligned}\phi : S_+ \cup S_- &\rightarrow S_0 \\ \phi(\mathbf{x}(t)) &= F_p^{m(\mathbf{x}(t))} + m(\mathbf{x}(t))\mathbf{v}_K,\end{aligned}\tag{B.11}$$

where  $S_+, S_-$  are defined by equations (B.3).

Using the above definitions, we can state the dynamics of the mean field system as

$$\begin{aligned}\dot{\mathbf{x}}(t) &= L_D\mathbf{x}(t) \quad \text{for } \mathbf{x}(t) \in S_0, \\ \mathbf{x}(t) &\mapsto \phi(\mathbf{x}(t)) \quad \text{for } \mathbf{x}(t) \in S_+ \cup S_-.\end{aligned}\tag{B.12}$$

## B.1 Construction of the map $G_0$

In the asynchronous state, isolated cascades (of size 1) occur in an alternating pattern originating from the two firing states 0 and  $2K$ . Therefore, we construct a map that takes the system state vector initially in set  $S_0$  (defined by Eqn. (B.3)) and describes the system undergoing an isolated (size 1) cascade originating from state  $2K$  (when the system state vector is in set  $S_+$  defined by Eqn. (B.3)), followed by a second diffusion and an isolated cascade originating from state 0 (when the system state vector is in set  $S_-$  defined by Eqn. (B.3)).

The physical actions in detail are as follows:

1. Initially the system has normalised state vector:

$$\mathbf{x} \in S_0$$

2. The system diffuses while in set  $S_0$  (under the relevant action given by Eqn (B.12)) for time  $\tau_1$  at which point the state vector is now in the set  $S_+$ . The state vector is now:

$$e^{\tau_1 L_D}\mathbf{x} \in S_+.$$

3. The system undergoes an isolated cascade given by  $\phi$  in Eqn. (B.11). Because

the cascade is of size 1,  $\phi$  is given by  $F_p$  defined in Eqn. (B.8), with  $p$ ,  $L_D$  and  $\mathbf{v}$  replaced with  $\varepsilon Kq$ ,  $L_{C,+}$  and  $\varepsilon \mathbf{v}_{2K}$  respectively. The state vector is now:

$$(I + \varepsilon KqL_{C,+})e^{\tau_1 L_D} \mathbf{x} - \varepsilon \mathbf{v}_{2K}.$$

4. After this cascade, the  $2K$ -th component of the state vector is reset (mapped) back to the  $K$ -th component of the state vector. Because we are considering an isolated (size 1) cascade, the  $2K$ -th component is  $\varepsilon$ , and so we must add  $\varepsilon \mathbf{v}_K$  back to the system state vector. The state vector is now:

$$(I + \varepsilon KqL_{C,+})e^{\tau_1 L_D} \mathbf{x} - \varepsilon(\mathbf{v}_{2K} - \mathbf{v}_K) \in S_0.$$

5. The system diffuses while in set  $S_0$  (under the relevant action given by Eqn (B.12)) for a time  $\tau_2$  at which point a the state vector is now in the set  $S_-$ . The state vector is now:

$$e^{\tau_2 L_D} [(I + \varepsilon KqL_{C,+})e^{\tau_1 L_D} \mathbf{x} - \varepsilon(\mathbf{v}_{2K} - \mathbf{v}_K)] \in S_-.$$

6. The system undergoes an isolated cascade given by  $\phi$  in Eqn. (B.11). Because the cascade is of size 1,  $\phi$  is given by  $F_p$  defined in Eqn. (B.8), with  $p$ ,  $L_D$  and  $\mathbf{v}$  replaced with  $\varepsilon Kq$ ,  $L_{C,-}$  and  $\varepsilon \mathbf{v}_0$  respectively. The state vector is now:

$$(I + \varepsilon KqL_{C,-})e^{\tau_2 L_D} [(I + \varepsilon KqL_{C,+})e^{\tau_1 L_D} \mathbf{x} - \varepsilon(\mathbf{v}_{2K} - \mathbf{v}_K)] - \varepsilon \mathbf{v}_0.$$

7. After this cascade, the 0-th component of the state vector is reset (mapped) back to the  $K$ -th component of the state vector. Because we are considering an isolated cascade (of size 1), the 0-th component is  $\varepsilon$  and therefore add  $\varepsilon \mathbf{v}_K$  back to the system state vector. The state vector is now:

$$(I + \varepsilon KqL_{C,-})e^{\tau_2 L_D} [(I + \varepsilon KqL_{C,+})e^{\tau_1 L_D} \mathbf{x} - \varepsilon(\mathbf{v}_{2K} - \mathbf{v}_K)] - \varepsilon(\mathbf{v}_0 - \mathbf{v}_K) \in S_0.$$

The map  $G_0 : S_0 \rightarrow S_0$  is defined as

$$G_0(\mathbf{x}) = (I + \varepsilon KqL_{C,-})e^{\tau_2 L_D} [(I + \varepsilon KqL_{C,+})e^{\tau_1 L_D} \mathbf{x} - \varepsilon(\mathbf{v}_{2K} - \mathbf{v}_K)] - \varepsilon(\mathbf{v}_0 - \mathbf{v}_K). \quad (\text{B.13})$$

When computing the solution, up to  $O(\varepsilon)$ , of the fixed point equation  $G_0(\mathbf{x}) = \mathbf{x}$ , it is

noted the times  $\tau_1$  and  $\tau_2$  are of order  $\varepsilon$ , and linearise the exponential matrix as

$$e^{\tau L_D} \approx I + \tau L_D. \quad (\text{B.14})$$

Furthermore, the matrix multiplications are performed while keeping careful track of simplifications arising from the kernel of the matrices  $L_D, L_{C,+}$  and  $L_{C,-}$ .

## B.2 Combinatorial methods for cascade probability

The composition [Stanley, 2012] of an integer,  $x$ , is the sequence of strictly positive summands of  $x$ . That is, if  $x = x_1 + x_2 + \dots + x_k$  then the sequence  $\{x_1, x_2, \dots, x_k\}$  is called a composition of  $x$ . There are exactly  $2^{x-1}$  distinct compositions of an integer  $x$ . We use the concept of integer compositions to derive Eqns. (4.16) and (4.17). To make it clear when we are working with compositions we use the notation  $x = [x_1, \dots, x_k]$ .

Consistent with Eqns. (4.10)-(4.12), an arbitrary (unsigned) cascade of size  $m > 0$ , initiated by a single agent, may be written in composition form as  $m = [1, x_1, \dots, x_k]$ , and therefore  $m - 1 = [x_1, \dots, x_k]$ . We identify  $x_i$  as being the number of internal nodes at level  $i$  in the tree representation of a cascade (see Fig. 4.7).

We proceed by enumerating the ways such a cascade can arise. Given a cascade expressed as  $[x_1, \dots, x_k]$ , at an arbitrary level  $i$  we have  $x_{i-1}$  copies of a single level  $(N - 1 - x_1 - \dots - x_i)$ -ary tree. We then have

$$x_{i-1}^{x_i} \binom{N - 1 - \sum_{j=1}^{i-1} x_j}{x_i} \quad (\text{B.15})$$

ways to select the  $x_i$  nodes. Proceeding recursively, we form the product

$$\begin{aligned} \binom{N-1}{x_1} \dots x_{i-1}^{x_i} \binom{N-1 - \sum_{j=1}^{i-1} x_j}{x_i} \dots x_{k-1}^{x_k} \binom{N-1 - \sum_{j=1}^{k-1} x_j}{x_k} \\ = \frac{(N-1)! x_1^{x_2} x_2^{x_3} \dots x_{k-1}^{x_k}}{(N-m)! x_1! x_2! \dots x_k!}, \end{aligned} \quad (\text{B.16})$$

where the right hand side of the equality is achieved after pairwise cancellation and

using the fact that  $m = 1 + [x_1, \dots, x_k]$ . Hence for a given composition (with  $k$  parts) we can write the probability as

$$P(m | [x_1, \dots, x_k]) = \frac{(N-1)! x_1^{x_2} x_2^{x_3} \dots x_{k-1}^{x_k}}{(N-m)! x_1! x_2! \dots x_k!} p^{m-1} (1-p)^Q, \quad (\text{B.17})$$

where  $p$  is the probability that an agent is induced to a firing state during a cascade and  $Q$  is the perimeter of the tree representation of the cascade. By simple counting, and using the fact that  $\sum_{i \geq 1, j > i} x_i x_j = \frac{1}{2} ((m-1)^2 - \sum_{i \geq 1} x_i^2)$  we can express  $Q = m(N-m) + \frac{1}{2}(m-1)^2 - \frac{1}{2} \sum_{i \geq 1} x_i^2$ . By removing the composition-dependent term,  $\frac{1}{2} \sum_{i \geq 1} x_i^2$ , from  $Q$  since it is relatively small, we can write the unconditional probability of a cascade of size  $m$  as

$$\begin{aligned} P(m) &= \sum_{k \geq 1, [x_1, \dots, x_k]} P(m | [x_1, \dots, x_k]) \\ &= p^{m-1} (1-p)^{m(N-m) + \frac{1}{2}(m-1)^2} \frac{(N-1)!}{(N-m)!} \sum_{k \geq 1, [x_1, \dots, x_k]} \frac{x_1^{x_2} x_2^{x_3} \dots x_{k-1}^{x_k}}{x_1! x_2! \dots x_k!} \\ &= p^{m-1} (1-p)^{m(N-m) + \frac{1}{2}(m-1)^2} \frac{(N-1)!}{(N-m)!} \frac{m^{m-2}}{(m-1)!}. \end{aligned} \quad (\text{B.18})$$

For large  $N, m$

$$\frac{(N-1)!}{(N-m)!} = \binom{N-1}{m-1} (m-1)! \sim N^{m-1} \quad (\text{B.19})$$

and

$$\frac{m^{m-2}}{(m-1)!} = \frac{m^{m-1}}{m!} \sim (2\pi)^{-\frac{1}{2}} m^{-\frac{3}{2}} e^m \quad (\text{B.20})$$

follow from Stirling's approximation. The final equality in Eqn. (B.18) can now be rewritten as

$$P(m) = (2\pi)^{-\frac{1}{2}} (pN)^{m-1} (1-p)^{m(N-m) + \frac{1}{2}(m-1)^2} m^{-\frac{3}{2}} e^m, \quad (\text{B.21})$$

and recalling  $p = qK/N$ , with  $K = 1$  as  $N \rightarrow \infty$  we obtain the asymptotic relation given by Eqn. (4.17).

### B.3 Mixture distribution moments and negative binomial density

First note that since cascade evolution is stochastic, each agent will undergo a random number of unsuccessful attempts before they are induced to fire - if at all. It is this simple observation that motivates the choice of the negative binomial statistical model to approximate the cascade distribution. The density of the negative binomial distribution used is

$$\frac{\Gamma(x+r)}{x!\Gamma(r)} p_{NB}^r (1-p_{NB})^x, \quad x = 0, 1, \dots, \quad r > 0, \quad 0 < p_{NB} \leq 1. \quad (\text{B.22})$$

Recall in the  $K = 1$  case, there is no symmetry breaking, and each cascade is an independent event occurring with equal probability either side of 0. Hence, the cascade distribution, for fixed  $q$ , is simply the equally weighted mixture distribution of negative binomial components: a negative tail and a positive tail. The resulting distribution,  $D$ , is symmetric about 0 and therefore  $\text{Var}(D) = \mathbb{E}(D^2)$ . The moments of  $D$  are obtained using standard methods. In particular,

$$\begin{aligned} \text{Var}(D) &= \frac{1}{2} \binom{2}{0} (\mathbb{E}^2(Y_1) + \mathbb{E}^2(Y_2)) \\ &\quad + \frac{1}{2} \binom{2}{2} (\mathbb{E}\{(Y_1 - \mu_1)^2\} + \mathbb{E}\{(Y_2 - \mu_2)^2\}) \\ &= \text{Var}(X) + (1 + \mathbb{E}(X))^2. \end{aligned} \quad (\text{B.23})$$

With  $Y_1 = 1 + X_1$  and  $Y_2 = -1 - X_2$ , with  $X_{1,2}(n, p)$  distributed negative binomial. For kurtosis we follow the same procedure as above.

$$\begin{aligned} \mathbb{E}\{D^4\} &= \frac{1}{2} (\mathbb{E}^4(Y_1) + \mathbb{E}^4(Y_2)) \\ &\quad + \frac{1}{2} \binom{4}{2} (\mathbb{E}^2(Y_1) \mathbb{E}\{(Y_1 - \mu_1)^2\} + \mathbb{E}^2(Y_2) \mathbb{E}\{(Y_2 - \mu_2)^2\}) \\ &\quad + \frac{1}{2} \binom{4}{3} (\mathbb{E}(Y_1) \mathbb{E}\{(Y_1 - \mu_1)^3\} + \mathbb{E}(Y_2) \mathbb{E}\{(Y_2 - \mu_2)^3\}) \\ &\quad + \frac{1}{2} (\mathbb{E}\{(Y_1 - \mu_1)^4\} + \mathbb{E}\{(Y_2 - \mu_1)^4\}). \end{aligned} \quad (\text{B.24})$$

The excess kurtosis expressed as a function of  $q$  is then,

$$\begin{aligned} \text{Kurt}(D) = C & \left( 1 - \frac{(q-2)q(a_1+a_2q)}{(q-1)^2} \right. \\ & - \frac{4(q-2)q(q^2-2q-1)(a_1+a_2q)(q^2(a_1-2a_2-1)-2(a_1-1)q+a_2q^3-1)}{(q-1)^8} \\ & - \frac{6(q-2)q(a_1+a_2q)(q^2(a_1-2a_2-1)-2(a_1-1)q+a_2q^3-1)^2}{(q-1)^8} \\ & \left. - \frac{(q-2)q(a_1+a_2q)(-3q^2(a_1-2a_2)+(6a_1+8)q-(3a_2+4)q^3+q^4+1)}{(q-1)^8} \right) - 3 \quad (\text{B.25}) \end{aligned}$$

where

$$C = \left( \left( \frac{(q-2)q(a_1+a_2q)}{(q-1)^2} - 1 \right)^2 - \frac{(q-2)q(a_1+a_2q)}{(q-1)^4} \right)^{-2}$$

## B.4 Power law distribution and Kolmogorov-Smirnov test

We use the discrete power law zeta distribution, which has density

$$f(x) = x^{-\alpha} / \zeta(\alpha), \quad (\text{B.26})$$

where  $\zeta(\alpha)$  is the Riemann zeta function  $\zeta(\alpha) = \sum_x x^{-\alpha}$  with the sum over all integers  $x$ . The computation of the MLEs and Kolmogorov-Smirnov test statistics follow the procedures described in Clauset et al. [2009].

# Appendix C

## Complexity model of herding in financial markets details - for chapter 5

### C.1 Model description

The model consists of  $N$  agents, or traders, operating in a financial market for a single asset, and represented as integrate-and-fire stochastic oscillators connected via an interaction network. For a fixed  $K$ , each agent can transition between  $2K + 1$  states, which is represented by a random-walk over the integers  $\{0, 1, \dots, 2K\}$ . During the integrate phase, agents accumulate information, or sentiment, unobserved by other agents. In the absence of any structure relating to how agents accumulate such private information, this is represented by the agents randomly transitioning between the states of the system (so-called noise traders). When agents have accumulated enough information so as to reach state 0 or  $2K$ , they execute a market transaction that reduces or increases the market asset price, respectively. Each transaction is assumed to impact the market price of the traded asset according to some specified price-impact function [Lillo et al., 2003]. Since market prices are observed by all agents, for each agent that transitions to the firing state  $X$ , where  $X = 0$  or  $X = 2K$ , each market agent not already in one of the firing states updates their private information by moving one state closer to state  $X$ , independently with probability equal to  $p$ . As a result, a cascade may form with agents inducing other agents into the same firing state. With probability  $(1 - p)$ , an

agent ignores the change in the asset price and does not update their private information. Thus, the agents form a pulse-coupled network, with coupling probability equal to  $p$ . We assume that cascades form instantaneously, and the time between a firing state being occupied is described by an exponential random variable with mean  $1/N$ . Once an agent has traded, its accumulation of private information is reset to a neutral level, represented by the state  $K$ . The network coupling probability is parametrised as  $p = Kq/N$ .

## **C.2 Recovery of the implied volatility smile**

We recover the implied volatility smile from quoted option prices using a numerical root search on the pricing formula for European call options [Black and Scholes, 1973]. Second, we use the simple empirical option pricing scheme outlined in Bouchaud and Sornette [1994] to compute the price an option via simulations of the probability distribution. From this we can again obtain the implied volatility from our model, and iterate the process until a reasonable fit is found to the market implied volatility.

## **C.3 Market data: implied volatility of 1-month expiry**

### **European call option on S&P 500 afternoon settled index**

Data for European call options written on the afternoon settled S&P 500 (SPXpm) index as of November 25 2014, with an expiry of December 20 2014. Options with a strike price between 2000 to 2220 are used, with the SPXpm index level at 2067.03 at the close of November 25 2014.

**Table C.1.** Implied volatility of SPXpm European call options of 1-month expiry as of November 25 2014

Strike Price	Implied Volatility
2000	11.91
2005	11.78
2010	11.6
2015	11.37
2020	11.23
2025	10.97
2030	10.78
2035	10.54
2040	10.34
2045	10.09
2050	9.87
2055	9.63
2060	9.41
2065	9.24
2070	9.04
2075	8.89
2080	8.73
2085	8.56
2090	8.43
2095	8.3
2100	8.21
2105	8.12
2110	8.12
2115	8.08
2120	8.08
2125	8.12
2130	8.23
2135	8.32
2140	8.46
2145	8.63
2150	8.82
2160	9.19
2170	9.64
2175	9.9
2180	10.14
2190	10.72
2200	11.09
2220	12.02

## Appendix D

# A result on the first passage time of $N$ Brownian motions - a result used in numerical programming

This brief section outlines computations that were used in the (C++) numerical programming work in simulating some parts of the models in chapter 4 and chapter 5. In particular, when an oscillator integrates stochastically to some boundary, by identification with continuous Brownian motion, it is possible to view the problem in terms of hitting times.

The result present here constructs an iterative approximation scheme for calculating the hitting time of  $N$  Brownian motion particles traversing to the same boundary. Pulse-coupling, then takes place at hitting times.

The theory regarding a single Brownian motion first hitting, a boundary is well studied (see Redner [2001] for summary). In order to present the result for  $N$  Brownian motions, some notation is introduced. Let  $W_t$  denote the standard Brownian motion with,  $W_0 = 0$ . The first passage time (FPT) for  $b \geq 0$  as

$$\tau_b = \inf\{t \geq 0 : W_t \geq b\}. \tag{D.1}$$

For all  $b$ , the FPT  $\tau_b$  is a random variable and is therefore described by a probability distribution. The Laplace transform of some function  $f(t)$  is stated in the form of an integral operator

$$\mathcal{L}[f(t)](s) = \int_0^{\infty} f(t)e^{-st} dt, \quad t \geq 0, s \in \mathbb{C}, \quad (\text{D.2})$$

which is denoted throughout this text by both  $F(s)$  or  $\check{f}(s)$ . In particular, when  $f$  is taken to be the probability density function of a random variable  $X$ , we can make use of the relation

$$F(s) = \mathbb{E}\{e^{-sX}\}, \quad (\text{D.3})$$

where  $\mathbb{E}$  denotes the expectation of the random variable  $e^{-sX}$ . The Laplace transform is a useful tool when investigating FPT problems, as in many cases it is easier to compute moments of the FPT distribution via the Laplace transform, rather than use direct integration. By using Eq. (D.3), moments of a random variable  $X$  can be obtained from

$$\mathbb{E}\{X^n\} = (-1)^n \left[ \check{f}^{(n)} \right] (0) \quad (\text{D.4})$$

$$= (-1)^n \left[ \frac{d^n}{ds^n} \mathbb{E}\{e^{-sX}\} \right] \Big|_{s=0}. \quad (\text{D.5})$$

Revuz and Yor [1999], state the Laplace transform of the law of FPT of standard Brownian motion (SBM) to a symmetric absorbing double barrier as

$$\mathbb{E}\{e^{-sT_V}\} = \frac{1}{\cosh(V\sqrt{2s})}, \quad V > 0, \quad (\text{D.6})$$

where  $T_V$  is the FPT random variable to barriers at  $\pm V$ . In contrast to the single barrier case the expectation for the double barrier case is finite as can be seen by computing the first moment using Equation. (D.5).

$$\mathbb{E}\{T_V\} = \lim_{s \rightarrow 0^+} \frac{V \tanh(V\sqrt{2s})}{\sqrt{2s} \cosh(V\sqrt{2s})} = V^2. \quad (\text{D.7})$$

Here we present a method to approximate the mean FPT of  $N$ -Brownian particles, useful for small  $N$ .

The idea is to compute the FPT of the minimum of two Brownian motions,  $B_1$  and  $B_2$ . We then use the inverse Laplace transform and an iterative scheme, to transform the initial Brownian motion  $B_1$  to  $\hat{B}_1^2$  via a variance transform, which approximates the mean FPT of  $\min(B_1, B_2)$ . In doing so, we have reduced the dimension by 1, and we repeat this process via  $\min(\hat{B}_1^2, B_3)$ , and so on.

Let  $K = \min(\tau_1, \tau_2)$  be the random variable representing the minimum of two independent FPTs for Brownian motion. Then,

$$\begin{aligned}\mathbb{E}\{e^{-sK}\} &= \mathcal{L}[f_K](s) = \int_0^\infty e^{-st} f_K(t) dt \\ &= \int_0^\infty e^{-st} \frac{\partial}{\partial t} G_K(t) dt = s\mathcal{L}[G_K](s),\end{aligned}$$

where  $G$  is the cumulative distribution function of  $K$  and the last equality follows from standard results. Now converting back to  $\tau$  variables gives

$$\begin{aligned}s\mathcal{L}[G_K](s) &= 2\mathcal{L}[f_\tau](s) - \frac{s}{2\pi i} \int_{\gamma-i\infty}^{\gamma+i\infty} \frac{1}{p} \mathcal{L}[f_\tau](p) \frac{1}{s-p} \mathcal{L}[f_\tau](s-p) dp \\ &= 2\mathcal{L}[f_\tau](s) - \frac{s}{2\pi i} \int_{\gamma-i\infty}^{\gamma+i\infty} \frac{1}{p \cosh(V\sqrt{2s})} \frac{1}{(s-p) \cosh(V\sqrt{2(s-p)})} dp,\end{aligned}$$

where we have used the FPT result from Equation. (D.6) in the final equality and  $\gamma$  is a vertical contour.

Using the method of residues to calculate the integral above, and Equation. (D.5), the

expected FPT of two identical Brownian motions to the double barriers  $\pm V$  is

$$\mathbb{E}\{T_{V,2}\} = \frac{2^4 V^2 \sinh(w)}{\sigma_1 \sigma_2 \pi^2 \cosh^2(w)}, \quad w = \frac{\pi}{2}. \quad (\text{D.8})$$

Starting with  $V = 1, \sigma_1 = \sigma_2 = 1$ , we equate Equation. (D.8) with  $\frac{V^2}{\beta^2}$  to make the identification to the FPT for a single Brownian motion with variance  $\beta^2$ , in order to compute the implied  $\beta$ . Successively replacing  $\sigma_1$  with  $\beta$  whilst keeping  $\sigma_2 = 1$  generates the mean FPT for  $N = 3, 4, \dots$ , etc. See Figure. D.1 for a comparison of the method to Monte Carlo generated values, for the case  $V = 1$ .

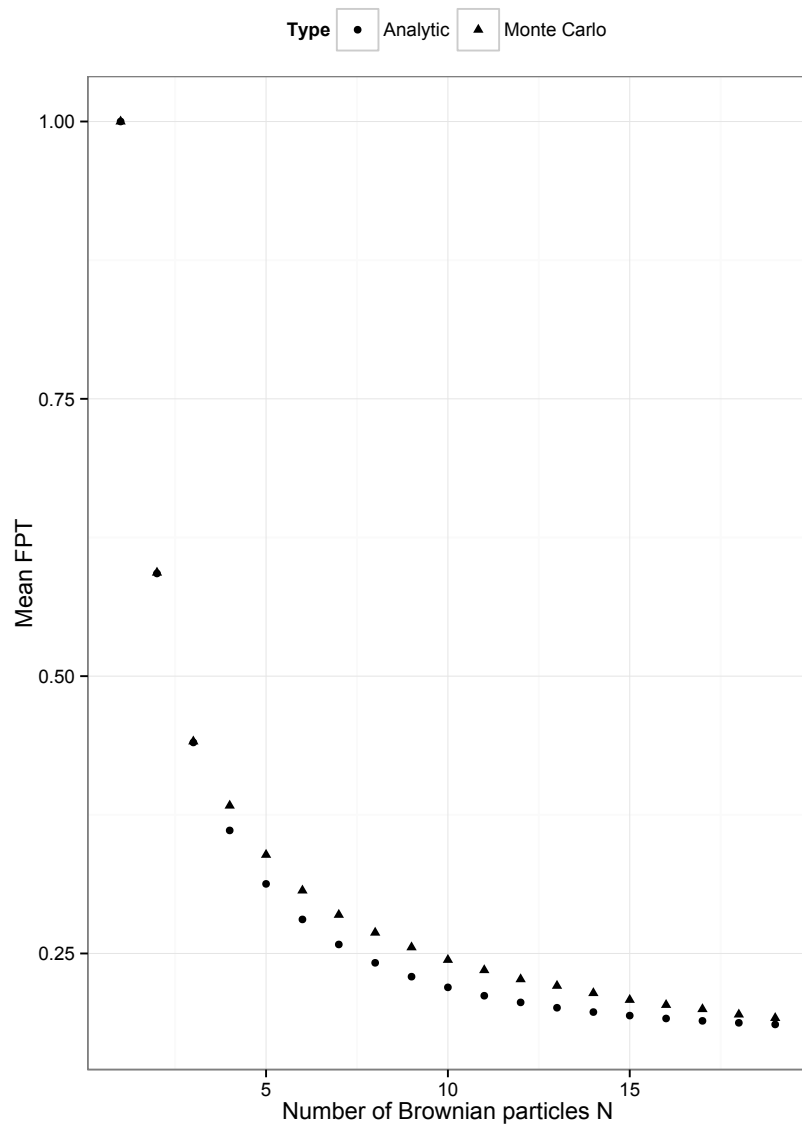


**Figure D.1.** Comparison of FPT for  $N$  Brownian motions computed using Monte Carlo and analytic approximation.

# References

- The role of macroprudential policy. Bank of England Discussion Paper. November, 2009.
- D. Abreu and M. K. Brunnermeier. Bubbles and Crashes. *Econometrica*, 71(1):173–204, 2003.
- V. V. Acharya. A theory of systemic risk and design of prudential bank regulation. *J. Financ. Stab.*, 5(3):224–255, 2009.
- D. Achlioptas and J. Spencer. Explosive percolation in random networks. *Science*, 323 (March):1453–1454, 2009.
- R. Albert and A. Barabási. Statistical mechanics of complex networks. *Rev. Mod. Phys.*, 74(1):47–97, 2002.
- R. Albert, H. Jeong, and A. Barabási. Error and attack tolerance of complex networks. *Nature*, 406(6794):378–82, 2000.
- S. Alfarano and T. Lux. A minimal noise trader model with realistic time series properties. In G. Teyssière and A. Kirman, editors, *Long memory in economics*, pages 345–362. Springer, 2007.
- S. Alfarano and M. Milaković. Network structure and N-dependence in agent-based herding models. *J. Econ. Dyn. Control*, 33:78–92, 2009.
- F. Allen and D. Gale. Optimal Financial Crises. *J. Finance*, 53(4):1245–1284, 1998.

- W. A. Allen and G. Wood. Defining and achieving financial stability. *J. Financ. Stab.*, 2(2):152–172, 2006.
- S. An and F. Schorfheide. Bayesian analysis of DSGE models. *Econom. Rev.*, 2007.
- K. Anand, P. Gai, S. Kapadia, S. Brennan, and M. Willison. A network model of financial system resilience. *J. Econ. Behav. Organ.*, 85:219–235, 2012.
- P. Anderson, K. Arrow, and D. Pines, editors. *The economy as a complex evolving system*. Addison-Wesley, Reading, 1988.
- P. W. Anderson. More Is Different. *Science*, 177(4047):393–396, 1972.
- A. Arenas, A. Díaz-Guilera, J. Kurths, Y. Moreno, and C. Zhou. Synchronization in complex networks. *Phys. Rep.*, 469(3):93–153, 2008.
- N. Arinaminpathy and R. M. May. Systemic risk: the dynamics of model banking systems. *Proc. Natl. Acad. Sci.*, 109(45):18338–18343, 2010.
- N. Arinaminpathy, S. Kapadia, and R. M. May. Size and complexity in model financial systems. *Proc. Natl. Acad. Sci.*, 109(45):18338–43, 2012.
- A. Arneodo, J.-F. Muzy, and D. Sornette. "Direct" causal cascade in the stock market. *Eur. Phys. J. B*, 2:277–282, 1998.
- W. Arthur. Inductive reasoning and bounded rationality. *Am. Econ. Rev.*, 1994.
- W. Arthur. Complexity Economics : A different framework for economic thought. In W. Arthur, editor, *Complexity and the economy*. Oxford university press, 2014.
- W. Arthur, J. Holland, B. LeBaron, and R. Palmer. Asset pricing under endogenous expectations in an artificial stock market. In *The economy as a complex evolving system II*, pages 15–44. Addison-Wesley, Reading, Ma, 1996.
- W. B. Arthur. Complexity in economic and financial markets: Behind the physical institutions and technologies of the marketplace lie the beliefs and expectations of real human beings. *Complexity*, 1:20–25, 1995.

- W. B. Arthur, S. Durlauf, and D. Lane. Economy as an Complex Evolving System II, 1997.
- E. Bacry, J. Delour, and J. Muzy. Modelling financial time series using multifractal random walks. *Phys. A Stat. Mech. its Appl.*, 299(1-2):84–92, 2001.
- E. Bacry, A. Kozhemyak, and J. F. Muzy. Log-normal continuous cascade model of asset returns: aggregation properties and estimation. *Quant. Financ.*, 13(5):1–24, 2012.
- R. T. Baillie. Long memory processes and fractional integration in econometrics. *J. Econom.*, 73(1):5–59, 1996.
- A. V. Banerjee. A simple-model of herd behavior. *Q. J. Econ.*, 107:797–817, 1992.
- Bank for International Settlements. International convergence of capital measurement and capital standards. Report. June, 2004.
- Bank for International Settlements. Statistical release : OTC derivatives statistics at end-December 2012. (May), 2013.
- A. Barabási and R. Albert. Emergence of scaling in random networks. *Science*, 286 (5439):509–512, 1999.
- O. E. Barndorff-Nielsen. Normal Inverse Gaussian Distributions and Stochastic Volatility Modelling. *Scand. J. Stat.*, 24(1):1–13, 1997.
- O. E. Barndorff-Nielsen and N. Shephard. Non-Gaussian Ornstein-Uhlenbeck-based models and some of their uses in financial economics. *J. R. Stat. Soc. Ser. B (Statistical Methodol.)*, 63(2):167–175, 2001.
- L. Barras, O. Scaillet, and R. Wermers. False discoveries in mutual fund performance: Measuring luck in estimated alphas. *J. Finance*, 65(1):179–216, 2010.
- M. Bartolozzi and A. Thomas. Stochastic cellular automata model for stock market dynamics. *Phys. Rev. E*, 69(4):046112, 2004.

- J. M. Bartunek and S. L. Rynes. Academics and practitioners are alike and unlike: The paradoxes of academic-practitioner relationships. *J. Manage.*, 40(5):1181–1201, 2014.
- J. Barunik, T. Aste, T. Di Matteo, and R. Liu. Understanding the source of multifractality in financial markets. *Phys. A Stat. Mech. its Appl.*, 391(17):4234–4251, 2012.
- Basel Committee. Global systemically important banks. Report. November, 2011.
- Basel Committee on Banking Supervision. Basel III: A global regulatory framework for more resilient banks and banking systems. Report., 2010.
- S. Battiston, G. Caldarelli, C.-P. Georg, R. May, and J. Stiglitz. Complex derivatives. *Nat. Phys.*, 9(3):123–125, 2013.
- M. Batty. *Cities and complexity: understanding cities with cellular automata, agent-based models, and fractals*. The MIT press, 2007.
- L. Bauwens, C. Hafner, and S. Laurent, editors. *Handbook of Volatility Models and Their Applications*. John Wiley and Sons, Inc., 2012.
- C. Bean. Asset prices, financial instability, and monetary policy. *Am. Econ. Rev.*, 94(2):14–18, 2004.
- J. M. Beggs. Neuronal networks: Focus amidst the noise. *Nat. Phys.*, 9(9):533–534, 2013.
- B. S. Bernanke. Financial reform to address systemic risk. *Counc. Foreign Relations*, 2009.
- B. S. Bernanke and M. Gertler. Should central banks respond to movements in asset prices? *Am. Econ. Rev.*, pages 253–257, 2001.
- S. Bikhchandani and S. Sharma. Herd behavior in financial markets. *IMF Staff Pap.*, 47(3):279–310, 2000.

- S. Bikhchandani, D. Hirshleifer, and I. Welch. A Theory of Fads, Fashion, Custom, and Cultural Change as Informational Cascades. *J. Polit. Econ.*, 100:992–1026, 1992.
- S. Bikhchandani, D. Hirshleifer, and I. Welch. Learning from the behavior of others: Conformity, fads, and informational cascades. *J. Econ. Perspect.*, 12(3):151–170, 1998.
- F. Black. Noise. *J. Finance*, 41(3):529–543, 1986.
- F. Black and M. Scholes. The pricing of options and corporate liabilities. *J. Polit. Econ.*, pages 637–654, 1973.
- O. Blanchard and M. Watson. Bubbles, rational expectations and financial markets. In P. Watchel, editor, *Crises in the Economic and Financial Structure*. Lexington Books, Lexington, 1982.
- R. Bloomfield, M. O’Hara, and G. Saar. How Noise Trading Affects Markets: An Experimental Analysis. *Rev. Financ. Stud.*, 22(6):2275–2302, 2009.
- S. Boccaletti, V. Latora, Y. Moreno, M. Chavez, and D. Hwang. Complex networks: structure and dynamics. *Phys. Rep.*, 424(4-5):175–308, 2006.
- N. Boccara. *Modeling complex systems*. Springer, 2 edition, 2010.
- T. Bohman. Emergence of connectivity in networks. *Science*, 323(March):1438–1439, 2009.
- J. Bollen, H. Mao, and X. Zeng. Twitter mood predicts the stock market. *J. Comput. Sci.*, 2(1):1–8, 2011.
- T. Bollerslev. Generalized autoregressive conditional heteroskedasticity. *J. Econom.*, 31(3):307–327, 1986.
- T. Bollerslev, R. Y. Chou, and K. F. Kroner. ARCH modeling in finance. *J. Econom.*, 52(1-2):5–59, 1992.

- B. Bollobás and O. Riordan. Mathematical results on scale-free random graphs. In S. Bornholdt and H. G. Schuster, editors, *Handbook of graphs and networks: From the Genome to the Internet*, volume 1, pages 1–34. Wiley, 2003.
- C. Borio. Towards a macroprudential framework for financial supervision and regulation? *CESifo Econ. Stud.*, 49(2):181–215, 2003.
- L. Borland. A non-Gaussian stock price model: Options, credit and a multi-timescale Memory. *Prog. Theor. Phys. Suppl.*, 162:155–164, 2006.
- L. Borland, J.-P. Bouchaud, J.-F. Muzy, and G. Zumbach. The dynamics of financial markets - Mandelbrot’s multifractal cascades, and beyond. *Wilmott Magazine*, 2005.
- J.-P. Bouchaud. An introduction to statistical finance. *Phys. A Stat. Mech. its Appl.*, 313(1-2):238–251, 2002.
- J.-P. Bouchaud. Economics needs a scientific revolution. *Nature*, 455(October):2008, 2008.
- J.-P. Bouchaud. Crises and collective socio-economic phenomena: Simple models and challenges. *J. Stat. Phys.*, 151(3-4):567–606, 2013.
- J.-P. Bouchaud and D. Sornette. The Black-Scholes option pricing problem in mathematical finance: generalization and extensions for a large class of stochastic processes. *J. Phys. I*, 4(6):863–881, 1994.
- J.-P. Bouchaud, I. Giardina, and M. Mezard. On a universal mechanism for long ranged volatility correlations. *pre-print cond-mat/0012156*, pages 212–216, 2001.
- F. Brauer. Models for the spread of universally fatal diseases. *J. Math. Biol.*, 28(4): 451–62, 1990.
- W. A. Brock. Tipping points, abrupt opinion changes, and punctuated policy change. In R. Repetto, editor, *Punctuated equilibrium and the dynamics of US environmental policy*. Yale University Press, Yale, 2006.

- W. A. Brock and C. H. Hommes. Heterogeneous beliefs and routes to chaos in a simple asset pricing model. *J. Econ. Dyn. Control*, 22(8-9):1235–1274, 1998.
- W. A. Brock, C. H. Hommes, and F. O. Wagener. Evolutionary dynamics in markets with many trader types. *J. Math. Econ.*, 41(1-2):7–42, 2005.
- D. C. Brody, L. P. Hughston, and E. Mackie. General theory of geometric Lévy models for dynamic asset pricing. *Proc. R. Soc. A Math. Phys. Eng. Sci.*, 468:1778–1798, 2012.
- J. Brogaard. High frequency trading and its impact on market quality. Working paper, Northwestern University Kellogg School of Management, 2010.
- J. Brogaard, T. Hendershott, and R. Riordan. High-Frequency Trading and Price Discovery. *Rev. Financ. Stud.*, 27(8):2267–2306, 2014.
- N. Brunel. Dynamics of sparsely connected networks of excitatory and inhibitory spiking neurons. *J. Comput. Neurosci.*, 8(3):183–208, 2000.
- S. V. Buldyrev, R. Parshani, G. Paul, H. E. Stanley, and S. Havlin. Catastrophic cascade of failures in interdependent networks. *Nature*, 464(7291):1025–8, 2010.
- N. Cai and S. G. Kou. Option Pricing Under a Mixed-Exponential Jump Diffusion Model. *Manage. Sci.*, 57(11):2067–2081, 2011.
- L. E. Calvet and A. J. Fisher. How to Forecast Long-Run Volatility: Regime Switching and the Estimation of Multifractal Processes. *J. Financ. Econom.*, 2(1):49–83, 2004.
- P. R. Carlile. Transferring, translating, and transforming: An integrative framework for managing knowledge across boundaries. *Organ. Sci.*, 15(5):555–568, 2004.
- S. R. Carpenter and W. Brock. Rising variance: a leading indicator of ecological transition. *Ecol. Lett.*, 9(3):311–318, 2006.
- P. Casini and F. Vestroni. Nonstandard bifurcations in oscillators with multiple discontinuity boundaries. *Nonlinear Dyn.*, pages 41–59, 2004.

- C. Castellano and R. Pastor-Satorras. Thresholds for epidemic spreading in networks. *Phys. Rev. Lett.*, 105(21):1–4, 2010.
- S. G. Cecchetti, H. Genberg, J. Lipsky, and S. Wadhvani. Asset prices and central bank policy. *Geneva Rep. world Econ.*, 2(2), 2000.
- C. Cella, A. Ellul, and M. Giannetti. Investors’ horizons and the amplification of market shocks. *Rev. Financ. Stud.*, 26(7):1607–1648, 2013.
- A. Chakraborti, I. M. Toke, M. Patriarca, and F. Abergel. Econophysics review: II. Agent-based models. *Quant. Financ.*, 11(7):1013–1041, 2011a.
- A. Chakraborti, I. M. Toke, M. Patriarca, and F. Abergel. Econophysics review: I. Empirical facts. *Quant. Financ.*, 11(7):991–1012, 2011b.
- D. Challet and M. Marsili. Phase transition and symmetry breaking in the minority game. *Phys. Rev. E*, 60(6):6271–6274, 1999.
- D. Challet, A. Chessa, M. Marsili, and Y.-C. Zhang. From Minority Games to real markets. *Quant. Financ.*, 1(1):168–176, 2001a.
- D. Challet, M. Marsili, and Y.-C. Zhang. Stylized facts of financial markets and market crashes in Minority Games. *Phys. A Stat. Mech. its Appl.*, 294(3-4):514–524, 2001b.
- S.-K. Chang. Herd behavior, bubbles and social interactions in financial markets. *Stud. Nonlinear Dyn. Econom.*, 18(1):89–101, 2014.
- W. Chen, J. Nagler, X. Cheng, X. Jin, H. Shen, Z. Zheng, and R. M. DSouza. Phase transitions in supercritical explosive percolation. *Phys. Rev. E*, 87(5):052130, 2013.
- S. Cincotti, D. Sornette, P. Treleven, S. Battiston, G. Caldarelli, C. Hommes, and A. Kirman. An economic and financial exploratory. *Eur. Phys. J. Spec. Top.*, 214(1): 361–400, 2012.
- M. Cipriani and A. Guarino. Estimating a Structural Model of Herd Behavior in Financial Markets . *Am. Econ. Rev.*, 104(1):224–251, 2014.

- A. Clauset, C. R. Shalizi, and M. E. J. Newman. Power-Law Distributions in Empirical Data. *SIAM Rev.*, 51(4):661–703, 2009.
- V. Colizza, A. Barrat, M. Barthélemy, and A. Vespignani. The role of the airline transportation network in the prediction and predictability of global epidemics. *Proc. Natl. Acad. Sci.*, 103(7):2015–20, 2006.
- R. Cont. Empirical properties of asset returns: stylized facts and statistical issues. *Quant. Financ.*, 1(2):223–236, 2001.
- R. Cont. Volatility clustering in financial markets : Empirical facts and agent - based models. In G. Teyssière and A. Kirman, editors, *Long memory in economics*, pages 289–310. Springer, 2007.
- R. Cont and J. Bouchaud. Herd behavior and aggregate fluctuations in financial markets. *Macroecon. Dyn.*, pages 170–196, 2000.
- R. M. Corless, G. H. Gonnet, D. E. G. Hare, D. J. Jeffrey, and D. E. Knuth. On the Lambert W function. *Adv. Comput. Math.*, 5(1):329–359, 1996.
- P. Crucitti, V. Latora, and M. Marchiori. Model for cascading failures in complex networks. *Phys. Rev. E*, 69(4):045104, 2004.
- C. Curme, T. Preis, H. E. Stanley, and H. S. Moat. Quantifying the semantics of search behavior before stock market moves. *Proc. Natl. Acad. Sci.*, 111(32):11600–5, 2014.
- R. A. Da Costa, S. N. Dorogovtsev, A. V. Goltsev, and J. F. F. Mendes. Explosive percolation transition is actually continuous. *Phys. Rev. Lett.*, 105(25):2–5, 2010.
- R. A. Da Costa, S. N. Dorogovtsev, A. V. Goltsev, and J. F. F. Mendes. Critical exponents of the explosive percolation transition. *Phys. Rev. E*, 89(4):1–6, 2014.
- J. Da Fonseca, M. Grasselli, and F. Ielpo. Estimating the Wishart Affine Stochastic Correlation Model using the empirical characteristic function. *Stud. Nonlinear Dyn. Econom.*, 18(3):253–289, 2014.

- V. Dakos, M. Scheffer, E. H. van Nes, V. Brovkin, V. Petoukhov, and H. Held. Slowing down as an early warning signal for abrupt climate change. *Proc. Natl. Acad. Sci.*, 105(38):14308–14312, 2008.
- E. Derman and I. Kani. Riding on a smile. *Risk*, 7(2):32–39, 1994.
- C. Detken and F. Smets. Asset price booms and monetary policy. In H. Sibert, editor, *Macroeconomic Policies in the World Economy*. Springer, 2004.
- R. E. L. DeVille and C. S. Peskin. Synchrony and asynchrony in a fully stochastic neural network. *Bull. Math. Biol.*, 70(6):1608–33, 2008.
- R. E. L. DeVille and C. S. Peskin. Synchrony and asynchrony for neuronal dynamics defined on complex networks. *Bull. Math. Biol.*, 74(4):769–802, 2012.
- R. E. L. DeVille, C. S. Peskin, and J. H. Spencer. Dynamics of Stochastic Neuronal Networks and the Connections to Random Graph Theory. *Math. Model. Nat. Phenom.*, 5(2):26–66, 2010.
- R. D’Hulst and G. J. Rodgers. Exact Solution of a Model for Crowding and Information Transmission in Financial Markets. *Int. J. Theor. Appl. Financ.*, 03(04):609–616, 2000.
- M. di Bernardo, C. Budd, and A. Champneys. Grazing and Border-Collision in Piecewise-Smooth Systems: A Unified Analytical Framework. *Phys. Rev. Lett.*, 86(12):2553–2556, 2001.
- T. Di Matteo. Multi-scaling in finance. *Quant. Financ.*, 7(1):21–36, 2007.
- Z. Ding, C. W. Granger, and R. F. Engle. A long memory property of stock market returns and a new model. *J. Empir. Financ.*, 1:83–106, 1993.
- I. Dobson, B. A. Carreras, V. E. Lynch, and D. E. Newman. Complex systems analysis of series of blackouts: cascading failure, critical points, and self-organization. *Chaos*, 17(2):026103, 2007.

- J. C. Doyle, D. L. Alderson, L. Li, S. Low, M. Roughan, S. Shalunov, R. Tanaka, and W. Willinger. The ‘robust yet fragile’ nature of the internet. *Proc. Natl. Acad. Sci.*, 102(41):14497–14502, 2005.
- J. M. Drake and B. D. Griffen. Early warning signals of extinction in deteriorating environments. *Nature*, 467(7314):456–459, 2010.
- M. Drmota. *Random trees*. Springer, Wien, 2009.
- D. Easley, M. M. Lopez de Prado, and M. O’Hara. The microstructure of the flash crash: Flow toxicity, liquidity crashes and the probability of informed trading. *J. Portf. Manag.*, 37:118–128, 2011.
- D. Easley, M. M. Lopez de Prado, and M. O’Hara. Flow Toxicity and Liquidity in a High-frequency World. *Rev. Financ. Stud.*, 25(5):1457–1493, 2012.
- R. M. Edge and R. S. Gürkaynak. How Useful Are Estimated DSGE Model Forecasts for Central Bankers? *Brookings Papers on Economic Activity*, 2010(2):209–244, 2010.
- V. Eguíluz and M. Zimmermann. Transmission of Information and Herd Behavior: An Application to Financial Markets. *Phys. Rev. Lett.*, 85(26):5659–5662, 2000.
- L. Eisenberg and T. Noe. Systemic risk in financial systems. *Manage. Sci.*, 47(2): 236–249, 2001.
- P. Erdős and A. Rényi. On random graphs. *Publ. Math. Debrecen*, 6:290–297, 1959.
- E. F. Fama. Efficient capital markets: A review of theory and empirical work. *J. Finance*, 25:383–417, 1970.
- E. F. Fama and K. R. French. Luck versus skill in the cross-section of mutual fund returns. *J. Finance*, 65(5):1915–1947, 2010.
- J. D. Farmer and D. Foley. The economy needs agent-based modelling. *Nature*, 460 (7256):685–6, 2009.

- W. Feller. *An introduction to probability theory and its applications: Volume 1*. John Wiley and Sons, Inc., New York, 3 edition, 1968.
- L. Feng, B. Li, B. Podobnik, T. Preis, and H. E. Stanley. Linking agent-based models and stochastic models of financial markets. *Proc. Natl. Acad. Sci.*, 109(22):8388–93, 2012.
- J.-P. Fouque and J. A. Langsam. *Handbook on Systemic Risk*. Cambridge University Press, 2013.
- G. Frankfurter and E. McGoun. Anomalies in finance: What are they and what are they good for? *Int. Rev. Financ. Anal.*, 10(4):407–423, 2001.
- D. Fricke and A. Gerig. Too fast or too slow? Determining the optimal speed of financial markets. 2015. URL <http://www.sec.gov/dera/staff-papers>.
- M. Friedman. *The case for flexible exchange rates*. University of Chicago Press, 1953.
- X. Gabaix, P. Gopikrishnan, V. Plerou, and H. E. Stanley. A theory of power-law distributions in financial market fluctuations. *Nature*, 423(6937):267–70, 2003.
- P. Gai and S. Kapadia. Contagion in financial networks. *Proc. R. Soc. A Math. Phys. Eng. Sci.*, 466(2120):2401–2423, 2010.
- P. Gai, A. Haldane, and S. Kapadia. Complexity, concentration and contagion. *J. Monet. Econ.*, 58(5):453–470, 2011.
- G. Galati and R. Moessner. Macroprudential policy - a literature review. *J. Econ. Surv.*, 27(5):846–878, 2013.
- M. Galbiati and K. Soramäki. An agent-based model of payment systems. Bank of England Discussion Paper., 2008.
- J. Galí. The Basic New Keynesian Model. In *Monetary Policy , Inflation and the Business Cycle*, number August. Princeton University Press, 2009.

- M. Gallegati and A. Kirman. Reconstructing economics: Agent based models and complexity. *Complex. Econ.*, 1:5–31, 2012.
- A. Gerali, S. Neri, L. Sessa, and F. M. Signoretti. Credit and Banking in a DSGE Model of the Euro Area. *J. Money, Credit Bank.*, 2010.
- I. Giardina and J. P. Bouchaud. Volatility clustering in agent based market models. *Phys. A Stat. Mech. its Appl.*, 324(1-2):6–16, 2003.
- R. J. Gibbens. *Dynamic routing in circuit-switched networks: the dynamic alternative routing strategy*. Phd, Cambridge, 1988.
- R. J. Gibbens, P. J. Hunt, and F. P. Kelly. Bistability in communication networks. *Disord. Phys. Syst.*, (1973):113–128, 1990.
- J. Gleeson and D. Cahalane. Seed size strongly affects cascades on random networks. *Phys. Rev. E*, 75(5):056103, 2007.
- A. Golub, J. Keane, and S. Poon. High frequency trading and mini flash crashes. *pre-print SSRN 2182097*, page 22, 2012.
- V. Gontis and A. Kononovicius. Consentaneous agent-based and stochastic model of the financial markets. *PLoS One*, 9(7), 2014.
- P. Gopikrishnan, V. Plerou, L. A. Nunes Amaral, M. Meyer, and H. E. Stanley. Scaling of the distribution of fluctuations of financial market indices. *Phys. Rev. E*, 60(5): 5305–5316, 1999.
- G. Grimmett. *Percolation*. Springer Berlin Heidelberg, 2 edition, 1999.
- X. Guardiola, A. Diaz-Guilera, M. Llas, and C. Perez. Synchronization, diversity, and topology of networks of integrate and fire oscillators. *Phys. Rev. E*, 62(4):5565–5570, 2000.
- A. Hackett and J. P. Gleeson. Cascades on clique-based graphs. *Phys. Rev. E*, 87(6): 062801, 2013.

- A. Hackett, S. Melnik, and J. P. Gleeson. Cascades on a class of clustered random networks. *Phys. Rev. E*, 83(5):056107, 2011.
- A. G. Haldane. Rethinking the Financial Network. *Bank of England*, pages 1–41, 2009.
- A. G. Haldane and R. M. May. Systemic risk in banking ecosystems. *Nature*, 469(7330):351–5, 2011.
- S. G. Hanson, A. K. Kashyap, J. C. Stein, and G. Hanson. A macroprudential approach to financial regulation. *J. Econ. Perspect.*, 25(1):3–28, 2011.
- J. Hasbrouck and G. Saar. Low-latency trading. *J. Financ. Mark.*, 16(4):646–679, 2013.
- S. Havlin, D. Y. Kenett, E. Ben-Jacob, a. Bunde, R. Cohen, H. Hermann, J. W. Kantelhardt, J. Kertész, S. Kirkpatrick, J. Kurths, J. Portugali, and S. Solomon. Challenges in network science: Applications to infrastructures, climate, social systems and economics. *Eur. Phys. J. Spec. Top.*, 214(1):273–293, 2012.
- D. Helbing. Pluralistic modeling of complex systems. CCSS Working Paper, 10-009 September, 2010.
- D. Helbing. Systemic risks in society and economics. International Risk Governance Council Report. October, 2012.
- D. Helbing. Globally networked risks and how to respond. *Nature*, 497(7447):51–9, 2013.
- D. Helbing, S. Baliatti, S. Bishop, and P. Lukowicz. Understanding, creating, and managing complex techno-socio-economic systems: Challenges and perspectives. *Eur. Phys. J. Spec. Top.*, 195(1):165–186, 2011.
- S. L. Heston. A closed-form solution for options with stochastic volatility with applications to bond and currency options. *Rev. Financ. Stud.*, 6:327–343, 1993.

- S. L. Heston and S. Nandi. A Closed-Form GARCH Option Pricing Model. *Rev. Financ. Stud.*, 13(3):585–625, 2000.
- D. A. Hibbs Jr. Political parties and macroeconomic policy. *Am. Polit. Sci. Rev.*, 71(4): 1467–1487, 1977.
- P. Hilton and J. Pedersen. Catalan numbers, their generalization, and their uses. *Math. Intell.*, 13(2):64–75, 1991.
- D. Hirshleifer and S. Hong Teoh. Herd behaviour and cascading in capital markets: A review and synthesis. *Eur. Financ. Manag.*, 9(1):25–66, 2003.
- D. Hodson and D. Mabbett. UK economic policy and the global financial crisis: paradigm lost? *J. common Mark. Stud.*, 47(5):1041–1061, 2009.
- R. P. Holt, J. B. Rosser, and D. Colander. The Complexity Era in Economics. *Rev. Polit. Econ.*, 23(3):357–369, 2011.
- C. Hommes. *Behavioral rationality and heterogeneous expectations in complex economic systems*. Cambridge University Press, 2013.
- C. Hommes and G. Iori. Introduction special issue crises and complexity. *J. Econ. Dyn. Control*, 50:1–4, 2015.
- C. Hommes and F. Wagener. Complex Evolutionary Systems in Behavioral Finance. In T. Hens and K. R. Schenk-Hoppé, editors, *Handbook of Financial Markets Dynamics and Evolution*. 2009.
- C. H. Hommes. Financial markets as nonlinear adaptive evolutionary systems. *Quant. Financ.*, 1(1):149–167, 2001.
- C. H. Hommes. Modeling the stylized facts in finance through simple nonlinear adaptive systems. *Proc. Natl. Acad. Sci.*, 99 Suppl 3:7221–8, 2002.
- C. H. Hommes. Heterogeneous agent models in economics and finance. *Handbook of computational economics*, 2:1109–1186, 2006.

- J. Hull. *Options, futures and other derivatives*. Prentice Hall, Boston, 8 edition, 2011.
- International Monetary Fund. *Financial Soundness Indicators*. 2006.
- G. Iori and J. Porter. Agent-based modelling for financial markets. Technical Report 12/08, City University, London, 2012. URL <http://openaccess.city.ac.uk/1744/>.
- E. Ising. Beitrag zur theorie des ferromagnetismus. *Zeitschrift für Phys.*, 31(1):253–258, 1925.
- K. E. Iverson. *A programming language*. Wiley, New York, 1 edition, 1962.
- A. Johansen, O. Ledoit, and D. Sornette. Crashes as critical points. *Int. J. Theor. Appl. Financ.*, 3(2):219–255, 2000.
- N. F. Johnson, P. Jefferies, and P. M. Hui. *Financial market complexity*. Oxford University Press, 2003.
- M. Joyce, M. Tong, and R. Woods. The United Kingdom’s quantitative easing policy: design, operation and impact. *Bank of England Quarterly Bulletin*, (3):200–212, 2011.
- T. Kaizoji, S. Bornholdt, and Y. Fujiwara. Dynamics of price and trading volume in a spin model of stock markets with heterogeneous agents. *Phys. A Stat. Mech. its Appl.*, 316:441–452, 2002.
- N. Kaldor. Capital accumulation and economic growth. In F. A. Lutz and D. C. Hague, editors, *The Theory of Capital*, pages 177–222. Macmillan and Co, 1961.
- P. Kaluza, A. Kölzsch, M. T. Gastner, and B. Blasius. The complex network of global cargo ship movements. *J. R. Soc. Interface*, 7(48):1093–1103, 2010.
- I. Karatzas and S. E. Shreve. *Brownian motion and stochastic calculus*, volume 113. Springer, 2 edition, 1991.

- J. Kari. Theory of cellular automata: A survey. *Theor. Comput. Sci.*, 334:3–33, 2005.
- F. P. Kelly. The Clifford Paterson lecture , 1995 : Modelling communication networks , present and future. *Philos. Trans. Math. Phys. Eng. Sci.*, 354(1707):437–463, 1996.
- D. Y. Kenett, E. Ben-Jacob, H. E. Stanley, and G. Gur-Gershgoren. How high frequency trading affects a market index. *Sci. Rep.*, 3:2110, 2013.
- W. O. Kermack and A. G. McKendrick. Contributions to the mathematical theory of epidemics. II. The problem of endemicity. *Proc. R. Soc. A Math. Phys. Eng. Sci.*, 138(834):55–83, 1932.
- A. Khandani and A. Lo. What happened to the quants in August 2007? *J. Invest. Manag.*, 5(August):10–12, 2007.
- A. E. Khandani and A. W. Lo. What happened to the quants in August 2007? Evidence from factors and transactions data. *J. Financ. Mark.*, 14(1):1–46, 2011.
- G.-R. Kim and H. M. Markowitz. Investment rules, margin, and market volatility. *J. Portf. Manag.*, 16(1):45–52, 1989.
- M. Kim and M. Kim. Group-wise herding behavior in financial markets: an agent-based modeling approach. *PLoS One*, 9(4):e93661, 2014.
- A. Kirman. Ants, Rationality, and Recruitment. *Q. J. Econ.*, 108(1):137–156, 1993.
- A. Kirman. The economic crisis is a crisis for economic theory. *CESifo Econ. Stud.*, 56(4):498–535, 2010a.
- A. Kirman. *Complex economics: individual and collective rationality*. Routledge, 2010b.
- K. Klemm and V. Eguíluz. Growing scale-free networks with small-world behavior. *Phys. Rev. E*, 65(5):057102, 2002.
- D. E. Knuth. *The art of computer programming*. Addison Wesley, Reading, Ma, 2 edition, 1998.

- A. N. Kolmogorov. A refinement of previous hypotheses concerning the local structure of turbulence in a viscous incompressible fluid at high Reynolds number. *J. Fluid Mech.*, 13(01):82, 1962.
- A. Kononovicius and V. Gontis. Control of the socio-economic systems using herding interactions. *Phys. A Stat. Mech. its Appl.*, 405:80–84, 2014.
- C. Kuehn. A mathematical framework for critical transitions: Bifurcations, fast-slow systems and stochastic dynamics. *Phys. D Nonlinear Phenom.*, 240(12):1020–1035, 2011.
- Y. Kuramoto. Collective synchronization of pulse-coupled oscillators and excitable units. *Phys. D*, 50:15–30, 1991.
- F. Kydland and E. Prescott. Time to build and aggregate fluctuations. *Econom. J. Econom. Soc.*, 1982.
- A. S. Kyle. Continuous auctions and insider trading. *Econometrica*, 53(6):1315–1335, 1985.
- S. J. Lade and T. Gross. Early warning signals for critical transitions: a generalized modeling approach. *PLoS Comput. Biol.*, 8(2):e1002360, 2012.
- Y.-C. Lai. Symmetry-breaking bifurcation with on-off intermittency in chaotic dynamical systems. *Phys. Rev. E*, 53(5):R4267–R4270, 1996.
- B. LeBaron. Stochastic volatility as a simple generator of apparent financial power laws and long memory. *Quant. Financ.*, 1(6):621–631, 2001.
- B. LeBaron. Heterogeneous gain learning and the dynamics of asset prices. *J. Econ. Behav. Organ.*, 83(3):424–445, 2012.
- M. Levy. Stock market crashes as social phase transitions. *J. Econ. Dyn. Control*, 32(1):137–155, 2008.
- P. Lévy. *Calcul des probabilités*. Gauthier-Villars Paris, 1925.

- F. Lillo, J. D. Farmer, and R. N. Mantegna. Econophysics: Master curve for price-impact function. *Nature*, 421(6919):129–30, 2003.
- M. Liu. Modeling long memory in stock market volatility. *J. Econom.*, 99(1):139–171, 2000.
- X. Liu, D. Margaritis, and P. Wang. Stock market volatility and equity returns: Evidence from a two-state Markov-switching model with regressors. *J. Empir. Financ.*, 19(4):483–496, 2012.
- Y.-F. Liu, W. Zhang, and H.-C. Xu. Collective behavior and options volatility smile: An agent-based explanation. *Econ. Model.*, 39:232–239, 2014.
- T. A. Lubik and P. Surico. The lucas critique and the stability of empirical models. *Journal of Applied Econometrics*, 25(1):177–194, 2010.
- T. Lux. Herd behaviour, bubbles and crashes. *Econ. J.*, 105(431):881–896, 1995.
- T. Lux. Financial power laws: Empirical evidence, models, and mechanism. Technical report, Economics working paper/Christian-Albrechts-Universität Kiel, Department of Economics, 2006.
- T. Lux and M. Marchesi. Scaling and criticality in a stochastic multi-agent model of a financial market. *Nature*, 397(February):498–500, 1999.
- T. Lux and M. Marchesi. Volatility clustering in financial markets: a microsimulation of interacting agents. *Int. J. Theor. Appl. Financ.*, 03(04):675–702, 2000.
- P. E. Lynch and G. O. Zumbach. Market heterogeneities and the causal structure of volatility. *Quant. Financ.*, 3(4):320–331, 2003.
- W. Maass and C. Bishop. *Pulsed neural networks*. Mit Press, Cambridge, Mass, 2001.
- A. Majdandzic, B. Podobnik, S. V. Buldyrev, D. Y. Kenett, S. Havlin, and H. Eugene Stanley. Spontaneous recovery in dynamical networks. *Nat. Phys.*, 10(1):34–38, 2013.

- B. Mandelbrot. The variation of certain speculative prices. *J. Bus.*, 36(4):394–419, 1963.
- B. B. Mandelbrot. Intermittent turbulence in self-similar cascades: divergence of high moments and dimension of the carrier. *J. Fluid Mech.*, 62(02):331, 1974.
- R. May, S. Levin, and G. Sugihara. Complex systems: Ecology for bankers. *Nature*, 451(February):893–895, 2008.
- R. M. May. Will a large complex system be stable? *Nature*, 238(5364):413–414, 1972.
- A. J. Menkveld. High-Frequency Traders and Market Structure. *Financ. Rev.*, 49(2): 333–344, 2014.
- R. C. Merton. Theory of rational option pricing. *Bell J. Econ. Manag. Sci.*, pages 141–183, 1973.
- R. C. Merton. Option pricing when underlying stock returns are discontinuous. *J. financ. econ.*, 3:125–144, 1976.
- F. Milani and A. Rajbhandari. Expectation formation and monetary DSGE models: Beyond the rational expectations paradigm. *Adv. Econom.*, 2012.
- P. Milgrom and N. Stokey. Information, trade and common knowledge. *J. Econ. Theory*, 26(1):17–27, 1982.
- R. Mirollo and S. Strogatz. Synchronization of pulse-coupled biological oscillators. *SIAM J. Appl. Math.*, 50(6):1645–1662, 1990.
- M. Mizen and W. Rhode. Breaking down the uk equity market: Executable liquidity, dark trading, high frequency and swaps. Technical report, TABB Group, 2011.
- A. E. Motter, C. S. Zhou, and J. Kurths. Enhancing complex-network synchronization. *Europhys. Lett.*, 69(3):334–340, 2005.
- J. Muhle-Karbe, O. Pfaffel, and R. Stelzer. Option Pricing in Multivariate Stochastic Volatility Models of OU Type. *SIAM J. Financ. Math.*, 3(1):66–94, 2012.

- J. F. Muth. Rational expectations and the theory of price movements. *Econometrica*, 29:315–335, 1961.
- J.-F. Muzy, R. Baïle, and E. Bacry. Random cascade model in the limit of infinite integral scale as the exponential of a nonstationary  $1/f$  noise: Application to volatility fluctuations in stock markets. *Phys. Rev. E*, 87(4):042813, 2013.
- M. E. J. Newman. Spread of epidemic disease on networks. *Phys. Rev. E*, 66(1):016128, 2002.
- M. E. J. Newman. Complex Systems: A Survey. *Am. J. Phys.*, 79:800–810, 2011.
- G. Nicosia and C. Nicosia. Foundations of Complex Systems. *Eur. Rev.*, 17(April):237, 2009.
- V. Nicosia, G. Bianconi, V. Latora, and M. Barthelemy. Growing Multiplex Networks. *Phys. Rev. Lett.*, 111(5):058701, 2013.
- Office of National Statistics-UK. Datasets and Tables, 2013.
- M. Ortisi and V. Zuccolo. From minority game to Black & Scholes pricing. *Appl. Math. Financ.*, 20(6):578–598, 2013.
- S. E. Page. *Diversity and complexity*. Princeton University Press, 2010.
- J. Pan. The jump-risk premia implicit in options: evidence from an integrated time-series study. *J. financ. econ.*, 63(1):3–50, 2002.
- A. Park and D. SgROI. Herding, contrarianism and delay in financial market trading. *Eur. Econ. Rev.*, 56(6):1020–1037, 2012.
- R. Pastor-Satorras and A. Vespignani. Epidemic spreading in scale-free networks. *Phys. Rev. Lett.*, 86(14):3200–3203, 2001.
- T. Persson and G. Tabellini. Political economics and macroeconomic policy. In J. B. Taylor and M. Woodford, editors, *Handbook of Macroeconomics*, volume 1, pages 1397–1482. 1999.

- C. S. Peskin. *Mathematical aspects of heart physiology*. Courant Institute of Mathematical Sciences, New York University, New York, 1975.
- A. M. Petersen, F. Wang, S. Havlin, and H. E. Stanley. Market dynamics immediately before and after financial shocks: Quantifying the Omori, productivity, and Bath laws. *Phys. Rev. E*, 82(3):036114, 2010.
- V. Plerou, P. Gopikrishnan, and H. E. Stanley. Econophysics: Two-phase behaviour of financial markets. *Nature*, 421(6919):130, 2003.
- B. Podobnik, T. Lipic, D. Horvatic, A. Majdandzic, S. R. Bishop, and H. Eugene Stanley. Predicting the Lifetime of Dynamic Networks Experiencing Persistent Random Attacks. *Sci. Rep.*, 5:14286, 2015.
- T. Preis, H. S. Moat, and H. E. Stanley. Quantifying trading behavior in financial markets using Google Trends. *Sci. Rep.*, 3:1684, 2013.
- V. Ramiah, X. Xu, and I. A. Moosa. Neoclassical finance, behavioral finance and noise traders: A review and assessment of the literature. *Int. Rev. Financ. Anal.*, 41:89–100, 2015.
- J. C. Reboredo, M. A. Rivera-Castro, and E. Machado de Assis. Power-law behaviour in time durations between extreme returns. *Quant. Financ.*, 14(12):2171–2183, 2014.
- S. Redner. A FORTRAN program for cluster enumeration. *J. Stat. Phys.*, 29(2):309–315, 1982.
- S. Redner. *A guide to first-passage processes*. Cambridge University Press, first edition, 2001.
- D. Revuz and M. Yor. *Continuous martingales and Brownian motion*, volume 293. Springer Verlag, 1999.
- J. J. Rotemberg and M. Woodford. An optimization-based econometric framework for the evaluation of monetary policy. *NBER Macroecon. Annu.*, 12:297–346, 1997.

- A. Rothkegel and K. Lehnertz. Multistability, local pattern formation, and global collective firing in a small-world network of nonleaky integrate-and-fire neurons. *Chaos*, 19(1):015109, 2009.
- T. Roukny, H. Bersini, H. Pirotte, G. Caldarelli, and S. Battiston. Default cascades in complex networks: topology and systemic risk. *Sci. Rep.*, 3:2759, 2013.
- S. L. Rynes, J. M. Bartunek, and R. L. Daft. Across the Great Divide: Knowledge Creation and Transfer between Practitioners and Academics. *Acad. Manag. Rev.*, 44(2):340–355, 2001.
- E. Salinas and T. J. Sejnowski. Correlated neuronal activity and the flow of neural information. *Nat. Rev. Neurosci.*, 2(8):539–50, 2001.
- P. Samuelson. Proof that properly anticipated prices fluctuate randomly. *Ind. Manag. Rev.*, 6(2):41–49, 1965.
- M. Scheffer. Foreseeing tipping points. *Nature*, 467:6–7, 2010.
- M. Scheffer, S. Carpenter, J. a. Foley, C. Folke, and B. Walker. Catastrophic shifts in ecosystems. *Nature*, 413(6856):591–596, 2001.
- M. Scheffer, J. Bascompte, W. A. Brock, V. Brovkin, S. R. Carpenter, V. Dakos, H. Held, E. H. van Nes, M. Rietkerk, and G. Sugihara. Early-warning signals for critical transitions. *Nature*, 461(7260):53–9, 2009.
- G. J. Schinasi. *Safeguarding financial stability: theory and practice*. International Monetary Fund, 2005.
- J. Shao. *Mathematical statistics*. Springer, New York, 4 edition, 2007.
- N. Shephard and T. Andersen. Stochastic volatility: origins and overview. In T. Andersen, R. Davis, J. Kreiss, and T. Mikosch, editors, *Handbook of Financial Time Series*, number 389, pages 233–254. Springer-Verlag Berlin Heidelberg.

- R. J. Shiller. Do stock prices move too much to be justified by subsequent changes in dividends? *Am. Econ. Rev.*, 71(3):421–436, 1981.
- R. J. Shiller. Conversation, information, and herd behavior. *Am. Econ. Rev.*, 85(2): 181–185, 1995.
- R. J. Shiller. Speculative asset prices. *Am. Econ. Rev.*, 104(6):1486–1517, 2014.
- R. J. Shiller. *Irrational exuberance*. Princeton University Press, Princeton, N. J, 3 edition, 2015.
- Y. Shin Kim, S. T. Rachev, M. Leonardo Bianchi, and F. J. Fabozzi. Tempered stable and tempered infinitely divisible GARCH models. *J. Bank. Financ.*, 34(9):2096–2109, 2010.
- N. Shiwakoti and M. Sarvi. Understanding pedestrian crowd panic: a review on model organisms approach. *Journal of transport geography*, 26:12–17, 2013.
- A. Shleifer and L. Summers. The noise trader approach to finance. *J. Econ. Perspect.*, 4(2):19–33, 1990.
- P. Singh, S. Sreenivasan, B. K. Szymanski, and G. Korniss. Threshold-limited spreading in social networks with multiple initiators. *Sci. Rep.*, 3:2330, 2013.
- D. Sornette. *Why Stock Markets Crash: Critical Events in Complex Financial Systems*. Princeton University Press, 1 edition, 2003.
- D. Sornette and A. Johansen. Large financial crashes. *Phys. A Stat. Mech. its Appl.*, 245(3-4):411–422, 1997.
- D. Sornette and S. Von der Becke. Computer trading: crashes and high frequency trading. UK Government Office for Science Technical Report. August, 2011.
- D. Sornette and W.-X. Zhou. Importance of positive feedbacks and overconfidence in a self-fulfilling Ising model of financial markets. *Phys. A Stat. Mech. its Appl.*, 370(2):704–726, 2006.

- T. O. Sprenger, A. Tumasjan, P. G. Sandner, and I. M. Welp. Tweets and trades: The information content of stock microblogs. *Eur. Financ. Manag.*, 20(5):926–957, 2014.
- H. E. Stanley. *Introduction to phase transitions and critical phenomena*. Oxford University Press, 1 edition, 1988.
- R. Stanley. *Enumerative Combinatorics, Volume 1*. Cambridge University Press, Cambridge, second edition, 2012.
- J. E. Stiglitz. Rethinking macroeconomics: What failed, and how to repair it. *J. Eur. Econ. Assoc.*, 9(4):591–645, 2011.
- S. H. Strogatz. Exploring complex networks. *Nature*, 410(6825):268–76, 2001.
- D. Stuckler, S. Basu, M. Suhrcke, A. Coutts, and M. Mckee. The public health effect of economic crises and alternative policy responses in Europe : an empirical analysis. *Lancet*, 374(9686):315–323, 2009.
- G. Tedeschi, G. Iori, and M. Gallegati. Herding effects in order driven markets: The rise and fall of gurus. *J. Econ. Behav. Organ.*, 81(1):82–96, 2012a.
- G. Tedeschi, A. Mazlounian, M. Gallegati, and D. Helbing. Bankruptcy cascades in interbank markets. *PLoS One*, 7(12):e52749, 2012b.
- R. H. Thaler. *Quasi rational economics*. Russell Sage Foundation, 1994.
- The European Commission. Improving knowledge transfer between research institutions and industry across Europe. Technical report, 2007.
- The Financial Crisis Inquiry Commission. The financial crisis inquiry report. Technical report, 2011.
- S. Thurner and S. Poledna. DebtRank-transparency: Controlling systemic risk in financial networks. *Sci. Rep.*, page 8, 2013.

- S. Thurner, J. D. Farmer, and J. Geanakoplos. Leverage Causes Fat Tails and Clustered Volatility. *Quant. Financ.*, 12(5):19, 2012.
- M. Timme, F. Wolf, and T. Geisel. Coexistence of regular and irregular dynamics in complex networks of pulse-coupled oscillators. *Phys. Rev. Lett.*, 89(25):258701, 2002.
- J. Tirole. Asset Bubbles and Overlapping Generations. *Econometrica*, 53(6):1499–1528, 1985.
- C. Tovar. DSGE models and central banks. *Econ. Open-Access, Open-Assessment E-Journal*, (258), 2009.
- J.-C. Trichet. Reflections on the nature of monetary policy non-standard measures and finance theory. In *ECB Central Banking Conference*, 2010.
- J. J. Tseng and S. P. Li. Asset returns and volatility clustering in financial time series. *Phys. A Stat. Mech. its Appl.*, 390(7):1300–1314, 2011.
- H. Uhlig. *A toolkit for analyzing nonlinear dynamic stochastic models easily*. 1995.
- A. H. Van De Ven and P. E. Johnson. Knowledge for theory and practice. *Acad. Manag. Rev.*, 31(4):802–821, 2006.
- B. B. Vladimirovski, J. Tabak, M. J. O’Donovan, and J. Rinzel. Episodic activity in a heterogeneous excitatory network, from spiking neurons to mean field. *J. Comput. Neurosci.*, 25(1):39–63, 2008.
- A. Walker, E. Cox, J. Loughhead, and J. Roberts. Counting the cost: the economic and social costs of electricity shortfalls in the UK. Technical Report November, Royal Academy of Engineering, 2014.
- H. W. Watson and F. Galton. On the probability of the extinction of families. *J. R. Anthropol. Inst.*, 4:138–144, 1875.

- D. J. Watts. A simple model of global cascades on random networks. *Proc. Natl. Acad. Sci.*, 99(9):5766–5771, 2002.
- D. J. Watts and S. H. Strogatz. Collective dynamics of 'small-world' networks. *Nature*, 393(6684):440–2, 1998.
- M. Wickens. How useful are DSGE macroeconomic models for forecasting? CEPR Discussion Paper. DP9049, 2012.
- S. Wolfram. Statistical mechanics of cellular automata. *Rev. Mod. Phys.*, 55(3):601–644, 1983.
- C. M. Wray and S. R. Bishop. Cascades on a stochastic pulse-coupled network. *Sci. Rep.*, 4:6355, 2014.
- C. M. Wray and S. R. Bishop. A financial market model incorporating herd behaviour. 2015. Submitted.
- D. Xiao and J. Wang. Modeling stock price dynamics by continuum percolation system and relevant complex systems analysis. *Phys. A Stat. Mech. its Appl.*, 391(20):4827–4838, 2012.
- Y. Xue and R. Gençay. Trading frequency and volatility clustering. *J. Bank. Financ.*, 36(3):760–773, 2012.
- R. Yalamova and B. McKelvey. Explaining what leads up to stock market crashes: A phase transition model and scalability dynamics. *J. Behav. Financ.*, 12(3):169–182, 2011.
- S. Yan. Jump risk, stock returns, and slope of implied volatility smile. *J. financ. econ.*, 99(1):216–233, 2011.
- X. Zhang, H. Fuehres, and P. A. Gloor. Predicting stock market indicators through Twitter 'I hope it is not as bad as I fear'. *Procedia - Soc. Behav. Sci.*, 26:55–62, 2011.

- L. Zhao, G. Yang, W. Wang, Y. Chen, J. P. Huang, H. Ohashi, and H. E. Stanley. Herd behavior in a complex adaptive system. *Proc. Natl. Acad. Sci.*, 108(37):15058–63, 2011.
- B. Zheng, T. Qiu, and F. Ren. Two-phase phenomena, minority games, and herding models. *Phys. Rev. E*, 69(4):046115, 2004.
- Z. Zheng, Z. Qiao, T. Takaishi, H. E. Stanley, and B. Li. Realized volatility and absolute return volatility: a comparison indicating market risk. *PLoS One*, 9(7), 2014.
- R. M. Ziff. Getting the jump on explosive percolation. *Science*, 339(6124):1159–60, 2013.
- G. Zumbach. Volatility processes and volatility forecast with long memory. *Quant. Financ.*, 4(1):70–86, 2004.
- G. Zumbach. Characterizing heteroskedasticity. *Quant. Financ.*, 11(9):1357–1369, 2011.
- G. Zumbach and P. Lynch. Heterogeneous volatility cascade in financial markets. *Phys. A Stat. Mech. its Appl.*, 298(3-4):521–529, 2001.